

# Real Algebraic Geometry of the Sextic Curves

Von der Fakultät für Mathematik und Informatik  
der Universität Leipzig  
angenommene

D I S S E R T A T I O N

zur Erlangung des akademischen Grades

DOCTOR RERUM NATURALIUM  
(Dr.rer.nat.)

im Fachgebiet  
Mathematik

vorgelegt von

Mahsa Sayyary Namin  
geboren am 24.04.1990 in Teheran

Die Annahme der Dissertation wurde empfohlen von:

1. Professor Dr. Bernd Sturmfels, Max-Planck-Institute MIS, Leipzig
2. Professor Dr. Peter Schenzel, Martin-Luther-Universität, Halle

Die Verleihung des akademischen Grades erfolgt mit Bestehen der Verteidigung am  
11.02.2021 mit dem Gesamtprädikat *magna cum laude*.



## Abstract

The main areas in mathematics in which this thesis lies are real algebraic geometry, computational algebraic geometry, and commutative algebra. This dissertation mainly revolves around the real algebraic geometry of curves, especially curves of degree six and the hyperplanes that have special intersections with them.

Chapter 2 consists of our computational study on smooth curves of degree six in the real projective plane. In the Rokhlin–Nikulin classification, there are 56 topological types, refined into 64 rigid isotopy classes. We develop methods for determining the topological type of a given sextic and, using our implementation, we compute empirical probability distributions on the various types. We list 64 explicit representatives with integer coefficients, and we perturb these to draw many samples from each class. This allows us to explore how many of the bitangents, inflection points and tensor eigenvectors are real. We also study the real tensor rank and the avoidance locus, which is the locus of all real lines that do not meet a given sextic. This is a union of up to 46 convex regions, bounded by the dual curve. Finally, we use the correspondence between surfaces of degree four and plane sextic curves to construct quartic surfaces with prescribed topology.

The objects of our study in Chapters 3 and 4 are canonical curves of genus four, called space sextics. These curves are the intersections of a quadric and a cubic surface in three dimensional projective space. A space sextic curve has exactly 120 complex tritangent planes corresponding to its 120 odd theta characteristics.

In Chapter 3, we present algorithms for computing real tritangent planes to space sextics, and we study the associated discriminants. However, our main focus is on sextic curves that arise from blowing up the projective plane at eight points. In particular, we give algorithms to construct such sextic curves and their tritangents. The number of planes that are tangent to a space sextic at three points with real coordinates vary widely. We show that both 0 and 120 are attained. This solves a problem suggested by Arnold Emch in 1928.

In Chapter 4, we develop efficient inverses to the algorithm of constructing space sextics arising from del Pezzo surfaces of degree one. This means, we present an algorithm to either reconstruct the original eight points in the projective plane from a space sextic or certify that this is not possible. Moreover, we extend a construction of Lehavi [60]

which recovers a space sextic from its tritangents and Steiner system. All algorithms in this chapter have been implemented in MAGMA.

Chapter 5 offers an algebraic study of an optimization problem with a long history. The Fermat-Weber point is the unique point that minimizes the sum of distances from  $n$  given points in the real Euclidean space. For  $n$  points with integer coordinates where  $n \geq 5$ , the Fermat-Weber point is no longer expressible by radicals over the field of rational numbers. It is the root of an irreducible monic polynomial of high degree with rational coefficients. We present our computational results on the algebraic degree of the Fermat-Weber point over rationals. We also derive a conjectured formula for that degree.



## Authorship

The contents of this manuscript are either my own work or represent joint work of my co-authors and myself. The first chapter is written by me. Most of the Chapter 2 grew out of the results in the article “Sixty-Four Curves of Degree Six” [45] with Nidhi Kaihnsa, Mario Kummer, Daniel Plaumann, and Bernd Sturmfels. This article is published in *Experimental Mathematics*, 2019, pages 132-150.

Chapters 3 and 4 are based on my collaborative work with Türkü Özlüm Çelik, Avinash Kulkarni, Yue Ren, and Bernd Sturmfels in the two joint articles [54] and [15]. The article “Real space sextics and their tritangents” [54] is published in *Proceedings of the International Symposium on Symbolic and Algebraic Computation (ISSAC)*, 2018, pages 247-254. The follow-up article “Tritangents and their space sextics” [15] is published in *Journal of Algebra*, 2019, pages 290 - 311.

Chapter 5 is entirely due to me. It represents my results on the algebraic properties of the Fermat-Weber point.

## Acknowledgments

First and foremost I want to thank my advisor Bernd Sturmfels. He has certainly been an inspiring character in my mathematical world. I am grateful to him for introducing me to different subjects in algebraic geometry, connecting me to experts, and patiently collaborating with me in different projects. His enthusiasm in the research that he does and his excellent and fast communications, made me feel supported at any moment during my doctoral work.

It has been an honor to be a member of Nonlinear Algebra Group since its birth at the Max Planck Institute for Mathematics in the Sciences (MPI MIS). Doing my Ph.D. in the nonlinear algebra group and being surrounded by many experts on different topics helped me being up to date in my research area, having several collaborations, and getting to know many outstanding mathematicians.

I gratefully thank my co-authors Türkü Özlüm Çelik, Nidhi Kainha, Avinash Kulkarni, Mario Kummer, Daniel Plaumann, and Yue Ren. I had a great time interacting with them and, needless to say, working beside them was the most joyful way for me to grow as a mathematician.

I am particularly thankful to Yue Ren, Avinash Kulkarni, Türkü Özlüm Çelik, Peter Schenzel, Yuhua Jiang, Paul Görlach, and Mateusz Michałek from whom I have learned the most.

I am grateful to many people who helped me during my Ph.D. by patiently proofreading my writings and listening to my preparatory presentations. In particular, thanks to Francesco Galuppi, Christiane Görden, and Stephan Mescher for their most friendly assistance.

I acknowledge the financial support of the International Max Planck Research School “Mathematics in the Sciences”. MPI MIS has been an excellent environment for me to pursue my doctoral studies. I am very thankful to Heike Rackwitz, Saskia Gutzschebauch, and Robert Gille for helping me with several personal and administrative tasks during my time at the institute. I am grateful to the librarians whose help always came faster than I imagined. Additionally, their effort in improving the social life at the institute is very much appreciated.

It was a great pleasure for me to join the geometry group of the University of Leipzig during the last year of my Ph.D. I thank Matthias Schwarz for giving me this opportunity and for trusting me to be his assistant in his newly formed lecture “Mathematical physics 1&2”. I

am very thankful to all the people in the geometry group to make a welcoming atmosphere for me to finish writing my Dissertation.

Lastly, I would like to thank my friends Azadeh, Sara, Masud, Fer-eydoon and Anja for all the help during my years in Leipzig. And thanks to my beloved sisters, Mahnaz and Parisa, for their unconditional support.

# Contents

List of Figures	vii
List of Tables	viii
Chapter 1. Introduction	1
Chapter 2. Plane Sextic Curves, an Experimental Approach	10
2.1. The rigid isotopy classification of plane sextics	16
2.2. Classifier and empirical distributions	18
2.3. Examples of polynomials and their constructions	24
2.4. Local sampling and rigid isotopy transitions	33
2.5. Avoidance locus, dual curve, and bitangents	40
2.6. Reality questions for plane sextics	49
2.7. Connections to K3 surfaces	54
Chapter 3. Real Space Sextics and their Tritangents	58
3.1. Space sextics from del Pezzo surfaces of degree 1	60
3.2. Constructing the tritangents	62
3.3. 120 totally real tritangents	65
3.4. Space sextics with fewer ovals	68
3.5. Solving the tritangent equations	70
3.6. Discriminants	74
3.7. What next?	78
Chapter 4. Tritangents and Their Space Sextics	80
4.1. Steiner systems and syzygetic quadruples	82
4.2. Space sextics on smooth quadrics	83
4.3. Space sextics on singular quadrics	85
4.4. Reconstruction of eight points from space sextics	88
4.5. Steiner systems to space sextics	95
Chapter 5. The Algebraic Degree of the Fermat-Weber Point	103
5.1. Explaining the degree formula	105
5.2. The ideal of the derivatives is determinantal	107
5.3. Computational results	114
Bibliography	116

## List of Figures

1.1 Emch and his construction of a space sextic curve	3
2.1 Using Bézout’s theorem to classify smooth plane quartics	11
2.2 The topological classification of smooth plane quartics	12
2.3 The topological classification of smooth plane quintics	12
2.4 Hilbert’s sixteen problem	14
2.5 The topological and rigid isotopy classifications of plane sextics	18
2.6 Perturbing the union of three quadrics intersecting transversally	31
2.7 Constructing dividing/non-dividing types by local perturbation	32
2.8 The division of the Robinson net by its discriminant	34
2.9 Discriminantal transitioning by turning an oval inside out	37
2.10 Edge quartic, its dual, and its avoidance locus	41
2.11 A sextic of Type 8nd and its 68 real relevant bitangents	45
2.12 A smooth sextic with 10 ovals and empty avoidance locus	49
2.13 A Kummer surface and the corresponding plane sextic	54
3.1 Totally real tritangent of a curve with three ovals	59
3.2 A space sextic with no totally real tritangents	59
3.3 Constructing space sextics from del Pezzo surfaces of degree 1	62
3.4 Twenty-eight lines pair with twenty-eight rational quintics	63
3.5 Fifty-six conics pair with fifty-six rational quartics	64
3.6 Twenty-eight pairs of rational cubics	64
3.7 Totally real tritangents of space sextics with 3 and 4 ovals	70
3.8 Emch’s construction has 108 totally real tritangents	73
4.1 Using pairs of exceptional curves to construct Steiner system	87
5.1 Fermat-Weber point for the set of three points	103
5.2 Fermat-Weber point for the set of four points	104

## List of Tables

2.1	Rokhlin–Nikulin classification of smooth sextics in $\mathbb{P}_{\mathbb{R}}^2$	16
2.2	Randomly chosen sextics with the $U(3)$ -invariant distribution	21
2.3	Sextics from random symmetric matrices with linear entries	22
2.4	Sextics from signed sums of $n$ sixth powers of linear forms	22
2.5	Sextics with uniformly distributed integer coefficients	23
2.6	Symmetric sextics with uniformly distributed coefficients	23
2.7	Reality of the four major features associated to plane sextics	51
3.1	The number of real and totally real tritangents of space sextics	69

## CHAPTER 1

### Introduction

Algebraic geometry, the broad area in which this manuscript falls, explores solution sets of systems of polynomial equations. They are called *varieties*. In classical algebraic geometry, for some fundamental theorems to hold, the ground field is often assumed to be algebraically closed, such as the field of complex numbers  $\mathbb{C}$ . By restricting the main objects of study, i.e. varieties and mappings between them, to the field of real numbers  $\mathbb{R}$ , we restrict to a branch of algebraic geometry known as *real algebraic geometry*.

Working with the real numbers as the ground field brings the very abstract objects and methods of algebraic geometry into applications in industry and science. For instance, several optimization and convex geometry problems arising from economics, chemistry, and biology can be formulated as real algebraic geometry problems. Another important aspect of restricting to  $\mathbb{R}$  is the ability to produce fast computations and visualizations for numerous problems in small dimensions.

This chapter aims for making the reader familiar with the main objects of study in this thesis as well as their brief history and importance. In addition, the overall scope of the chapters is given in this introduction. We start by introducing some notation and elementary definitions. Apart from Chapter 4, which inherits the key definitions and notations from Chapter 3, the remaining chapters are self-contained. Furthermore, each chapter starts with a detailed outline of its sections.

The *projective space*, of dimension  $n$  over a field  $k$ , is denoted by  $\mathbb{P}_k^n$ , or simply  $\mathbb{P}^n$  when the field is arbitrary or known from context. For readers that are not familiar with projective spaces, it is intuitive to think of the  $n$  dimensional (affine) space  $k^n$ . Varieties in  $\mathbb{P}^n$  are defined by homogeneous polynomial equations. A *hypersurface* is the zero set of a single polynomial and a *hyperplane* is a hypersurface defined by a linear form. The one-dimensional varieties in  $\mathbb{P}^n$  are called *algebraic curves*, or *curves* for short. The *degree* of a curve in  $\mathbb{P}_k^n$  is geometrically defined as the number of intersection points of a generic hyperplane with the curve in  $\mathbb{P}_{\bar{k}}^n$ , where  $\bar{k}$  is the algebraic closure of  $k$ .

There are several intrinsic properties assigned to curves that are well-studied over the field of complex numbers. However, there is not much known about these properties when restricting to curves over the real numbers. A crucial direction of inquiry is the study of hyperplanes associated with the curve. The possibility of reconstructing some families of curves from hyperplanes that have special intersections with them, highlights this importance. We now explore two such examples in projective spaces of dimensions two and three, both of which will be discussed in detail within this thesis.

Curves and lines in the *projective plane*  $\mathbb{P}^2$  are the simplest examples of hypersurfaces and hyperplanes. A curve in the projective plane is called a *plane curve*, and it is the zero set of a single homogeneous polynomial with three unknowns. Let  $C \subseteq \mathbb{P}^2$  be a plane curve defined by  $f(x, y, z) = 0$ . Its *dual*  $C^\vee \subseteq (\mathbb{P}^2)^\vee$  is a plane curve that consists of points  $(a : b : c)$  corresponding to the lines  $ax + by + cz = 0$  that are tangent to  $C$ . Plücker's formula relates certain numeric invariants of algebraic curves to corresponding invariants of their dual curves. In particular, it counts the *singularities* of curves over an algebraically closed field.

The lines that are tangent to a plane curve  $C$  of degree  $d$  at two points, called *bitangents*, correspond to certain singularities of the dual curve  $C^\vee$ . Bézout's theorem says that for a bitangent line to exist,  $d$  has to be larger than three and by Plücker's formula over  $\mathbb{C}$  the number of such lines only depends on  $d$  and equals  $\frac{1}{2}(d-3)(d-2)d(d+3)$ . Therefore, for a curve  $C \subseteq \mathbb{P}_{\mathbb{C}}^2$  of any given degree  $d$ , the number of lines that are tangent to  $C$  at two points is known.

After passing to  $\mathbb{R}$ , the largest degree for which this number has been well-studied is four, i.e. the first case for which a bitangent is defined. There are only experimental results regarding the count of real bitangents to a curve in  $\mathbb{P}_{\mathbb{R}}^2$  for higher degrees. The 'experiment' can be to write a program to generate many random curves of a certain degree  $d$  and to count how many of the complex bitangents are real. Advanced computational tools are indispensable for such studies.

In three-dimensional projective space  $\mathbb{P}^3$ , hypersurfaces and hyperplanes are called *surfaces* and *planes*, respectively. The common zero set of two homogeneous polynomials in four variables, i.e. the intersection of two surfaces, is a curve in  $\mathbb{P}^3$ , which we call a *space curve*. The natural analogous to lines that are tangent to a plane curve at two points are planes tangent to a space curve at three points.

Examples of space curves for which these planes are well-studied over the complex numbers are curves of degree six, called *space sextics*. The *smooth* space sextics in  $\mathbb{P}_{\mathbb{C}}^3$  arise from intersecting a quadric and a cubic surface. These are surfaces defined by polynomials of degrees two and three, respectively. The definition of the degree of a curve implies that a plane intersects a space sextic at six points in  $\mathbb{P}_{\mathbb{C}}^3$ .



There are exactly 120 planes, called *tritangents*, corresponding to 120 *odd theta characteristics* of a space sextic  $C$ . Geometrically, tritangents are planes that are tangent to  $C$  at every points of intersection. If  $C$  lies on a smooth quadric surface, every such plane is a tritangent. However, if the quadric surface is singular, there are infinitely many planes passing through its singularity that are tangent to  $C$  at every intersection point. In this case, tritangents are the planes tangent to  $C$  at three points and do not pass through the singularity of the quadric surface. The tritangent planes reflect notable facts about the intrinsic properties of a space sextic as well as its extrinsic geometry. For instance a space sextic curve can be reconstructed from its tritangent planes.

In early 20th century the answer to many questions regarding space sextics over the real numbers seemed to be known to real algebraic geometers. However, recently it has been shown that not all of them were correct: Let  $C$  be a smooth space sextic. The number of connected components of the real part  $C_{\mathbb{R}} \subseteq \mathbb{P}_{\mathbb{R}}^3$  is at most five, due to the Harnack bound [37]. From 120 complex tritangent planes associated to  $C$ , the count of the real ones only depends on the number of real components. All complex tritangents are real if and only if  $C_{\mathbb{R}}$  has five components. Such a curve was constructed by Arnold Emch [26] in 1928. Furthermore, he used the symmetry of his construction and claimed that all 120 tritangents intersect the curve only at real points.

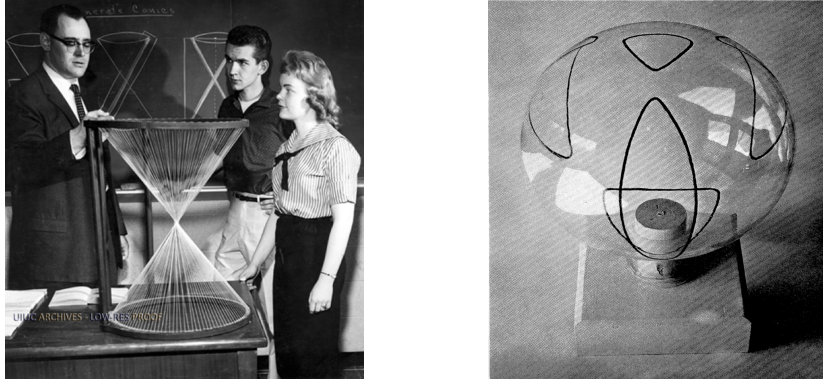


FIGURE 1.1. Arnold Emch and his construction of a space sextic with five real components on a smooth quadric surface.

This claim was proven wrong by Corey Harris and Yoav Len in 2018, which left the problem open again [38]:

★ *Does there exist a space sextic  $C$  with 120 real tritangent planes, all intersecting  $C$  only at real points?*

This thesis mainly revolves around curves of degree six and their ‘reality problems’ in two and three-dimensional projective spaces. Broadly speaking, reality problems treat the real solutions to the defining equations of a curve and the hypersurfaces intersecting it in special manners. It also includes the investigation of several other features associated with the real part of the curve as well as the complex curve which can be viewed as a two-dimensional real manifold. Plane sextics and space sextics, are both of great importance, especially in computational and real algebraic geometry.

In the projective plane, the topological classification of plane sextic curves offers several problems that can be investigated over the real numbers:

- \* The real *topological classification of smooth plane curves* is a classical theme in algebraic geometry. It basically asks: by plotting the zero set of a degree  $d$  polynomial in the real projective plane  $\mathbb{P}_{\mathbb{R}}^2$ , what are the possible mutual positions of the connected components that one can expect? More than a century ago, David Hilbert asked for the first non-trivial case, i.e. the topological classification of curves of degree six:

*A thorough investigation of the relative position of the separate branches when their number is the maximum seems to me to be of very great interest, and not less so the corresponding investigation as to the number, form, and position of the sheets of an algebraic surface in space.*

In 1978, after about seven decades of proof and disproof, D. A. Gudkov [35] solved this problem which is known as *Hilbert’s 16th problem*. The difficulty of the topological classification increases dramatically as  $d$  increases. So far, it is only solved up to degree seven. A complete classification of plane sextics in  $\mathbb{P}_{\mathbb{R}}^2$  would provide a viable source to explore their features and in particular, several related reality problems.

The study of the *avoidance locus* associated to a plane curve is one such example: points corresponding to the lines that miss a curve  $C \subseteq \mathbb{P}_{\mathbb{R}}^2$  form a union of convex connected components in the dual projective plane  $(\mathbb{P}^2)_{\mathbb{R}}^{\vee}$ . Exploring these components is directly related to the real topological type of the curve and its real bitangents. More examples of invariants associated with a plane sextic that can be investigated over  $\mathbb{R}$  are its *rank* and the number of its *inflection points*. Additionally, one can ask analogous questions for surfaces of degree four in  $\mathbb{P}^3$  arising from plane sextic curves.

In three-dimensional projective space  $\mathbb{P}^3$ , an important family of space sextics arises from blowing up the projective plane at eight points. This simplifies several reality problems concerning such curves:

- \* Smooth space sextics are the *canonical curves of genus four* in  $\mathbb{P}^3$ , where the genus of a curve is the number of holes in the corresponding manifold. Space sextics provide a rich example for us to understand several geometric features of non-planar curves. There is a classical construction that relates *del Pezzo surfaces of degree one* to a family of space sextics.

This construction starts with a del Pezzo surface of degree one which is the *blow-up* of the projective plane  $\mathbb{P}^2$  at eight points in *general position*. The resulting space sextic is smooth and it lies on a singular quadric surface in  $\mathbb{P}^3$ . Several reality problems related to such sextics have equivalent descriptions in terms of the reality of given points and their relative configurations.

Answering the question by Harris and Len with intersecting samples of quadric and cubic surfaces, if possible, is computationally very hard. In this approach one needs to keep track of the number of real components in the intersection of two surfaces along with the reality of their intersections with all tritangents. However, by restricting to sextics that are constructed from blowing up the plane at eight points, we can rephrase this question:

- ★ What are the coordinates of eight points in the plane that give rise to the desired space sextic?

Roughly speaking, this construction translates the problem of intersecting surfaces in three dimensional space to the intersections of planar curves where exact computations are much more feasible. Apart from dealing with the historical problem due to Emch, the ‘eight points construction’ of space sextics has advantages in answering more general questions regarding the real part of the curve. For instance it relates the number of components of the real curve to the number of real points among the original eight points. Therefore, it simplifies the exploration of features associated to real space sextics with different number of connected components.

The structure of this manuscript is as follows. Chapter 2 addresses plane sextics and Chapters 3 and 4 revolve around the space sextics and their tritangents. In Chapter 5, we report on computational results to an optimization problem which arose historically in economics due to Alfred Weber. Although this problem has a different flavor in its main objects of study, the computational methods and tools that we apply are similar to the ones used in the chapters before. Advanced computational tools including MATHEMATICA, MAPLE, and in particular

specialized computer algebra systems such as SINGULAR, MACAULAY2 and MAGMA play a major role in all chapters.

Chapter 2 starts with introducing two important classifications of smooth plane sextics: the topological and *rigid isotopy* classifications. The latter is a finer classification since, in addition to the topology of the curve in the real plane, it concerns the behavior of its real part inside the complex curve. This classification is based on a hypersurface, called the *discriminant*, in the space of all real plane sextic curves  $\mathbb{P}_{\mathbb{R}}^{27}$ . The discriminant has degree 75 and it divides the whole space into 64 connected components, one for each rigid isotopy type. Crossings of the discriminant, which we call *discriminantal transitions*, come in three different forms. The 64 rigid isotopy types, grouped into 56 topological types, carry a *poset structure* where the *cover relations* are the discriminantal transitions. The exact computation of the discriminant as well as a detailed study of all three forms of transitions are presented in this chapter.

Several different methods from the literature combined with our systematic tricks are applied to construct a ‘nice’ representative in each component of the complement of the discriminant in  $\mathbb{P}_{\mathbb{R}}^{27}$ . We wrote code that given the defining polynomial of a plane sextic returns its topological type after checking its smoothness. Using the 64 representatives to produce many curves in each component together with our fast code to check the type provided us with a large and reliable sample space. We use our samples to explore several features associated to plane sextics over the field of real numbers.

In addition to the experimental results on reality questions, we give an algorithm which uses the real bitangents to construct the avoidance locus. We prove that for a smooth plane curve of degree  $d$  the avoidance locus is the union of  $m$  convex connected components where  $m$  is bounded above by a degree four polynomial in  $d$ . The upper bound evaluates to 46 for plane sextics, and we show that any number between 0 and 46 is realizable by plane sextic curves.

In Chapter 3 we answer the historical problem originating from Emch’s mistake in the construction of a space sextic where all the real tritangents only touch the curve at real points. We call such planes *totally real tritangents* and we prove that there exists a space sextic with 120 totally real tritangents by presenting one such curve.

Although we give a method to compute the tritangents for an arbitrary space sextic, we advise against using it for the purpose of computational proof. Instead, we recommend restricting to the family of sextics that lie on a singular quadric and therefore, they are constructed from del Pezzo surfaces of degree one. In particular, we give an algorithm to construct space sextic curves that arise from blowing up  $\mathbb{P}^2$  at eight points and provide algorithms to compute the 120 tritangents.

In  $\mathbb{P}^2$  eight given points define 120 pairs of curves that satisfy certain properties. Each pair maps to a unique tritangent plane. The intersection of two planar curves in such a pair contains three points which do not lie in the set of our eight original points. We show that there is a one-to-one correspondence between these points and the three points in  $\mathbb{P}^3$  where the corresponding tritangent plane touches the space sextic.

Therefore, to answer the above-mentioned question asked by Harris and Len, we present the coordinates of eight points in the projective plane and show that the reality of coordinates of eight points together with the reality of all intersections between planar curves in 120 pairs results in the desired space sextic.

More generally, in this chapter we show how to control the number of components of a real space sextic curve by the choices of coordinates of eight original points: By picking  $s$  pairs of 8 points to be complex conjugated non-real pairs, for  $0 \leq s \leq 4$ , we obtain a space sextic with  $5 - s$  components in  $\mathbb{P}_{\mathbb{R}}^3$ . Since the number of real tritangents only depends on the number of components of the real curve, this is a powerful tool to keep track of the count of real and totally real tritangents.

Furthermore, in the space of all configurations of eight points  $(\mathbb{P}^2)^8$ , we define the *tritangent discriminant locus*. It divides the whole space into open subsets in such a way that within each subset the number of totally real tritangents to the arising space sextics is constant. We show that the tritangent discriminant locus is a union of 120 hypersurfaces, one for each pair of special curves in the plane. Next, we discuss such a division in the more general space  $\mathbb{P}^9 \times \mathbb{P}^{19}$ , i.e. the space of an arbitrary space sextic from intersecting a quadric and a cubic surface. In both cases, we compute the degrees of all hypersurfaces that are involved.

Finally, at the end of Chapter 3, there is a list of ten questions presented as the ‘natural follow-ups’. The last one is motivation for the next chapter: David Lehavi [60] shows that a general space sextic can be reconstructed from its 120 tritangents. How to do this in practice?

In Chapter 4, which relies on Chapter 3, we present several algorithms, all implemented in MAGMA. In the construction of a space sextic  $C$  from a del Pezzo surface  $X$  of degree one, the 120 pairs of special plane curves that we discussed above map to 120 pairs of *exceptional curves* on  $X$ . There is a rational function that maps  $X$  to a double cover of a singular quadric surface in  $\mathbb{P}^3$  branched along the space sextic  $C$ . It maps each of the exceptional pairs to a tritangent plane. This intermediate step whose explanation we skipped before, is the key point for the inverse direction:

Given a space sextic curve  $C$  which comes from a del Pezzo surface of degree one, we give an algorithm that constructs a collection of eight points in the plane which give rise to a space sextic isomorphic to  $C$ .

First we compute the defining equation of the del Pezzo surface  $X$  of degree one. Among the 240 exceptional curves on  $X$ , we find a (non-unique) set of 8 curves that satisfy certain properties. The *blow-down* of  $X$  along these 8 exceptional curves into  $\mathbb{P}^2$  marks the desired 8 points.

Over the complex numbers, Lehavi [60] explained how to recover a generic space sextic  $C$  on a smooth quadric surface from its 120 tritangent planes. In this method, first we present the reconstruction of the unique quadric surface containing  $C$  and then the reconstruction of a cubic surface which cuts out the curve on the quadric.

Lehavi uses the *Steiner system* associated to  $C$  in this reconstruction method. This is a set consisting of 255 blocks called *Steiner complexes*. Each block is a set of 28 pairwise disjoint length-two-subsets of the 120 tritangents. There are certain *syzygetic* relations defining these sets, where four tritangents are syzygetic if  $4 \times 3 = 12$  pairwise intersection points of them with  $C$  lie on a quadric surface in  $\mathbb{P}^3$ .

We give algorithms to compute the Steiner system associated to a space sextic, in both of the cases that  $C$  lies on a smooth or on a singular quadric surface. Moreover, we extend Lehavi's reconstruction results to space sextics on singular quadrics and to space sextics over more general ground fields.

Chapter 5 tackles an optimization problem with real and computational algebraic geometry methods. We translate a minimization problem into finding the number of solutions to a system of polynomial equations with integer coordinates.

The first roots of the problem go back to the 17th century when Pierre de Fermat started the challenge by asking for the location of a point that minimizes the sum of the Euclidean distances from three given points in the plane. By the end of the 18th century, the exact location of the minimizer was found for three and for four given points in the plane, using basic geometrical tools such as straight-edge and compass. Therefore, it is expressible in terms of the coordinates of given points and by radicals over the rational numbers  $\mathbb{Q}$ .

Later, the economist Alfred Weber generalized Fermat's question to  $n$  given points. The point that minimizes the Euclidean sum of the distances from  $n$  given points in the plane is called *Fermat-Weber point*. Chandrajit Bajaj [4] in 1984 proved that in general for  $n$  given points, where  $n \geq 5$ , the Fermat-Weber point is no longer expressible by radicals over  $\mathbb{Q}$ . He showed that the coordinates of this point are roots of irreducible monic polynomials of high degree with rational coefficients. This unique degree is called the *algebraic degree of the Fermat-Weber point over  $\mathbb{Q}$* .

In 2015, Jean-Charles Faugère, Mohab Safey El Din, Bernd Sturmfels and Rekha Thomas conjectured this degree for the more general case where  $n$  given points are in  $d$  dimensional space  $\mathbb{R}^d$ . Chapter 5

offers an algebraic study of this optimization problem. We give an algebraic explanation of the conjecture for the case that  $n$  given points are in  $\mathbb{R}^2$ . Finally, we present partial and computational results regarding the proof of the conjecture.

## CHAPTER 2

### Plane Sextic Curves, an Experimental Approach

The topological classification of the real algebraic curves in the projective plane has become a prominent topic in mathematics since it has appeared in the well-known *Hilbert's problems list*. In 1900, a German mathematician David Hilbert published a list of twenty-three problems that were all unsolved at the time. Some of these problems are still open and several of them were very influential for 20th and 21st century mathematics. The topological classification of smooth real algebraic curves in  $\mathbb{P}_{\mathbb{R}}^2$  is a classical theme in real algebraic geometry that originates from the Hilbert's sixteenth problem.

An *algebraic curve*  $C$  in the real projective plane  $\mathbb{P}_{\mathbb{R}}^2$  is the zero set of a homogeneous polynomial in three variables. The *degree* of  $C$  is defined to be the degree of the defining polynomial. In this chapter an algebraic curve is simply called a *curve*. The *topological type* of a curve  $C$  in  $\mathbb{P}_{\mathbb{R}}^2$  is the mutual position of the connected components of  $C$ . More precisely, two plane curves  $C$  and  $C'$  have the same type if some homeomorphism of  $\mathbb{P}_{\mathbb{R}}^2 \rightarrow \mathbb{P}_{\mathbb{R}}^2$  restricts to a homeomorphism  $C_{\mathbb{R}} \rightarrow C'_{\mathbb{R}}$ . *Hilbert's sixteenth problem* asks for the topological classification of smooth curves of degree six as the classification is quite manageable for the lower degrees.

Let  $C$  be a smooth curve of degree  $d$  in  $\mathbb{P}_{\mathbb{R}}^2$ . For odd  $d$ , the curve  $C$  consists of exactly one *pseudoline* and some *ovals*. The complement of a pseudoline has only one connected component in the real projective plane  $\mathbb{P}_{\mathbb{R}}^2$  while the complement of an oval has two, namely, inside and outside of the oval. The *inside* of an oval  $O$  is homeomorphic to a disk, and the *outside* to a Möbius strip. An oval  $O_1$  *contains* another oval  $O_2$  if  $O_2$  lies in the inside of  $O_1$ . In that case,  $O_1$  and  $O_2$  are *nested ovals*. An oval is *empty* if it contains no other ovals. If  $d$  is even then it only consists of ovals. The number of connected components of a smooth plane curve  $C$  together with the information of how the ovals are nested determines the topological type of  $C$ . The number of connected components of  $C$  is bounded above by

$$\frac{1}{2}(d-1)(d-2) + 1,$$

which is known due to Harnack (1876) and is called the *Harnack bound*.

The topological classification is trivial for smooth plane curves of degree less than six. The triviality follows from a well-known result of Bézout's theorem which states that *any line in the real projective plane*



intersects a smooth curve  $C$  of degree  $d$  in at most  $d$  real points. Let  $m$  be the maximum number of ovals of  $C$ . Thus,  $m$  is the Harnack bound for even  $d$  and one less for odd  $d$ . For  $d \leq 5$ , any mutual position of the 0 to  $m$  ovals, together with the unique pseudoline for the odd degree case, corresponds to a topological type if it does not contradict the stated result of Bézout's theorem. Example 2.1 shows the topological classification for  $d = 4$ .

**Example 2.1** Let  $C$  be a smooth plane curve of degree four. It has at most  $\frac{1}{2}(4-1)(4-2) + 1 = 4$  connected components that are all ovals. Figure 2.1 shows all of the possible topological types of  $C$ . This can either be empty or consist of one to four empty ovals. If there is a nesting of ovals then there can not be more than two ovals, otherwise there will be a line intersecting  $C$  in more than 4 real points as it is shown in the right-most picture.

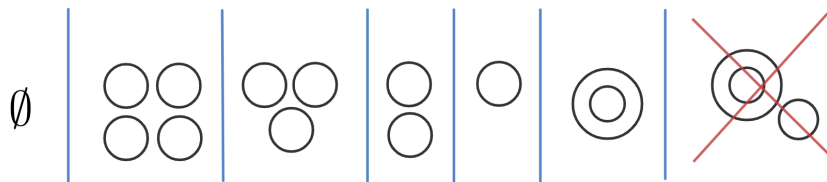


FIGURE 2.1. The topological classification of the smooth plane quartics. The configuration that is crossed out contradicts Bézout's theorem.

There is a unique topological type for smooth curves of degree two since conics are all homeomorphic in  $\mathbb{P}_{\mathbb{R}}^2$ . Cubic forms can be either a pseudoline or the union of a pseudoline and an oval. Curves of degrees four, and five are called quartics and quintics, respectively. There are simple constructions for the smooth plane curves of these degrees. Figures 2.2 and 2.3 present one singular curve in red for each of them. You can see that perturbing these singular curves at their nodes gives rise to all the topological types of the smooth plane quartics and quintics.

The challenge of the topological classification for smooth plane curves increases dramatically with  $d$ , where  $d$  is the degree. The reason is that not all the configurations of ovals that satisfy the Harnack bound and do not contradict Bézout's theorem, can be easily constructed or proven to be non existence for  $d \geq 6$ . The topological classification problem has been solved up to  $d = 7$ , thanks to contributions by many mathematicians, including Hilbert [41], Rohn [75], Petrovsky [69], Rokhlin [76], Gudkov [35], Nikulin [68], Kharlamov [48], and Viro [84, 88, 85].

In this chapter the focus is on the case  $d = 6$  which is part of the Hilbert's sixteenth problem. Curves of degree six are called *sextics*. The Harnack bound for the smooth plane sextics is 11. There are 68 mutual

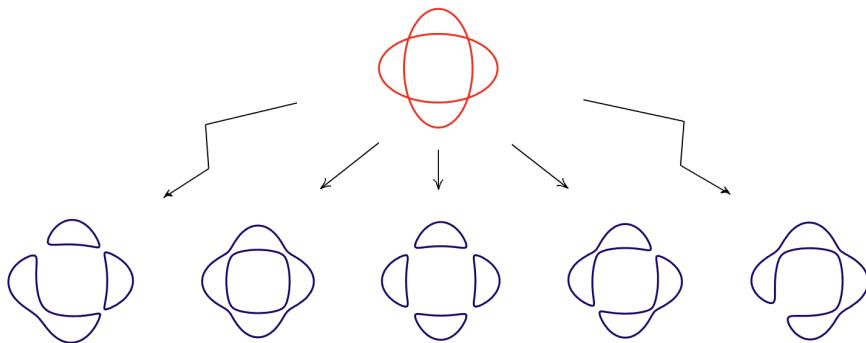


FIGURE 2.2. All non-empty topological types for the smooth plane quartics are constructible by perturbing the union of two conics, intersecting transversally.

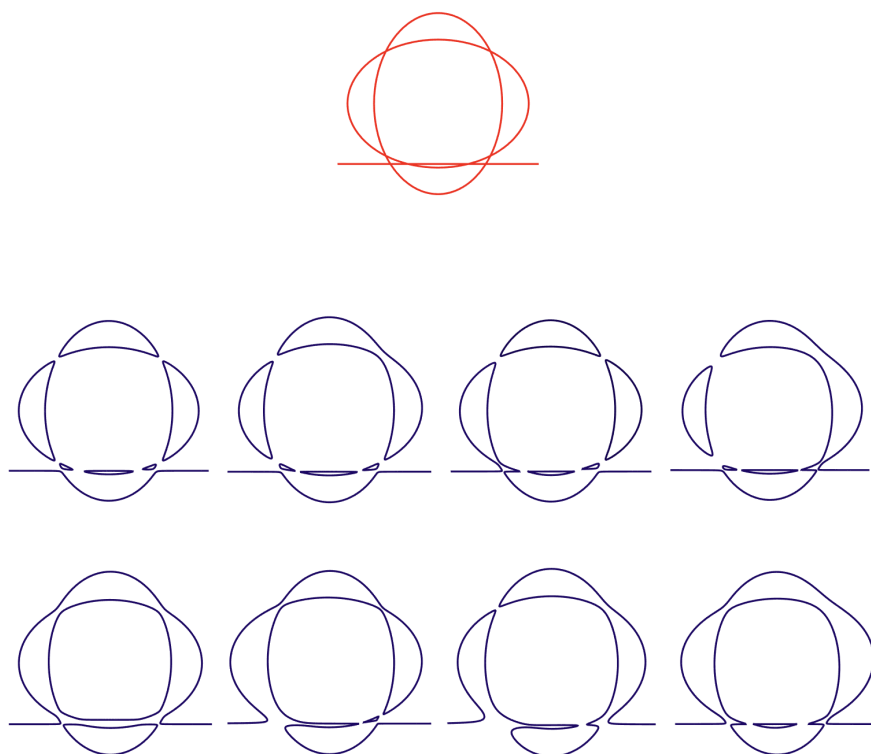


FIGURE 2.3. A smooth plane quintic has eight possible topological types. It can be the union of a pseudoline and  $n$  empty ovals, where  $0 \leq n \leq 6$ , or it is the union of a pseudoline and one oval nested in another. All of these types are constructible from the singular quintic that is the union of two conics and a line, intersecting transversally as shown in the red picture.

positions for 0 to 11 ovals that any line in  $\mathbb{P}_{\mathbb{R}}^2$  intersects them in less than 7 points. Hilbert and Harnack proved that 54 of them correspond to the topological types of plane sextic curves by introducing a construction for each. Furthermore, Hilbert conjectured that the type with 11 empty ovals does not exist. Many mathematicians including Hilbert's students Kahn [44] and Löbberstein [62], Wrigh [87], Rohn [75], and McDonald [65] attempted to prove it. The first rigorous proof was given by I. G. Petrowsky [69]. Although the non existence of the remaining 13 cases was not proven, Hilbert strongly believed and conjectured that these 54 types complete the topological classification for plane sextics. This conjecture was shown to be wrong after 69 years, by the Russian mathematician Dmitrii Andreevich Gudkov. In 1978, he completed the answer to the classification problem by finding a construction for two of the 13 unknown cases and proving that the remaining 11 candidates can not represent a topological type of a smooth plane sextic. See Figure 2.4. In addition to the stated result of Bézout's theorem and the Harnack bound, there are more prohibitions for the configurations of ovals. These new limits explain the elimination of 12 out of 68 cases. To formulate these restrictions we need two more numerical characteristics of a curve. An oval is called *even* if it lies inside even number of ovals and is *odd* otherwise. Denote the number of even ovals and the number of odd ovals by  $p$  and  $n$ , respectively.

**Theorem 2.2** (Gudkov-Rokhlin congruence) *Let  $C$  be a plane curve of degree  $d = 2k$  with the maximal number of ovals. The following congruence holds:*

$$p - n \equiv k^2 \pmod{8}.$$

This congruence explains why in the top row of Figure 2.4 only three cases are plane sextic types. Gudkov [34] proved this congruence for the specific case of  $d = 6$ ; later Rokhlin [77] gave the first proof for the general case that was conjectured by Gudkov.

**Theorem 2.3** (Gudkov-Krakhnov-Kharlamov congruence) *Let  $C$  be a plane curve of degree  $d = 2k$  with one less than the maximum number of ovals, i.e., with  $\frac{1}{2}(d-1)(d-2)$  ovals. The following congruence holds:*

$$p - n \equiv k^2 \pm 1 \pmod{8}.$$

This congruence explains why in the second top row of Figure 2.4, four cases do not correspond to plane sextic types. Gudkov and Krahnov [36], and Kharlamov [50] proved this independently.

As Figures 2.2 to 2.4 suggest, a small perturbation of a smooth curve does not change its topology. The natural question to ask is this: given two curves of the same degree, when is it possible to deform one of them to the other one continuously, i.e. without passing any singular curve? More precisely, take two distinct points in the space of all degree

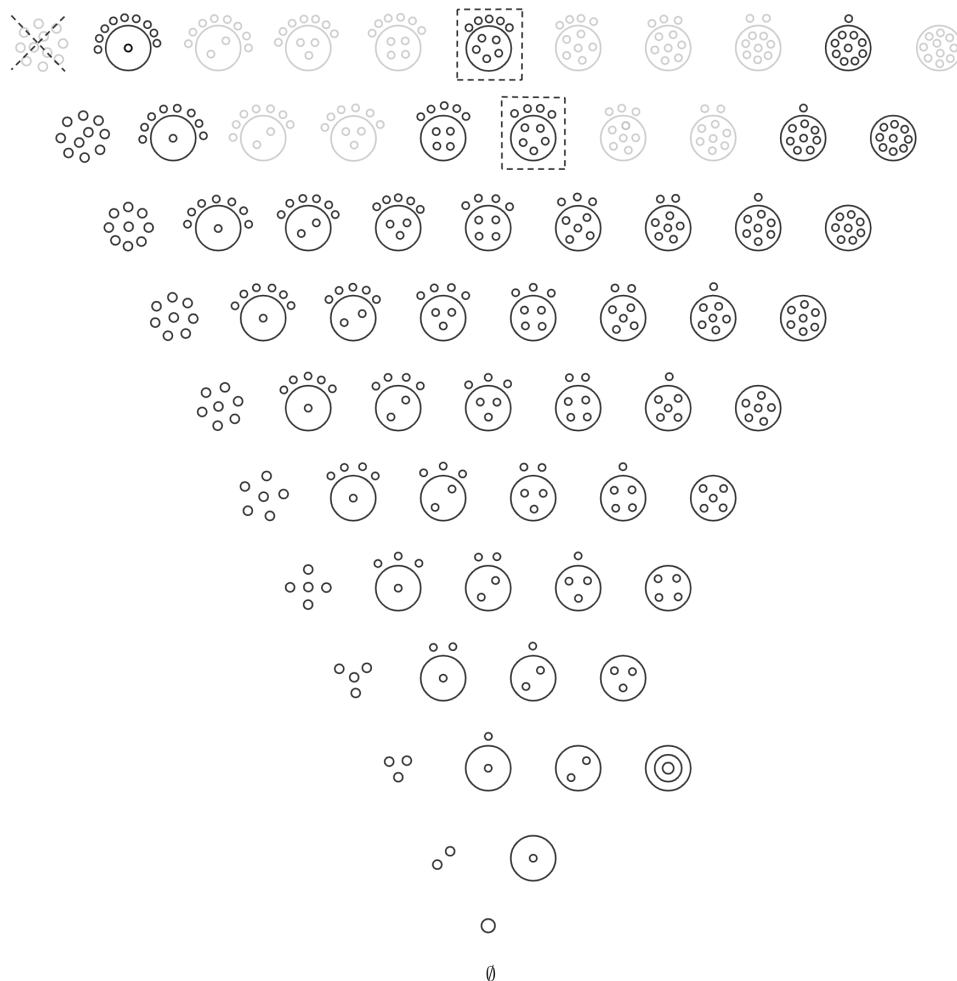


FIGURE 2.4. The picture shows all 68 candidates for the topological type of a plane smooth sextic at the time that Hilbert formulated his 16th problem. Hilbert and Harnack constructed 54 of them. Petrovski proved the nonexistence of the one that is crossed out. Later, Gudkov found the two missing cases that are boxed. The configurations in black are 56 topological types.

$d$  curves that correspond to two curves with the same topological type. Does there always exist a continuous path from one to the other not passing through any point that corresponds to a singular curve? This motivates us to introduce a finer classification.

Another notion of equivalence comes from the discriminant. The space of all the plane curves of degree  $d$  in  $\mathbb{P}_{\mathbb{R}}^2$  is the projective space  $\mathbb{P}_{\mathbb{R}}^{d(d+3)/2}$ . The points of this space that correspond to the singular curves form an irreducible hypersurface of degree  $3(d-1)^2$  which is called the *discriminant* and is denoted by  $\Delta \subset \mathbb{P}_{\mathbb{R}}^{d(d+3)/2}$ .

The *rigid isotopy classes* are the connected components of the complement  $\mathbb{P}_{\mathbb{R}}^{d(d+3)/2} \setminus \Delta$ . If two curves  $C$  and  $C'$  are in the same rigid isotopy class, then they have the same topological type, but the converse is not true for  $d \geq 5$ , as shown by Kharlamov [48]. In the case of  $d = 5$ , there are 9 rigid isotopy types and therefore only one of the topological types appears in two different components of  $\mathbb{P}_{\mathbb{R}}^{20} \setminus \Delta$ . This is the type with 4 ovals and one pseudoline. The rigid isotopy classification of plane sextics was completed by Nikulin. It first appeared in his paper [68] on the arithmetic of real K3 surfaces.

This chapter presents an experimental study of the objects above for planar degree six curves, conducted with a view towards applied algebraic geometry. Numerous emerging applications, notably in the analysis of data from the life sciences, now rely on computational tools from topology and algebraic geometry. A long-term goal that motivated this project is the development of connections between such applications and existing knowledge on the topology of real algebraic varieties.

The ecosystem to be explored in this particular study is the 27-dimensional space of plane sextic curves. Our focus lies on experimentation and exact computation with ternary sextics over the integers. Thus, our model organisms are homogeneous polynomials in  $\mathbb{Z}[x, y, z]_6$ .

The following proposition shows one of the many new results and questions that can be derived by the computational framework developed in this chapter. It concerns reducible sextic curves consisting of six distinct lines. This 12-dimensional family in  $\mathbb{P}_{\mathbb{R}}^{27}$  is the *Chow variety* of factorizable forms.

**Proposition 2.4** *Configurations of six general lines appear in the closure of precisely 35 of the 64 rigid isotopy classes. These are the classes that meet the Chow variety in a generic point. These 35 classes are marked with an asterisk in Table 2.7, in the column on eigenvectors.*

The structure of this chapter is as follows. Section 2.1 is a discussion on the rigid isotopy classification for planar sextics. In Section 2.2 we describe methods for classifying a given ternary sextic according to Theorem 2.1.1. To determine the topological type we wrote fast code in **Mathematica** based on the built-in tool for *cylindrical algebraic decomposition* (CAD, [7]). This is used to sample sextics from natural probability distributions on  $\mathbb{R}[x, y, z]_6 \simeq \mathbb{R}^{28}$ , so as to find the empirical distributions on the 56 topological types. Distinguishing between dividing and non-dividing types is harder. Our primary tool for this is Proposition 2.4.2. For an alternative approach see [46]. In Section 2.3 we present a list of 64 polynomials in  $\mathbb{Z}[x, y, z]_6$  that serve as representatives for the 64 rigid isotopy types and we explain several constructions which we use to find the satisfactory representatives.

In Section 2.4, a method for computing the discriminant is presented and we discuss different types of discriminantal transitions. Moreover, we use the 64 polynomial exemplar and the discriminant to sample from each of the rigid isotopy types for our further experiments. Section 2.5 concerns the subdivision of the dual projective plane  $(\mathbb{P}^2)_{\mathbb{R}}^{\vee}$  by a curve  $C^{\vee}$  of degree 30, namely that dual to a given sextic  $C$ . The nodes of  $C^{\vee}$  are the 324 bitangents of  $C$ . We study how many of them are real for each of the 64 types. These numbers do not depend on the topological or rigid isotopy type alone. They are reported in Table 2.7. Real lines that miss  $C_{\mathbb{R}}$  form the avoidance locus  $\mathcal{A}_C$ . This is a union of up to 46 convex regions, bounded by the dual curve. In Section 2.6 we use our local samples to explore inflection points, tensor eigenvectors, real tensor rank and the final section briefly connects our studies on plane sextic curves to K3 surfaces.

### 2.1. The rigid isotopy classification of plane sextics

The discriminant of plane sextic curves is a hypersurface of degree 75 in  $\mathbb{P}_{\mathbb{R}}^{27}$  whose complement has 64 connected components. Therefore, there are 64 rigid isotopy types for smooth sextic curves in  $\mathbb{P}_{\mathbb{R}}^2$ . The following theorem summarizes both topological and rigid isotopy classifications for the plane sextics [88, §7].

**Theorem 2.1.1** (Rokhlin–Nikulin) *A degree six smooth plane curve consists of 0 to 11 ovals. It has 64 rigid isotopy types that are grouped into 56 topological types with the distribution that is shown in Table 2.1.*

ovals	0	1	2	3	4	5	6	7	8	9	10	11	all
topological types	1	1	2	4	4	5	6	7	8	9	6	3	56
rigid isotopy types	1	1	2	4	4	7	6	10	8	12	6	3	64

TABLE 2.1. Rokhlin–Nikulin classification of smooth sextics in the real projective plane. The first row is the number of ovals, the second and third rows are the counts of rigid isotopy and topological types corresponding to each number of ovals, respectively.

We denote the type of a smooth plane sextic  $C$  in  $\mathbb{P}_{\mathbb{R}}^2$  by (hyp) if  $C$  consists of three ovals, one nested in another and together they are inside the third oval (“hyp” stands for “hyperbolic”); by  $n$  if  $C$  consists of  $n$  empty ovals; and finally by  $(n1)m$  if  $C$  consists of an oval  $O$  with  $n$  empty ovals inside and of  $m$  further empty ovals lying outside it.

For an irreducible curve  $C$  in  $\mathbb{P}_{\mathbb{R}}^2$ , the set  $C_{\mathbb{C}} \setminus C_{\mathbb{R}}$  of non-real points in the Riemann surface has either one or two connected components. In other words, the real curve  $C_{\mathbb{R}}$  either divides the Riemann surface

$C_{\mathbb{C}}$  of real dimension two or not. The rigid isotopy type of a smooth plane sextic determines whether it is *dividing* or *non-dividing* and we denote it by  $d$  or  $nd$  in front of the topological type.

All but eight of the 56 topological types correspond to exactly one rigid isotopy class. Each of the following eight types consists of two rigid isotopy classes [68, p. 107], explaining the difference between the second row and third row of the table in Theorem 2.1.1:

$$(2.1) \quad (41) \quad (21)2 \quad (51)1 \quad (31)3 \quad (11)5 \quad (81) \quad (41)4 \quad 9.$$

These can be dividing or not, by [68, Remark 3.10.10]. There are six topological types that are necessarily dividing:

$$(2.2) \quad (91)1 \quad (51)5 \quad (11)9 \quad (61)2 \quad (21)6 \quad (\text{hyp}).$$

Finally, the remaining 42 types are all only non-dividing. Therefore, the subset of  $\mathbb{P}_{\mathbb{R}}^{27}$  consisting of all dividing sextics is the closure of the union of 14 rigid isotopy types appearing in (2.1) and (2.2). In Figure 2.5, which is a refinement of Viro's diagram in [85, Figure 4], the blue and red configurations are the non-dividing types and dividing types, respectively. Those 8 configurations that can be both dividing or non-dividing are colored in purple. Therefore each curve with the color red or blue corresponds to exactly one connected components of  $\mathbb{P}_{\mathbb{R}}^{27} \setminus \Delta$  while each of the purple ones corresponds to two. This accounts for all  $64 = 42 + 6 + 2 \times 8$  rigid isotopy types in Theorem 2.1.1.

For exploring these 64 components of  $\mathbb{P}_{\mathbb{R}}^{27} \setminus \Delta$ , it is important to understand their adjacencies. A general point in the discriminant  $\Delta$  is a sextic curve  $f$  that has precisely one ordinary node. If  $f$  is in the real locus  $\Delta_{\mathbb{R}}$ , then that node is a point in the real plane  $\mathbb{P}_{\mathbb{R}}^2$ . Two of the 64 types are connected by a *discriminantal transition* if there is a curve in the closure of both of the components having only one singular point which is an ordinary node.

All 56 topological types that are covering the whole 64 components, together form a poset, where the cover relation is either fusing two ovals or shrinking an oval until it vanishes (cf. Theorem 2.4.5). These relations are shown by the green line segments in Figure 2.5. Note the one to one correspondence between the maximal elements of this poset and the 6 types that can only be dividing. Apart from the type (hyp) which ruins the symmetry, if we exchange the inside and outside of the biggest oval in a configuration of Figure 2.5, the resulting type is the one obtained by vertical reflection with respect to the broken line.

For now we have an insight into the actions *shrinking* an oval, *fusing* two ovals, and *turning* an oval *inside out*, however, we have not yet mathematically defined them. The explicit definitions come in Section 2.4. Furthermore, in Theorem 2.4.4 we prove that any discriminantal transition corresponds to exactly one of these actions. Before that, we start with the experiments. We study the probability that each of the

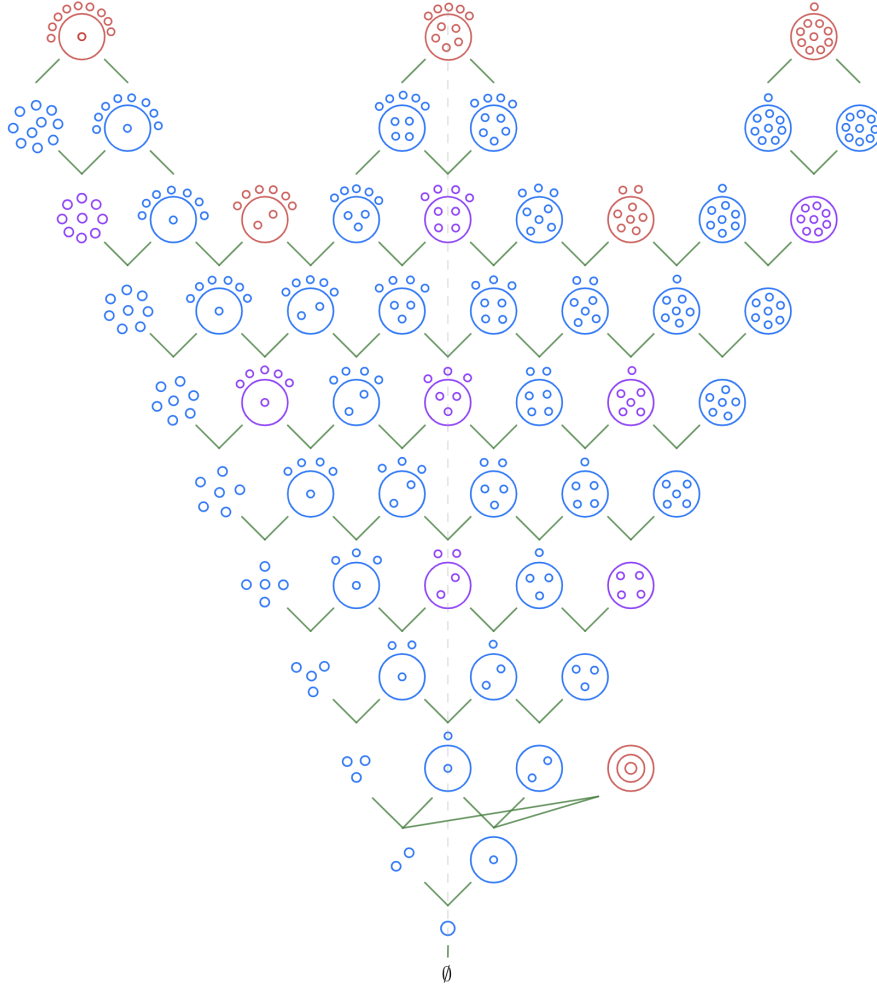


FIGURE 2.5. The 56 types of smooth plane sextics form a partially ordered set. The color code indicates whether the real curve divides its Riemann surface. The red curves are dividing, the blue curves are non-dividing, and the purple curves can be either dividing or non-dividing.

56 topological types will occur at random and afterwards we present representative polynomials, one for each 64 rigid isotopy components.

## 2.2. Classifier and empirical distributions

Given the equation of a plane curve how to find its topological type in  $\mathbb{P}_{\mathbb{R}}^2$ ? This problem is well-studied in computational geometry and the key idea is to construct isotopic graphs whose nodes are the singular and extreme points. Despite the existence of several methods and packages for this task, we wrote our own program based on the build-in quantifier elimination techniques of the software **Mathematica**. At the



end of this section we introduce some other methods and their drawbacks that motivated us to have our own specialized implementation for sextic curves in  $\mathbb{P}_{\mathbb{R}}^2$ .

For now, we first illustrate how our code works and then we use it to do some probabilistic study on the topological type of the sextic curves. In the following section, it is easy to observe that some of the representative polynomials are simpler than the other ones in terms of the size of their coefficients. Naturally, we have tried to present the simplest form that we could obtain for each type. By having a code to identify the topological type there are natural questions arising: Could we obtain all fifty-six types by randomly assigning reasonably small integers into the 28 coefficients of a general plane sextic? With different probability distributions, what is the chance that a specific topological type will occur in a large sample of randomly chosen sextics?

One advantage of our program that allows us to do the probabilistic experiments is its speed. For all sextics in Section 2.3, it terminates in less than four seconds and if the absolute value of the coefficients are smaller than  $10^8$ , then it takes less than one second. The entire code, which we called `SexticClassifier`, is written in `Mathematica` and is available on our supplementary materials website

(2.3) <https://software.mis.mpg.de/planeSexticCurves/index.html>.

The input to `SexticClassifier` is a homogeneous polynomial  $f$  of degree six in three variables  $x, y$ , and  $z$  with integer coefficients,  $f \in \mathbb{Z}[x, y, z]_6$ . At first, the code checks whether the curve that is defined by the polynomial  $f$  has singularities in  $\mathbb{P}_{\mathbb{C}}^2$  or not. If yes, then it returns “**Singular**” and if no then the output shows the topological type of the curve  $V_{\mathbb{R}}(f)$  in the real projective plane:

- **Empty** for the type with no ovals.
- **n** for the type with n empty ovals.
- **{1,1,1}** for the type (hyp) with three nested ovals.
- **{{n,1},m}** for the type (n1)m with n+m+1 ovals. This type consists of an oval with n empty ovals inside and m empty ovals outside it.

This covers the whole fifty-six topological types. The last case that could occur as the output is “**Please change the coordinates**”. This happens when the curve is smooth in  $\mathbb{P}_{\mathbb{C}}^2$  but its ovals in the real plane arrange a certain position that our code can not proceed. A linear transformation in the coordinates of  $f$  can change the exposition of the ovals without changing the topology of the real curve  $V_{\mathbb{R}}(f)$ .

We now explain how `SexticClassifier` works. After checking the smoothness, we start with setting  $z = 1$  in our input polynomial  $f \in \mathbb{Z}[x, y, z]_6$  so that the curve  $C := V_{\mathbb{R}}(f)$  is in the affine chart  $\mathbb{R}^2$

with coordinates  $x$  and  $y$ . Next we use the build-in function *Cylindrical Algebraic Decomposition* (CAD; see e.g. [5, 7]) of the curve  $C \subset \mathbb{R}^2$ . Our goal is to build up a graph  $G_C$  whose connected components are in one-to-one correspondence with the ovals of  $C$ , and furthermore, the final graph reveals the relative positions of the ovals.

To construct such a graph we project  $C$  into the  $x$ -axis. The nodes of  $G_C$  are the critical points of this projection. We draw an edge between the two nodes if the preimages of them is connected by an arc in  $C$ . The message “Please change the coordinates” is to avoid multiple preimages for a critical point. Having in mind that by restricting our curve to the affine chart  $\mathbb{R}^2$  we might lose the information of some components that are not compact in our choice of the chart, we add further edges corresponding to arcs crossing the line at infinity. Finally, by having the one-to-one correspondence between the ovals and the connected components of  $G_C$ , for each pair of ovals we have to find their relative positions. This is done by first checking whether the center of projection is inside or outside an oval and then looking at the parity of the number of branches of both ovals.

One of our goals for the future is to extend `SexticClassifier` so that it decides rapidly whether the curve is dividing or non-dividing. At present, our code is only determining the topological type of a given curve. Since out of fifty-six topological types, forty-eight of them each corresponds to a unique component of the  $\mathbb{P}_{\mathbb{R}}^{27}$  to extend our code for determining between ‘d’ and ‘nd’ we only need to check the types that appear in more than one connected components, namely the eight Nikulin [68] cases in (2.1). To find this, we need to build the Riemann surface  $V_{\mathbb{C}}(f)$  to see whether  $V_{\mathbb{C}}(f) \setminus V_{\mathbb{R}}(f)$  has one or two connected components. Kalla and Klein [46] developed and implemented a method for this verification, however, we found their code not suitable for curves of genus 10, which is the case that we are interested in.

Our first use of `SexticClassifier` is answering the question: “what is the probability that a particular topological type arises when we pick a sextic curve at random?”. This, of course, depends on the probability distribution that we choose on  $c_{ijk}$  in the equation of a general plane curve of degree six:

$$(2.4) \quad f = \sum_{i+j+k=6} c_{ijk} x^i y^j z^k.$$

We computed the empirical distributions of the topological types over the space of plane sextics. Recently, Lerario and Lundberg [61] did a theoretical study for curves of large degree. They employed the real Fubini-Study ensemble and the Kostlan distribution. Our experiments below are meant to inform this line of inquiry with some empirical probability distributions.

As the first experiment we take our sample space to be the set of all homogeneous polynomials as (2.4) where the 28 coefficients  $c_{ijk}$  are independently chosen from a univariate normal distribution, with center at 0 and with variance equal to  $6!/(i!j!k!)$ . This is the unique  $U(3)$ -invariant probability measure on  $\mathbb{R}[x, y, z]_6$  by [11, §16.1]. Table 2.2 shows the count of the topological types that appear by running **SexticClassifier** on 1,500,000 samples with this distribution.

Type	Evidences	Type	Evidences
0	127	(hyp)	1
1	875109	(31)	2
(11)	90316	(21)1	8
2	423099	(11)2	118
(21)	1180	4	7594
(11)1	4360	5	245
3	97834	6	7

TABLE 2.2. Counts of topological types appearing in a sample of 1,500,000 randomly chosen sextics with the  $U(3)$ -invariant distribution

The result shows that the empirical distribution is very skewed:

- In total, only 14 of the 56 types were observed.
- Only six types had an empirical probability of  $\geq 1\%$ .
- No type with more than six ovals was observed.
- The average number of connected components is approximately 1.50.
- The average *energy* is approximately 2.99.

Another numerical invariant of the topological type of a smooth real plane curve is the *energy*. This nonnegative integer, which was introduced in [61, page 8], measures the nesting of the ovals. For curves of degree six, the maximal energy is 38 and attained by the Harnack-type curve (91)1. The average energy that we observe in our sample of 1,500,000 sextics is considerably smaller.

We expand our experiment to several distributions on  $\mathbb{R}[x, y, z]_6$ . We sample 500,000 random sextics with each probability distribution. After running **SexticClassifier** on our samples, we ignore the types with empirical probability less than 0.01% and report the appearance-percentage of the rest in the following tables.

Table 2.3 shows the largest variety of types with the most number of ovals that appears among our considered distributions. In this experiment, we sample sextics of the form  $\det(xA + yB + zC)$  where  $A, B$

and  $C$  are symmetric  $6 \times 6$ -matrices with entries uniformly distributed random integers with absolute value less than 1000. Some types appear with this probability distribution that did not show up among the 1,500,000 samples in Table 2.2. This is also the only distribution in our experiments where the most common type is not the sextic consisting of only one oval. The type (11)3 is our unique observation of nesting in a type with more than four ovals.

Type	Probability	Type	Probability
1	16.44%	(21)1	0.12%
(11)	8.02%	(11)2	0.98%
2	29.12%	4	11.06%
(21)	1.19%	(11)3	0.13%
(11)1	4.30%	5	2.46%
3	25.77%	6	0.30%
(31)	0.07%	7	0.02%

TABLE 2.3. Sextics that are determinants of random symmetric matrices with linear entries

Our most skewed distribution appears when we are restricting to sextics of real rank 10, the case considered in [66, §6]. Here we sample signed sums (with the signs chosen uniformly at random) of ten sixth powers of linear forms whose coefficients are uniformly distributed integers with absolute values less than 1000. More than 90% of the samples are of the type consisting of only one oval. Table 2.4 shows the result for this distribution. Furthermore, it reveals that if we pass to eleven and twelve summands, no more type will show up. Although, we observe that by increasing the number of summands, the percentage of types with zero or one ovals decreases while the appearance of other three types increases.

Type \ n	10	11	12
0	5.14%	4.75%	4.28%
1	90.17%	89.95%	89.90%
(11)	0.09%	0.12%	0.15%
2	4.50%	5.06%	5.53%
3	0.09%	0.12%	0.15%

TABLE 2.4. Probability of sextics that are signed sums of  $n$  sixth powers of linear forms

In our last two experiments with random sextics, the coefficients are uniformly distributed integers with absolute value smaller than  $10^{12}$ .

Table 2.5 shows the general result if we sample our sextics in this way and in Table 2.6 we see the empirical distribution obtained from sampling only symmetric sextics, i.e. linear combinations of the monomial symmetric polynomials of degree six. By restricting our random sample to symmetric sextics, the variety of types increases from 6 to 10. The type consisting of seven empty ovals appears as a random symmetric sextic, however, it was not among 1,500,000 sextics in our first  $U(3)$ -invariant distribution. Another interesting observation is that Table 2.6 is the only one missing the type consisting of two empty ovals.

Type	Probability	Type	Probability
0	0.66%	2	18.19%
1	77.52%	3	2.11%
(11)	1.46%	4	0.06%

TABLE 2.5. Sextics with uniformly distributed integer coefficients of absolute value  $\leq 10^{12}$

Type	Probability	Type	Probability
0	28.38%	(31)	0.03%
1	45.69%	4	2.17%
(11)	7.40%	(11)3	0.03%
3	16.15%	6	0.13%
(hyp)	0.01%	7	0.01%

TABLE 2.6. Symmetric sextics with uniformly distributed integer coefficients of absolute value  $\leq 10^{12}$

The experiments with four large sets of samples and different probability distributions demonstrate that it is extremely rare to observe topological types consisting of more than four ovals when sextic curves are generated at random. Only 15 out of 56 types occurred in our samples and we never encountered a sextic with 8, 9, 10 or 11 ovals. This underlines the importance of having the representatives listed in Section 2.3. Our sixty-four explicit polynomials in  $\mathbb{Z}[x, y, z]_6$  allow us to do local sampling for further experiments on different properties of each type in  $\mathbb{P}_{\mathbb{R}}^2$ . Section 2.6 covers all the results for our local experiments.

The program enabling us to obtain the above results, not only needed to be reasonably fast, but also had to handle other sort of difficulties with the non-compactness of a randomly generated curve. Our first attempt was trying several existing algorithms ([16, 24, 33, 78]) given by many authors including Nicola Wolpert, Raimund

Seidel, Hoon Hong, M’hammed El Kahoui, Ioana Necula, Laureano González-Vega, Elias Tsigaridas, Fabrice Rouillier, Luis Peñaranda, Marc Pouget, Sylvain Lazard, and Jinsan Cheng.

The main idea of building the corresponding graph for each type is the same in all methods, including ours in `SexticClassifier`. The algorithm in [16] is called `ISOTOP`. It uses certain `C` packages and is implemented in `Maple`. For comparisons between `ISOTOP` and `Top`, as well as with `INSULATE`, `AlciX` [24], and `Cad2d` [7], we refer to [16, Table 1, page 28]. The implementation of the last two is in `C++`.

After first experiments with these packages, it was not obvious how to extract the topological type of the curve in  $\mathbb{P}_{\mathbb{R}}^2$  from the output with a reasonable amount of coding effort since all of them are restricted to the affine chart  $\{z = 1\}$ . It is not hard to imagine that some of our samples are not compact in this affine chart. On the other hand, although curves of even degrees consist of only ovals, it is not true that they can be compact after some linear transformation of the coordinates. More precisely, unlike curves of degrees two and four, there are real plane sextics that any line in  $\mathbb{P}_{\mathbb{R}}^2$  will intersect them. Here is an example of such curve. More details on this topic will show up in Section 2.5 where we define the *avoidance locus*.

**Example 2.2.1** Let  $f$  be the following polynomial of degree six:

$$\begin{aligned} 7(x+y+2z)(x+2y+z)(2x+y+z)(x-2y+3z)(y-2z+3x)(z-2x+3y) \\ + xyz(x^3+y^3+z^3). \end{aligned}$$

The input to `SexticClassifier` is the polynomial  $f$  and the output is the label 3. This means, after checking that the complex curve  $V_{\mathbb{C}}(f)$  has no singularities in  $\mathbb{P}_{\mathbb{C}}^2$ , our code reveals that the real curve  $V_{\mathbb{R}}(f)$  consists of three empty ovals and therefore has no nesting. Since the topological type of  $V_{\mathbb{R}}(f)$  is not in (2.2) or (2.1), `SexticClassifier` shows that the real curve  $V_{\mathbb{R}}(f)$  is not dividing the Riemann surface defined by  $f$ . Every real line in  $\mathbb{P}_{\mathbb{R}}^2$  meets  $V_{\mathbb{C}}(f)$  in at least one real point, regardless of which line serves as the line at infinity. Thus, the real curve  $V_{\mathbb{R}}(f)$  is not compact in any affine chart of  $\mathbb{P}_{\mathbb{R}}^2$ .

Apart from the speed, our main reason to have our own specialized implementation to determine the topological type of a given degree six curve was to include such “non-compactible” curves. `SexticClassifier` has been designed to handle them well. The vast experiments that we did using our code demonstrate that to build most of the types certain constructions, to be provided in the following section, are needed as they will not appear at random.

### 2.3. Examples of polynomials and their constructions

We list sixty-four polynomials with integer coefficients that represent sixty-four rigid isotopy types of smooth sextic curves in  $\mathbb{P}_{\mathbb{R}}^2$ .

**SexticClassifier** helped us to verify the correctness of our polynomial list. An algorithm for sampling from the connected components of  $\mathbb{P}_{\mathbb{R}}^{27} \setminus \Delta$  using our representatives is presented in Section 2.4.

Afterwards, we explain the constructions and give some explicit examples of how we find the representatives. Each sextic is labeled by its topological type and an indicator d or nd showing whether it is a dividing or a non-dividing type. This list is available in a computer-algebra-friendly format at (2.3).

Types with less than four ovals are all non-dividing:

One type with no ovals:

$$0 \quad \text{nd} \quad x^6 + y^6 + z^6$$

One type with only one oval:

$$1 \quad \text{nd} \quad x^6 + y^6 - z^6$$

Two types with two ovals:

$$(11) \quad \text{nd} \quad 6(x^4 + y^4 - z^4)(x^2 + y^2 - 2z^2) + x^5y$$

$$2 \quad \text{nd} \quad (x^4 + y^4 - z^4)((x + 4z)^2 + (y + 4z)^2 - z^2) + z^6$$

One of the types with three ovals, namely (hyp) appears in the maximal elements of the poset in Figure 2.5, therefore it can be only dividing. The other three are non-dividing. Four types with three ovals:

$$(21) \text{ nd} \quad 16((x + z)^2 + (y + z)^2 - z^2)(x^2 + y^2 - 7z^2)((x - z)^2 + (y - z)^2 - z^2)x^3y^3$$

$$(11)1 \text{ nd} \quad ((x + 2z)^2 + (y + 2z)^2 - z^2)(x^2 + y^2 - 3z^2)(x^2 + y^2 - z^2) + x^5y$$

$$3 \quad \text{nd} \quad (x^2 + y^2 - z^2)(x^2 + y^2 - 2z^2)(x^2 + y^2 - 3z^2) + x^6$$

$$(\text{hyp}) \quad \text{d} \quad 6(x^2 + y^2 - z^2)(x^2 + y^2 - 2z^2)(x^2 + y^2 - 3z^2) + x^3y^3$$

Four types with four ovals, all non-dividing:

$$(31) \quad \text{nd} \quad (10(x^4 - x^3z + 2x^2y^2 + 3xy^2z + y^4) + z^4)(x^2 + y^2 - z^2) + x^5y$$

$$(21)1 \quad \text{nd} \quad (10(x^4 - x^3z + 2x^2y^2 + 3xy^2z + y^4) + z^4)((x + z)^2 + y^2 - 2z^2) + x^5y$$

$$(11)2 \quad \text{nd} \quad (10(x^4 - x^3z + 2x^2y^2 + 3xy^2z + y^4) + z^4)(x^2 + (y - z)^2 - z^2) + x^5y$$

$$4 \quad \text{nd} \quad x^6 + y^6 + z^6 - 4x^2y^2z^2$$

There are only five topological types with five ovals. Two types, namely (41) and (21)2 can be both dividing or non-dividing. Therefore, there are seven rigid isotopy types with five ovals:

$$\begin{aligned}
(41) \quad \text{nd} \quad & (x^2 + 3y^2 - 20z^2)(4x^2 + y^2 - 16z^2) + 18x^2z^2)(x^2 + y^2 - 10z^2) - 2z^6 \\
(41) \quad \text{d} \quad & 10(((x^2 + 2y^2 - 16z^2)(2x^2 + y^2 - 16z^2) + x^2y^2)(10x + y + 5z) + xz^4)(10x \\
& \quad - y - 8z) - xz^5 \\
(31)1 \quad \text{nd} \quad & ((x^2 + 3y^2 - 17z^2)(3x^2 + y^2 - 10z^2) + 15x^2z^2)(x^2 + 4(y + z)^2 - 25z^2) \\
& \quad + x^3y^3 \\
(21)2 \quad \text{nd} \quad & ((x^2 + 3y^2 - 20z^2)(4x^2 + y^2 - 16z^2) + 18x^2z^2)((x + y)^2 + 20(x - y \\
& \quad - 3z)^2 - 24z^2) + (y - x)z^5 \\
(21)2 \quad \text{d} \quad & ((x^2 + 3y^2 - 20z^2)(4x^2 + y^2 - 16z^2) + 18x^2z^2)(x^2 + 8y^2 - 16z^2) - 4z^6 \\
(11)3 \quad \text{nd} \quad & ((x^2 + 2y^2 - 30z^2)(3x^2 + y^2 - 20z^2) + 15x^2z^2)(x^2 + (4y + 16z)^2 - 15z^2) \\
& \quad + x^3y^3 \\
5 \quad \text{nd} \quad & 4((x^2 + 2y^2 - 4z^2)(2x^2 + y^2 - 4z^2) + z^4)(x^2 + y^2 - z^2) + x^3y^3
\end{aligned}$$

Six types with six ovals, all non-dividing:

$$\begin{aligned}
(51) \quad \text{nd} \quad & (3x^2 + 4xy + 2y^2 - 4z^2)(x^2 + 2(y - z)^2 - 8z^2)(2x^2 + y^2 - 3z^2) - z^6 \\
(41)1 \quad \text{nd} \quad & (4x^2 + 6x(y - z) + 3(y - z)^2 - 14z^2)(x^2 + 5(y - 2z)^2 - 9z^2)(2x^2 \\
& \quad + (y - z)^2 - 15z^2) - yz^5 \\
(31)2 \quad \text{nd} \quad & ((x + z)^2 + 4y^2 - 4z^2)(7(x + z)^2 + y^2 - 10z^2)((x + z)^2 + 4(2(x + y) \\
& \quad + 3z)^2 - 8z^2) + xz^5 \\
(21)3 \quad \text{nd} \quad & ((x + z)^2 + 3y^2 - 4z^2)(7(x + z)^2 + y^2 - 12z^2)((x + z)^2 + 3(2(x + y) \\
& \quad + 3z)^2 - 5z^2) + xz^5 \\
(11)4 \quad \text{nd} \quad & ((x^2 + 3y^2 - 20z^2)(4x^2 + y^2 - 16z^2) + 18x^2z^2)(8x^2 + y^2 - 16z^2) \\
& \quad + (x + y)z^5 \\
6 \quad \text{nd} \quad & (3x^2 + 5xy + 2y^2 - 7z^2)(x^2 + 2(y - z)^2 - 8z^2)(2x^2 + y^2 - 5z^2) - z^6
\end{aligned}$$

There are seven topological types with seven ovals. Three types, namely (51)1, (31)1, and (11)5 can be both dividing or non-dividing. Therefore, there are ten rigid isotopy types with seven ovals:

$$\begin{aligned}
(61) \quad \text{nd} \quad & (4x^2 + 4xy + 3y^2 - 4z^2)(x^2 + 3y^2 - 4z^2)(4x^2 + y^2 - 4z^2) - z^6 \\
(51)1 \quad \text{nd} \quad & 30(((x - z)^2 + 3y^2 - 5z^2)(3(x - z)^2 + y^2 - 5z^2) + xz^3)((x - z)^2 + y^2 \\
& \quad - 2z^2) + (x - 2z)z^5
\end{aligned}$$



$$\begin{aligned}
(51)1 \quad d \quad & 7((x^2 + 3(y+z)^2 - 48z^2)(3(x+z)^2 + y^2 - 48z^2) - z^4)(x^2 + y^2 - 26z^2) + xz^5 + yz^5 \\
(41)2 \quad nd \quad & 15(4x^2 + y^2 - 3z^2)(x^2 + 3y^2 - 3z^2)((4x-z)^2 + 16y^2 - 22z^2) + (5xz^5 + (y-z)^3z^3) \\
(31)3 \quad nd \quad & 34((3x^2 + y^2 - 3z^2)(x^2 + 8y^2 - 3z^2) + x^2y^2)(2x^2 - yz - 2z^2) + (x-4z)yz^4 \\
(31)3 \quad d \quad & ((x^2 + 3y^2 - 28z^2)(4x^2 + y^2 - 20z^2) - z^4)((x+z)^2 + y^2 - 12z^2) - xz^5 \\
(21)4 \quad nd \quad & 27(2xz - 6y^2 + 2yz + 3z^2)(-(x+y)^2 - 4y^2 + 2z^2)(5(x+y)^2 + y^2 - 4z^2) - xz^5 \\
(11)5 \quad nd \quad & ((x^2 + 3y^2 - 20z^2)(4x^2 + y^2 - 16z^2) + 18x^2z^2)(16x^2 + y^2 - 20z^2) - (x+y)z^5 \\
(11)5 \quad d \quad & ((x^2 + 3y^2 - 20z^2)(4x^2 + y^2 - 16z^2) + 18x^2z^2)((x+y)^2 + 20(x-y-3z)^2 - 24z^2) + (x+y)z^5 \\
7 \quad nd \quad & 2(4x^2 + y^2 - 4z^2)(x^2 + 4y^2 - 5z^2)(x^2 + y^2 - 4z^2) + 3x^4y^2 + xy^5
\end{aligned}$$

Eight types with eight ovals, all non-dividing:

$$\begin{aligned}
(71) \quad nd \quad & 2(x^2 + y^2 - 26z^2)(x^2 + 3(y+z)^2 - 48z^2)(3(x+z)^2 + y^2 - 48z^2) - z^6 \\
(61)1 \quad nd \quad & (160075(5yz - x^2)(8(xz + 15z^2) - (y - 12z)^2) + 109(17x + 5y + 72z)(13x + 5y + 42z)(9x + 5y + 20z)(2x + 5y))(5yz - x^2) - (x + 3z)z^5 \\
(51)2 \quad nd \quad & (5435525((y+z)z - x^2)((x+2z)z - 2(y-x)^2) + 5(25x - 25y - 31z)(5x - 50y - 49z)(15x + 25y + 27z)(35x + 25y + 37z))((y+z)z - x^2) + x^5y \\
(41)3 \quad nd \quad & (14460138((y+z)z - x^2)((x+2z)z - 2(y-x)^2) + 5(25x - 25y - 31z)(5x - 50y - 49z)(15x + 25y + 27z)(37z + 35x + 25y))((y+z)z - x^2) + x^5y \\
(31)4 \quad nd \quad & (27867506((y+z)z - x^2)((x+2z)z - 2(y-x)^2) + 61(6x + 8y + 9z)(64y + 63z)(15x - 25y - 27z)(35x - 25y - 37z))((y+z)z - x^2) + x^5y \\
(21)5 \quad nd \quad & 40(3x^2 + y^2 - 3z^2)(x^2 + 8(y-z)^2 - 3z^2)(2x^2 - yz - 2z^2) - y^3z^3 - 2xz^5 + 2z^6 \\
(11)6 \quad nd \quad & 19(4x^2 + y^2 - 4z^2)(x^2 + 8(y-z)^2 - 3z^2)(2x^2 - yz - 2z^2) - (2y - 3z)z^5 \\
8 \quad nd \quad & 12(x^4 + 2x^2y^2 + y^4 - x^3z + 3xy^2z)(7(8x + 3z)^2 + 8y^2 - 10z^2) + x^5y + 2z^6
\end{aligned}$$

There are nine topological types with nine ovals, three of which namely (51)1, (31)1, and (11)5 can be both dividing or non-dividing. The two

types (61)2 and (21)6 are maximal elements in the poset in Figure 2.5 and they are only dividing. Twelve rigid isotopy types with eight ovals:

- (81) nd  $(1920981(yz - x^2)(57(x+z)z - (6x - y + 6z)^2) + 48(10x + 7y + 3z)(11x + 25y + z)(11x - 23y - z)(10x - 8y - 3z))(x^2 - yz) + x^2y^4 - 61y^6$
- (81) d  $((x^2 + 3y^2 - 28z^2)(4x^2 + y^2 - 20z^2) - z^4)(2x^2 + y^2 - 12z^2) - z^6$
- (71)1 nd  $(529321083(yz - x^2)(53(x+z)z - (6x - y + 6z)^2) + 25(10x + 8y + 3z)(12x + 30y + z)(12x - 32y - z)(10x - 8y - 3z))(x^2 - yz) - y^6$
- (61)2 d  $(19157935(5yz - x^2)(8(xz + 15z^2) - (y - 12z)^2) + 1185(17x + 5y + 72z)(13x + 5y + 42z)(9x + 5y + 20z)(2x + 5y))(5yz - x^2) - (x + 3z)z^5$
- (51)3 nd  $(28920269((y+z)z - x^2)((x+2z)z - 2(y-x)^2) + 10(25x - 25y - 31z)(5x - 50y - 49z)(15x + 25y + 27z)(35x + 25y + 37z))((y+z)z - x^2) + x^5y$
- (41)4 nd  $6761249083262(68794627464(1095368(118(x^2 + y^2 - 3z^2)y + (x - 2z)(x - 12z)(x - 13z))y + (x - 4z)(x - 9z)(x - 10z)(x - 11z))y + (x - 3z)(x - 5z)(x - 6z)(x - 7z)(x - 8z))y - z^6$
- (41)4 d  $13278270242890(52982089012(1610519(149(x^2 + y^2 - 4z^2)y + (x - 3z)(x - 13z)(x - 14z))y + (x - 5z)(x - 10z)(x - 11z)(x - 12z))y + (x - 4z)(x - 6z)(x - 7z)(x - 8z)(x - 9z))y - (x - 5z)z^5$
- (31)5 nd  $(26894836459((y+z)z - x^2)((x+2z)z - 2(y-2x)^2) + 1880(6x + 8y + 9z)(64y + 63z)(15x - 25y - 27z)(35x - 25y - 37z))((y+z)z - x^2) + x^5y$
- (21)6 d  $(93678589978((y+z)z - x^2)((x+2z)z - 2(y-2x)^2) + 50949(6x + 8y + 9z)(18x - 72y - 73z)(5x - 6y - 7z)(-27x + 18y + 28z))((y+z)z - x^2) + x^5y$
- (11)7 nd  $23(3x^2 + y^2 - 3z^2)(x^2 + 8(y-z)^2 - 3z^2)(2x^2 - yz - 2z^2) - (2y - 3z)z^5$
- 9 nd  $((x^2 + 3y^2 - 20z^2)(4x^2 + y^2 - 16z^2) + 18x^2z^2)((x+y)^2 + 20(x-y-3z)^2 - 24z^2) + y^2z^4$
- 9 d  $((x^2 + 3y^2 - 20z^2)(4x^2 + y^2 - 16z^2) + 18x^2z^2)(16x^2 + y^2 - 20z^2) + z^6$

Six types with ten ovals, all non-dividing:

- (91) nd  $(40008(yz - x^2)(57(x+z)z - (6x - y + 6z)^2) + (10x + 7y + 3z)(11x + 25y + z)(11x - 23y - z)(10x - 8y - 3z))(x^2 - yz) - y^6$
- (81)1 nd  $(622771068(yz - x^2)(57(x+z)z - (6x - y + 6z)^2) + 35(10x + 8y + 3z)(12x + 30y + z)(12x - 32y - z)(10x - 8y - 3z))(x^2 - yz) - y^6$

$$\begin{aligned}
(51)4 \text{ nd} \quad & -3401397120x^6 - 3195251840x^5y - 2164525440x^4y^2 - 869728640x^3y^3 \\
& + 332217600x^2y^4 + 316096000xy^5 + 53760001y^6 + 1597625920x^5z \\
& + 10^{11} \times 368484688x^4yz + 10^{11} \times 79881296x^3y^2z - 10^{11} \times 33732864x^2y^3z \\
& + 10^{11} \times 38247616xy^4z + 10^{23} \times 234256y^4z^2 - 1199390720x^4z^2 \\
& - 10^{11} \times 79881296x^3yz^2 - 10^{21} \times 127552392x^2y^2z^2 + 10^{12} \times 1618496y^5z \\
& + 764952320x^3z^3 + \frac{10^{31} \times 14172488y^3z^3}{10^{11} \times 36543936x^2yz^3} + 10^{11} \times 36543936x^2yz^3 \\
& - 10^{11} \times 38247616xyz^4 - 130099200x^2z^4 + 10^{23} \times 117128y^2z^4 \\
& + 10^{12} \times 650496yz^5 - 2z^6 \\
(41)5 \text{ nd} \quad & -3401397120x^6 - 3195251840x^5y - 2164525440x^4y^2 - 869728640x^3y^3 \\
& + 332217600x^2y^4 + 316096000xy^5 + 53760002y^6 + 1597625920x^5z \\
& + 10^{11} \times 368484688x^4yz + 10^{11} \times 79881296x^3y^2z - 10^{11} \times 33732864x^2y^3z \\
& + 10^{11} \times 38247616xy^4z + 10^{12} \times 1618496y^5z - 1199390720x^4z^2 \\
& - 10^{11} \times 79881296x^3yz^2 - 10^{21} \times 127552392x^2y^2z^2 + 10^{23} \times 234256y^4z^2 \\
& + 764952320x^3z^3 + 10^{11} \times 36543936x^2yz^3 - 10^{11} \times 38247616xyz^4 \\
& - 130099200x^2z^4 + \frac{10^{31} \times 14172488y^3z^3}{10^{11} \times 36543936x^2yz^3} + 10^{23} \times 117128y^2z^4 \\
& + 10^{12} \times 650496yz^5 - z^6 \\
(11)8 \text{ nd} \quad & (227693(yz - x^2)((x + 2z)z - 2(y - 2z)^2) + (10x - 8y - 3z)(10x - 23y \\
& - z)(11x + 22y + z)(10x + 7y + 3z))(x^2 - yz) + y^6 \\
10 \text{ nd} \quad & 19x^6 - 20x^4y^2 - 20x^2y^4 + 19y^6 - 20x^4z^2 + 60x^2y^2z^2 - 20y^4z^2 \\
& - 20x^2z^4 - 20y^2z^4 + 19z^6
\end{aligned}$$

Finally, there are three types with the maximum number of ovals and they are all dividing:

$$\begin{aligned}
(91)1 \text{ d} \quad & (1941536164(yz - x^2)(60(x + z)z - (6x + 6z - y)^2) + 118(10x + 8y \\
& + 3z)(12x + 32y + z)(12x - 32y - z)(10x - 8y - 3z))(x^2 - yz) - y^6 \\
(51)5 \text{ d} \quad & -3401397120x^6 - 3195251840x^5y - 2164525440x^4y^2 - 869728640x^3y^3 \\
& + 332217600x^2y^4 + 316096000xy^5 + 53760001y^6 + 1597625920x^5z \\
& + 10^{11} \times 368484688x^4yz + 10^{11} \times 79881296x^3y^2z - 10^{11} \times 33732864x^2y^3z \\
& - 130099200x^2z^4 - 1199390720x^4z^2 - 10^{11} \times 79881296x^3yz^2 \\
& - 10^{21} \times 127552392x^2y^2z^2 + 10^{23} \times 234256y^4z^2 + 764952320x^3z^3 \\
& + 10^{11} \times 36543936x^2yz^3 + \frac{10^{31} \times 14172488y^3z^3}{10^{11} \times 36543936x^2yz^3} + 10^{11} \times 38247616xyz^4 \\
& + 10^{12} \times 1618496y^5z - 10^{11} \times 38247616xyz^4 + 10^{23} \times 117128y^2z^4 \\
& + 10^{12} \times 650496yz^5 - z^6 \\
(11)9 \text{ d} \quad & (340291(yz - x^2)((x + 2z)z - 2(y - 2z)^2) + (10x - 8y - 3z)(12x \\
& - 27y - z)(12x + 28y + z)(10x + 7y + 3z))(x^2 - yz) + y^6
\end{aligned}$$

After furnishing explicit polynomial representatives, now we can derive the following result.

**Proposition 2.3.1** *Each of the 64 rigid isotopy types can be realized by a ternary sextic in  $\mathbb{Z}[x, y, z]_6$  whose integer coefficients have absolute value less than  $1.5 \times 10^{38}$ .*

The absolute value of the underlined coefficients is the closest to the bound  $1.5 \times 10^{38}$  in the proposition above. Our criterion for the desirable representative polynomial  $f$  are smoothness of  $V_{\mathbb{C}}(f)$  and having integer coefficients of small size. Let  $f$  be a polynomial of degree six as in (2.4). We say  $f$  is *optimal* if its complex curve  $V_{\mathbb{C}}(f)$  is smooth and its coefficients  $c_{ijk}$  are integers with minimal infinite norm. i.e, we attempt to minimize the largest absolute value  $|c_{ijk}|$  among all curves in the same rigid isotopy class. The simplest example is the Fermat sextics  $x^6 + y^6 \pm z^6$ . Four more examples of optimal representations are:

$$\begin{aligned}
(11) \quad \text{nd} \quad & x^5y + x^5z + x^4y^2 + x^4yz - x^3y^3 + x^3yz^2 - x^3z^3 - x^2y^4 + x^2y^3z + x^2y^2z^2 - x^2yz^3 \\
& + x^2z^4 - xy^4z + xy^3z^2 - xyz^4 + xz^5 - y^5z - y^4z^2 + y^3z^3 + y^2z^4 - yz^5 - z^6 \\
2 \quad \text{nd} \quad & x^6 - x^5y - x^5z - x^4yz + x^3y^3 + x^3yz^2 - x^2y^4 - x^2y^2z^2 + xy^4z \\
& - xy^3z^2 - xy^2z^3 - xyz^4 + y^6 + y^5z + y^4z^2 + y^3z^3 - yz^5 + z^6 \\
3 \quad \text{nd} \quad & x^6 - x^5y - x^4y^2 + x^4z^2 + x^3y^3 + x^3y^2z + x^3yz^2 + x^2y^3z - x^2y^2z^2 + x^2yz^3 + x^2z^4 \\
& + xy^4z + xy^3z^2 + xy^2z^3 + xyz^4 - xz^5 + y^6 + y^5z + y^4z^2 - y^2z^4 - yz^5 + z^6 \\
4 \quad \text{nd} \quad & -x^6 + x^5y + x^4y^2 - x^3y^3 + x^2y^4 + xy^5 - y^6 + x^5z + x^4yz + xy^4z \\
& + y^5z + x^4z^2 + y^4z^2 - x^3z^3 - y^3z^3 + x^2z^4 + xyz^4 + y^2z^4 + xz^5 + yz^5 - z^6
\end{aligned}$$

Although, these types might have shorter representatives, minimizing the number of monomials is not part of our criterion. In all four representatives, the largest absolute value of the coefficients is one and therefore they are optimal.

To find such optimal representatives, one approach is to start with all 28 integers  $c_{ijk}$  being zero or  $\pm 1$ , and slowly increase the range and check which types will appear. More precisely, we sample at random from sextics with  $|c_{ijk}| \in \{0, 1, \dots, m\}$  starting with  $m = 1$  and increase it one by one. The most frequent types in Table 2.2 could be constructed in this way, however, this approach is not useful for constructing the vast majority of types. As we have seen in our experiments in the previous section, most of the types are extremely rare to happen at random even without the restriction of the small coefficients. Note that the four types listed above appear when we set  $m = 1$ .

To construct our list of 64 representatives, we relied on different methodologies. Many types could be obtained by perturbing singular curves that are the union of three smooth conics intersecting transversally. Figure 2.2 shows that if we perturb a unique singular curve which is the union of two smooth conics intersecting transversally, we obtain all topological types of plane quartics.

Such a unique singular curve does not exist in the case of plane sextics. Although, varying the manner of transversal intersections in the union of three smooth quadratics and perturbing the resulting singular curve, result in all of the types with less than nine ovals. Several types

with more ovals can be constructed in this way as well. This is not hard to find these representatives in our list since we did not expand the multiplication of our quadratics in the final polynomial. Figure 2.6 shows two examples of such construction. Let

$$f = (x^2 + 2y^2 - z^2)(2x^2 + y^2 - z^2)(x^2 + 8y^2 - 2z^2) \pm \epsilon z^6.$$

If  $\epsilon = 0$  then  $V_{\mathbb{R}}(f)$  is the red curve and a small enough choice of  $\epsilon > 0$ , results in the two smooth blue sextics.

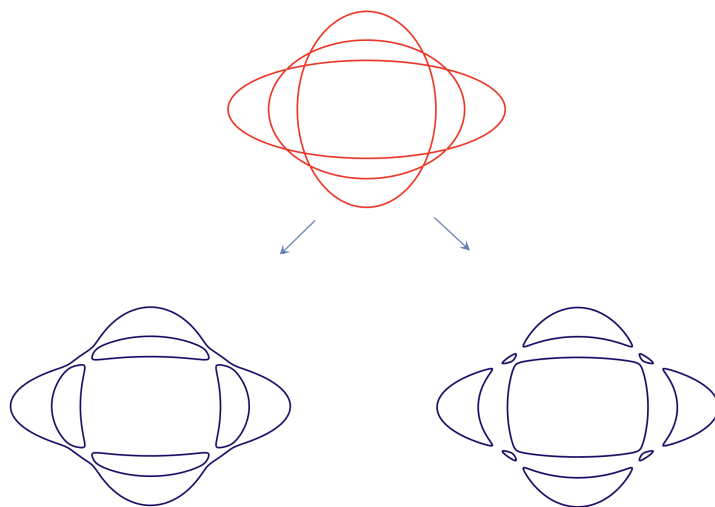


FIGURE 2.6. Many of the 56 topological types can be obtained by perturbing the union of three smooth quadrics intersecting transversally.

Later we present an important example of this construction with 10 ovals. The curve in Figure 2.12 is notable since any line in  $\mathbb{P}_{\mathbb{R}}^2$  intersects it in at least one point. We briefly explained this property in Example 2.2.1 where we had a sextic of Type 3. The complete discussion on this topic will come in Section 2.5.

For all other types, except the three types having underlined coefficients, we carried out the classical constructions of Harnack and Hilbert, as explained by Gudkov [35]. We start with two quadratics intersecting in four real points, pick eight points on the curves, and perturb the reducible quartic with the product of four lines through these points. The smooth quartic is intersected with one of the original quadratics and perturbed again to get a smooth sextic. The different ways in which the original curves and the points on them are selected give the different types.

For the construction of types (51)5, (51)4, and (41)5 we tried Gudkov's method but found it too complicated to carry out explicitly. For them, we employed the most recent method for constructing real varieties with prescribed topology, namely, Viro's *patchworking*

*method* [85]. All 56 topological types of smooth sextics can be realized by a version of patchworking known as *combinatorial patchworking*, which can also be interpreted in the language of tropical geometry.

In this method, one records the signs of the 28 coefficients  $c_{ijk}$  and represents their magnitudes by a regular triangulation of the Newton polygon. Transitioning from that representation to actual polynomials in  $\mathbb{Z}[x, y, z]_6$  yields integer coefficients  $c_{ijk}$  whose absolute values tend to be very large. We experimented with some of these sextics, but in the end we abandoned them for all but three types, because symbolic computation became prohibitively slow.

Although the constructions above enabled us to build our fifty-six topological types, yet it is remained to distinguish between dividing and non-dividing curves for the Nikulin cases (2.1). We followed Fiedler [29, §2] for this purpose. We start with the union of two smooth curves of degrees  $d_1$  and  $d_2$ , with prescribed orientations, in a way that they transversally intersect in  $d_1 \cdot d_2$  real points. Small perturbations of this reducible curve can lead to a smooth plane curve. Depending on how is the perturbation of the curve at the singular points, one can decide whether it is dividing or non-dividing as follows.

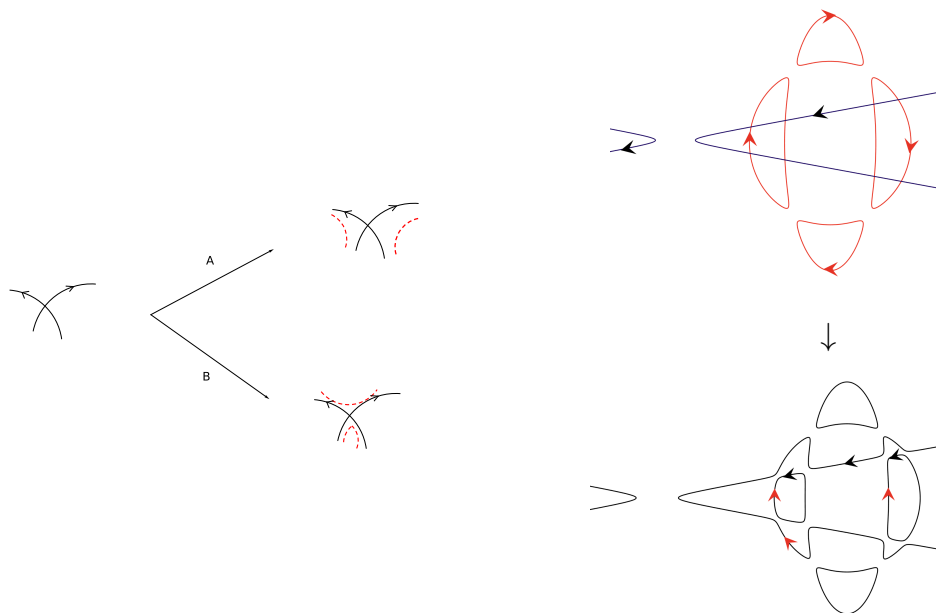


FIGURE 2.7. Using local perturbations to create sextics that are dividing or non-dividing

If the singular point is smoothen such that the two orientations agree on the final curve, it is called type A and otherwise type B. If *all* intersections are perturbed either using only A or using only B then it is dividing. However, if the smoothening is done via A at some crossings and via B at other crossings, then the resulting smooth curve does not divide its Riemann surface. Figure 2.7 shows the two possible ways

of smoothening a singular point and an example for construction of a dividing curve of type (21)2.

In this example the reducible curve is the union of smooth quartic and quadratic curves. After perturbation, all the intersection points are smoothen with type B since the black and the red directions disagree on all the mixed components. One can show that any other choice of prescribed directions for the quartic and quadratic leads to the same result. Proposition 2.4.2 will give us an extra tool to construct the type (21)2 by turning the type (21)2 d inside out. See Figure 2.9. In particular, for the construction of types (41)4d and (41)4nd we followed [31, page 273].

After having all the sixty-four representatives, the task is to make them look nicer. This means to make the expression smaller and closer to the optimal polynomial for each type. Except for our first method of construction the other two led to huge coefficients. We have two main methods to improve the representatives and their combination yields the best results for each type.

One way is to choose a prime number  $p$  and vary the polynomial without crossing the discriminant locus so that every coefficient of the resulting polynomial is divisible by  $p$ . The other is to shrink the absolute value of each coefficient of a given representative separately as far as possible without crossing the discriminant. For both methods we used our code `SexticClassifier`. In the following chapter we complete the discussion about discriminant and the later method appears in more details. In particular, we show that Sylvester's formula for the discriminant (Proposition 2.4.1) has a major role in improvement of the representatives.

## 2.4. Local sampling and rigid isotopy transitions

Representing explicit polynomials, one for each sixty-four connected components in the complement of the discriminant  $\mathbb{P}_{\mathbb{R}}^{27} \setminus \Delta$ , enables us to sample locally. Our experimental study in Section 2.6 on certain properties of curves belonging to each rigid isotopy class requires such sampling. In this section, we take a deeper look into the discriminant. After presenting a method to compute  $\Delta$ , we explain how to avoid crossing it. This avoidance is needed to sample from a component. Moreover, we study different possibilities to cross the discriminant and how they affect the rigid isotopy type.

Before we start with the computation of discriminant in the whole space  $\mathbb{P}_{\mathbb{R}}^{27}$ , let us see an example of such polynomial for a smaller subspace:

$$(2.5) \quad \begin{aligned} \mathcal{R}(a, b, c) = & a(x^6 + y^6 + z^6) + bx^2y^2z^2 \\ & + c(x^4y^2 + x^4z^2 + x^2y^4 + x^2z^4 + y^4z^2 + y^2z^4), \end{aligned}$$

where  $(a : b : c)$  is any point in  $\mathbb{P}_{\mathbb{R}}^2$ . The discriminant is now a curve in  $\mathbb{P}_{\mathbb{R}}^2$  and this allows us to visually explore how it divides the two dimensional subspace of  $\mathbb{P}_{\mathbb{R}}^{27}$  defined by  $\mathcal{R}(a, b, c)$ .

In 1973, R.M. Robinson showed that the sextic  $\mathcal{R}(1, 3, -1)$  is non-negative but is not a sum of squares which is the reason that we named this net of sextics after him [74]. The real locus of his special sextic curve consists of 10 isolated singular points, given by

$$(2.6) \quad \left\{ (1:1:1), (-1:1:1), (1:-1:1), (1:1:-1), (0:1:1), \right. \\ \left. (0:1:-1), (1:0:1), (-1:0:1), (1:1:0), (1:-1:0) \right\} \subset \mathbb{P}_{\mathbb{R}}^2.$$

By examining the complement of the discriminant  $\mathbb{P}_{\mathbb{R}}^2 \setminus \Delta_{\mathcal{R}}$  one can express how the topology of  $\mathcal{R}(a, b, c)$  varies with  $(a : b : c)$ . First, we compute the discriminant:

$$(2.7) \quad \Delta_{\mathcal{R}} = a^3 \times (a + c)^6 \times (3a - c)^{18} \times (3a + b + 6c)^4 \\ \times (3a + b - 3c)^8 \times (9a^3 - 3a^2b + ab^2 - 3ac^2 - bc^2 + 2c^3)^{12}.$$

This is a reducible polynomial of degree 75. The complement of the discriminant  $\mathbb{P}_{\mathbb{R}}^2 \setminus \Delta_{\mathcal{R}}$  has 15 connected components. The topological types 10, 4, 3 and 0 are appearing in 1, 3, 5 and 6 connected components, respectively. Setting  $(a : b : c) = (19 : 60 : -20)$ , results in a smooth sextic and its real locus has ten empty ovals. We included  $\mathcal{R}(19, 60, -20)$  as our representative for the Type 10nd in Section 2.3 because of its nice construction.

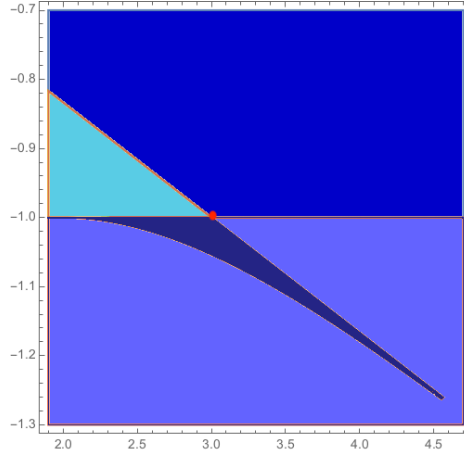


FIGURE 2.8. The Robinson net (2.5) is divided into 15 components by the discriminant (2.7). The darkest region shows the unique component corresponding to the type with 10 empty ovals. The red point represents the curve that is known as *Robinson form*.

The space of plane sextic curves  $\mathbb{P}_{\mathbb{R}}^{27}$  is divided into 64 connected components by a hypersurface of degree 75, namely the discriminant  $\Delta$ .



Intersecting this partition by the plane  $\mathbb{P}_{\mathbb{R}}^2$ , with coordinates  $(a : b : c)$  gives the simplified version that divides the Robinson net  $\mathcal{R}(a : b : c)$ . Figure 2.8 shows a selected region of this two-dimensional slice in the affine chart  $(a, b) \subset \mathbb{R}^2$ .

We are interested in this region since it contains all of the four topological types. From the darkest to the lightest blue, the number of ovals in the regions decreases. Therefore, the lightest blue belongs to one of the six components corresponding to the type that has no ovals. The unique component with 10 empty ovals is shown as the darkest region. The red point is where the zero locus of  $\mathcal{R}(a, b, c)$  in  $\mathbb{P}_{\mathbb{R}}^2$  is the set of ten points in (2.6).

Occurrence of the types 0, 3, and 4 in more than one components of this two dimensional slice proves that the 64 regions corresponding to the 64 rigid isotopy types are not necessarily convex.

Now we continue with the general case: For plane curves of degree six, as represented in (2.4), identify  $\Delta$  with its defining irreducible polynomial over  $\mathbb{Z}$  in the 28 unknowns  $c_{ijk}$ . We follow Gelfand, Kapranov and Zelevinsky [32, Theorem 4.10, Chapter 3] and evaluate  $\Delta$  using *Sylvester's formula* which expresses  $\Delta$  as the determinant of a  $45 \times 45$ -matrix  $\mathcal{S}_f$ . Each entry in the first 30 columns of  $\mathcal{S}_f$  is either 0 or one of the coefficients  $c_{ijk}$ . The entries in the last 15 columns are cubics in the  $c_{ijk}$ . Therefore, we have the required degree:

$$\deg(\det(\mathcal{S}_f)) = 75.$$

A Curve of degree eight is called an *octic*. Let

$$\mathcal{S}_f : (\mathbb{R}[x, y, z]_3)^3 \oplus \mathbb{R}[x, y, z]_4 \longrightarrow \mathbb{R}[x, y, z]_8$$

be a map taking a triple of real plane cubics and a real plane quartic and mapping them into a real plane octic as follows. It maps a triple of cubics to an octic via

$$(a, b, c) \mapsto a \frac{\partial f}{\partial x} + b \frac{\partial f}{\partial y} + c \frac{\partial f}{\partial z}.$$

and on the second summand, it takes a quartic monomial  $x^r y^s z^t$  to the octic  $\det(M_{rst})$ , where  $M_{rst}$  is any  $3 \times 3$ -matrix of ternary forms in the  $c_{ijk}$  satisfying the homogeneous identity

$$\begin{bmatrix} \partial f / \partial x \\ \partial f / \partial y \\ \partial f / \partial z \end{bmatrix} = M_{rst} \cdot \begin{bmatrix} x^{r+1} \\ y^{s+1} \\ z^{t+1} \end{bmatrix}.$$

The entries of  $M_{rst}$  are linear in the  $c_{ijk}$ . Thus,  $\det(M_{rst})$  is an octic in  $x, y, z$  whose coefficients are cubics in the  $c_{ijk}$ . These are the entries of the column indexed by  $x^r y^s z^t$  in the matrix representation of the  $\mathbb{R}$ -linear map  $\mathcal{S}_f$  in monomial bases. This representation of  $\mathcal{S}_f$  is exactly the *Sylvester matrix*  $\mathcal{S}_f$ .

**Proposition 2.4.1** *The discriminant  $\Delta$  is the determinant of the  $45 \times 45$  - matrix  $\mathcal{S}_f$ .*

PROOF. We use Sylvester's formula for the resultant of three ternary quintics. This is [32, Theorem III.4.10] by setting  $d = 5$  and  $k = 4$ . If we take the three quintics to be the three partial derivatives of  $f$ , then we get the matrix  $\mathcal{S}_f$  above. That resultant equals our discriminant because both are non-zero homogeneous polynomials in 28 unknowns  $c_{ijk}$  and the degree of both is 75.  $\square$

Let  $f$  and  $g$  be points in the space  $\mathbb{P}^{27}$  of all ternary curves of degree six, a *pencil of sextics* is a line  $\{f + tg\}$ . Its discriminant  $\Delta(f + tg)$  is a univariate polynomial in  $t$  of degree 75 which can be computed as the determinant of the Sylvester matrix  $\mathcal{S}_{f+tg}$ . If we pick  $f, g \in \mathbb{Z}[x, y, z]_6$  with reasonably small coefficients, the computation of discriminant takes only a few seconds. For the Robinson net of sextics, we tried a similar method with more than one parameter and computed the discriminant (2.7) of the curve (2.5) with three parameters  $a, b$ , and  $c$ . In this case the output is not large and factors in smaller components, therefore the computation took less than one second.

Due to our experiments, the symbolic evaluation of the  $45 \times 45$  determinant in Proposition 2.4.1 works well for pencils of sextics and, in principle, also for evaluating  $\Delta$  on families with more than one parameter, however, it generally fails for nets of plane sextics.

Sylvester's formula allows us to sample from a fixed rigid isotopy class. We start with a representative  $f$  with  $\Delta(f) \neq 0$ , for example one of the 64 sextics in Section 2.3. After picking a random sextic  $g$ , we compute the polynomial  $\Delta(f + tg)$  in the unique variable  $t$ . Next, we extract the real roots among the 75 complex ones, and we identify the smallest positive root and the largest negative root. The sextic  $f + tg$  has the same rigid isotopy type as  $f$  for any  $t$  in the open interval between these two roots. Repeating this process over and over, we make our sample from the unique connected component of  $\mathbb{R}[x, y, z]_6 \setminus \Delta$  that contains  $f$ . This produces sextics in the largest star domain with center  $f$  contained in that component. We have seen in 2.3 that the components of  $\mathbb{P}_{\mathbb{R}}^{27} \setminus \Delta$  are not necessarily convex. Therefore, this is wise to vary the center many times as well to reach the largest area of the desired component. We call this process the *local exploration method*. It will be used for the applications in Sections 2.5 and 2.6.

To understand the cover relations of the poset structure and the vertical reflection in Figure 2.5, we briefly introduced the *discriminantal transitions*. For any two connected components of  $\mathbb{P}_{\mathbb{R}}^{27} \setminus \Delta$ , the intersection of their Euclidean closures is a subset of  $\Delta$ . Therefore, it only contains singular curves. Recall from Section 2.1, two rigid isotopy types are connected by a discriminantal transition if this intersection contains a curve  $C$ , whose only singularity is an ordinary node.

The ordinary node of  $C$  is locally defined by either  $x^2 + y^2 = 0$  or  $x^2 - y^2 = 0$ . The former occurs when the singularity is an isolated real point called *acnode*. This transition corresponds to removing one empty oval and we call it *shrinking an oval*. The inverse operation to shrinking is adding an empty oval. In the later case, singularity of  $C$  is a *crunode*, i.e. it locally looks like the intersection of two crossing real branches. In this case, there are two possibilities: The ordinary node is the unique intersection of either two ovals or two pseudolines.

If two ovals are intersecting in one point the transition is two ovals coming together and forming one oval. We call this operation *fusing two ovals*. Itenberg [43] uses the terms *contraction* and *conjunction* for the operations shrinking an oval and fusing two ovals, respectively. Each of these two operations reduces the number of ovals by one.

The transition corresponding to the intersection of two pseudolines does not change the number of ovals. This operation exchanges the inside and outside of an oval that is not contained in any other ovals. We call this transition *turning inside out*. Figure 2.9 shows an example of turning inside out for two different smooth sextics with five ovals.

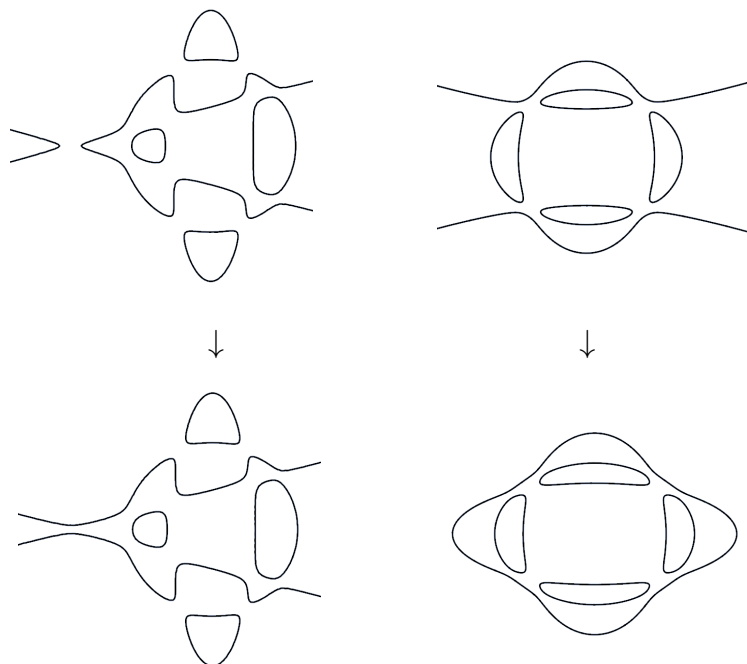


FIGURE 2.9. The left picture is Type (21)2 d transitioning into Type (21)2 nd and on the right Type 5 nd transitions into Type (41) which could be d/nd. Both transitions are turning inside out.

**Proposition 2.4.2** *The topological type of the resulting curve from turning inside out of a plane sextic is obtained by vertically reflecting Figure 2.5. Curves of diving type become non-dividing, however, non-dividing sextics can turn into either dividing or non-dividing.*

PROOF. Let  $C$  be a real plane curve with exactly one ordinary crunode  $p$ . In a neighborhood of  $p$ , the Riemann surface  $C_{\mathbb{C}}$  is homeomorphic to the union of two discs  $D_1$  and  $D_2$  with  $D_1 \cap D_2 = \{p\}$ . The real part  $C_{\mathbb{R}}$  divides  $D_1$  and  $D_2$  into two connected components  $D_1^+$ ,  $D_1^-$  and  $D_2^+$ ,  $D_2^-$  respectively. One of the two possible smoothenings of the node  $p$  connects  $D_1^+$  with  $D_2^+$  and the other one connects  $D_1^+$  with  $D_2^-$ . Thus, if  $C$  is dividing then exactly one of the two deformations results in a dividing curve. Otherwise, both are non-dividing.  $\square$

Turning inside out preserves the number of ovals, so it is an operation that acts on each of the rows in Figure 2.5 separately. In Figure 2.9, on the left we start from a curve with the topological type (21)2 that is diving. (See 2.7.) From the previous proposition we know that turning the outermost oval inside out is a non-dividing type. In the right picture, the same transition for the type with 5 empty ovals that is non-diving results in the topological type (41), which is one of the Nikulin cases in 2.1, therefore could be either dividing or non-dividing.

Not every vertical reflection in Figure 2.5 can be realized geometrically by a discriminantal transition. For instance, the types (91)1 and (11)9 are related by a vertical reflection. But both types are dividing, so Proposition 2.4.2 implies that they are not connected by turning inside out. Put differently, these two components of  $\mathbb{P}_{\mathbb{R}}^{27} \setminus \Delta$  do not share a wall of codimension one. In fact, turning inside out can only happen for curves with at most 9 ovals: Consider a plane sextic curve with exactly one crunode and  $r$  connected components, one of which is the intersection of two pseudolines. The normalization of such a curve has genus 9 and  $r + 1$  connected components. By Harnack's inequality this implies that  $r \leq 9$ .

In addition to turning inside out, the other discriminantal transition which helps us to determine whether the resulting plane sextic is diving or non-dividing type is shrinking an oval:

**Lemma 2.4.3** *A smooth sextic obtained from shrinking an oval is non-dividing.*

PROOF. Consider a singular real plane curve  $C$  with only one singularity  $p$  that is an acnode. We can assume that  $S$  is of dividing type since being of non-dividing type is an open condition. Therefore,  $C_{\mathbb{C}} \setminus C_{\mathbb{R}}$  has two connected components and  $p$  is in the closure of both. In particular,  $(C_{\mathbb{C}} \setminus C_{\mathbb{R}}) \cup \{p\}$  is connected. Thus, shrinking an oval leads to a curve that is non-dividing.  $\square$

The definitions of an acnode and a crunode are not restricted to curves of degree six. These are the only two possibilities of an ordinary node in any plane curve of degree  $d$ . Although, a crunode could also be the intersection of a pseudoline and an oval for odd  $d$ , in addition to the possibilities that we explained above. Therefore, it makes sense to have similar discussions on discriminantal transitions for other degrees. The transition turning inside out is only defined for curves of even degrees. In particular, this is the only transition for plane conics. All three discriminant transitions are possible for plane quartics.

We include our proof for the following theorem only for lack of a suitable reference. We expect that they are well-known to experts.

**Theorem 2.4.4** *Any discriminantal transition between rigid isotopy types for plane curves of even degree is one of the following: shrinking an oval, fusing two ovals, and turning inside out.*

PROOF. Let  $C$  be a general point on the discriminant  $\Delta \subset \mathbb{P}_{\mathbb{R}}^{\frac{d(d+3)}{2}}$ , where  $d$  is even. i.e.  $C \subset \mathbb{P}_{\mathbb{R}}^2$  is a singular plane curve of even degree with exactly one ordinary singularity  $p$ . If  $p$  is an acnode, then  $C$  corresponds to shrinking. Let  $p$  be a crunode. There are two subsets  $C_1, C_2 \subset C_{\mathbb{R}}$ , both homeomorphic to the circle, such that  $C_1 \cap C_2 = \{p\}$ . Let  $\pi : \tilde{C} \rightarrow C$  be the normalization map. The fiber  $\pi^{-1}(p)$  consists of exactly two points  $p_1, p_2 \in \tilde{C}_{\mathbb{R}}$ .

Suppose that  $p_1$  and  $p_2$  are in the same connected component of  $\tilde{C}_{\mathbb{R}}$ . If any of  $C_1$  or  $C_2$  does not disconnect  $\mathbb{P}_{\mathbb{R}}^2$ , there is a perturbation of  $C$  that results in a smooth curve with at least one pseudoline. Since this is not possible for a smooth plane curve to have a pseudoline as one of the connected components of its real part, both  $C_1$  and  $C_2$  disconnect  $\mathbb{P}_{\mathbb{R}}^2$ . This corresponds to fusing of ovals.

If both  $p_1$  and  $p_2$  belong to different connected components of  $\tilde{C}_{\mathbb{R}}$ , the number of components of the real curve stays the same for both bifurcations of the node. Suppose that  $C_1$  or  $C_2$  disconnected  $\mathbb{P}_{\mathbb{R}}^2$ , then besides  $p$ , there would be another intersection point of  $C_1$  and  $C_2$ .

Therefore,  $\mathbb{P}_{\mathbb{R}}^2 \setminus C_i$  is connected for  $i = 1, 2$ , and  $\mathbb{P}_{\mathbb{R}}^2 \setminus (C_1 \cup C_2)$  has two connected components, both homeomorphic to an open disc. Depending on the bifurcation of the node, one of these connected components remains homeomorphic to an open disc and the other one does not. This case corresponds to turning inside out.  $\square$

Back to our case of interest, namely smooth plane curves of degree six, let us examine the diagram in Figure 2.5 from the perspective of discriminantal transitions. We have already discussed the correspondence between turning inside out and the vertical reflections. Thus, the focus is now on the other two discriminantal transitions.

The edges in the poset correspond to shrinking or fusing. There are three possibilities for what might be geometrically possible: shrinking

only, fusing only, or shrinking and fusing. For instance, Type (11) can become Type 1 by either shrinking the inner oval, or by fusing the two nested ovals. Both possibilities are geometrically realized by a singular curve with a single node that lies in the common boundary between the two types.

**Theorem 2.4.5** (Itenberg) *Each of the edges in Figure 2.5 is realized by shrinking an empty oval, except the one between (hyp) and (11). Not every edge is realized by fusing two ovals.*

PROOF. The first statement is [43, Prop. 2.1]. Furthermore, it was shown in [43] that the transition from (11)9 to 10 cannot be realized by fusing.  $\square$

One possible way of explicitly realizing edges by fusing is to use Gudkov's constructions [35] and the following lemma which is a special case of a theorem due to Brusotti [10].

**Lemma 2.4.6** *Let  $C_1, C_2 \subset \mathbb{P}^2$  be two smooth real curves of degrees 2 and 4 (resp. 1 and 5) intersecting transversally. By a small perturbation, we can fix any one of the real nodes of the sextic curve  $C_1 \cup C_2$  and perturb all the others independently in any prescribed manner.*

PROOF. Let  $q, p_1, \dots, p_7 \in \mathbb{P}_{\mathbb{R}}^2$  be eight distinct real points lying on the smooth quadric  $C_1$ . We claim that, for every tuple  $\epsilon \in \{\pm 1\}^7$ , there is a sextic which is singular at  $q$  and whose sign at  $p_i$  is  $\epsilon_i$ . Let  $L$  be the linear system of all sextic curves that are singular at  $q$ . The pull-back of  $L$  to  $C_1 \cong \mathbb{P}^1$  is the set of all bivariate forms of degree 12 having a double root at  $q$ . Since for any distinct 7 points in  $\mathbb{R}$  there is a polynomial of degree 10 that vanishes on all but one of these points, the claim follows. The other case (degrees 1 and 5) is analogous.  $\square$

We might also approach these questions by computational means. This requires a software tool for the following task. Consider two general sextics  $f, g \in \mathbb{Z}[x, y, z]_6$  and compute the univariate polynomial  $\Delta(f + tg)$  of degree 75. For each of its real roots  $t^*$ , we must decide if the transition at  $t^*$  is a shrinking of ovals, a fusing of ovals, or turning inside out.

## 2.5. Avoidance locus, dual curve, and bitangents

In Section 2.2, we have seen that `SexticClassifier` has several advantages in comparison with many other software packages for plane curves. The most important one is handling the cases where the given curve is not compactible, e.g. the one in Example 2.2.1.

We say a real plane curve  $C$  is *compactible*, if there is a homeomorphism  $\mathbb{P}_{\mathbb{R}}^2 \rightarrow \mathbb{P}_{\mathbb{R}}^2$  such that the image of  $C$  is a compact curve in some affine chart, i.e. the closure of the image in  $\mathbb{P}_{\mathbb{R}}^2$  is disjoint from the

line at infinity. Odd degree curves are not compactible since they contain a pseudoline. Although any plane conic or quartic is necessarily compactible, this is no longer true for the higher even degrees.

Consider any line in  $\mathbb{P}_{\mathbb{R}}^2$  that do not intersect a given curve  $C$ . The image of  $C$  under the homeomorphism that maps this line to the line at infinity is compact in the corresponding affine chart. Therefore,  $C$  is compactible if such a non-intersecting line exists. This motivates the concept of the avoidance locus, to be introduced and studied in this section. This will lead us naturally to computing dual curves and bitangent lines, and to investigating the behavior of these objects over the field of real numbers.

We define the *avoidance locus* of a smooth curve  $C \subset \mathbb{P}^2$  of even degree  $d$  to be the set  $\mathcal{A}_C$  of all lines in  $\mathbb{P}_{\mathbb{R}}^2$  that do not intersect the real curve  $C_{\mathbb{R}}$ . Let  $(\mathbb{P}^2)^{\vee}$  be dual of the projective plane. We write  $C^{\vee}$  for the curve in  $(\mathbb{P}^2)^{\vee}$  that is dual to  $C$ . The dual curve has degree  $d(d-1)$  and points on  $C^{\vee}$  correspond to lines in  $\mathbb{P}^2$  that are tangent to  $C$ . The real dual curve  $C_{\mathbb{R}}^{\vee}$  divides the real projective plane  $(\mathbb{P}^2)_{\mathbb{R}}^{\vee}$  into connected components. The set  $\mathcal{A}_C$  is a semi-algebraic subset of  $(\mathbb{P}^2)_{\mathbb{R}}^{\vee}$  that comes from such division.

**Example 2.5.1** Let  $C$  be the smooth plane curve of degree four known as *Edge quartic*, defined by:

$$f = 25(x^4 + y^4 + z^4) - 34(x^2y^2 + x^2z^2 + y^2z^2)$$

This curve  $C \subset \mathbb{P}^2$  served as a running example in [70]. The affine picture by setting  $z = 1$  is shown on the left in Figure 2.10. We choose

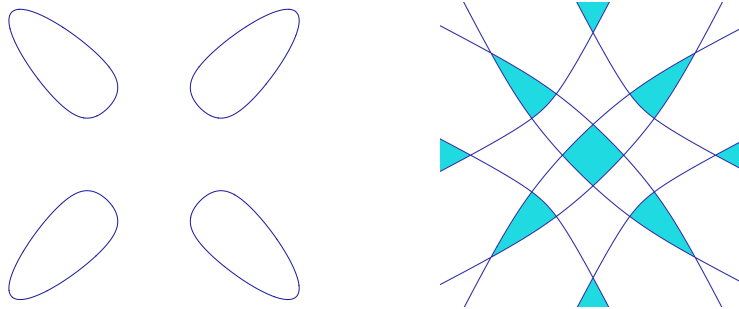


FIGURE 2.10. The dual curve to the Edge quartic  $C$  divides the real plane into 21 regions; the avoidance locus  $\mathcal{A}_C$  is colored.

coordinates  $(u : v : w)$  for points in the dual projective plane  $(\mathbb{P}^2)^{\vee}$ .

Such a point represents the line  $L = \{ux + vy + wz = 0\}$  in the primal  $\mathbb{P}^2$ . The dual curve  $C^\vee$  is given by

$$\begin{aligned} &10000u^{12} - 98600u^{10}v^2 - 98600u^{10}w^2 + 326225u^8v^4 + 85646u^8v^2w^2 + 326225u^8w^4 \\ &- 442850u^6v^6 - 120462u^6v^4w^2 - 120462u^6v^2w^4 - 442850u^6w^6 + 326225u^4v^8 \\ &- 120462u^4v^6w^2 + 398634u^4v^4w^4 - 120462u^4v^2w^6 + 326225u^4w^8 - 98600u^2v^{10} \\ &+ 85646u^2v^8w^2 - 120462u^2v^6w^4 - 120462u^2v^4w^6 + 85646u^2v^2w^8 - 98600u^2w^{10} \\ &+ 10000v^{12} - 98600v^{10}w^2 + 326225v^8w^4 - 442850v^6w^6 + 326225v^4w^8 \\ &- 98600v^2w^{10} + 10000w^{12} = 0. \end{aligned}$$

The real dual curve  $C_{\mathbb{R}}^\vee$  divides  $(\mathbb{P}^2)_{\mathbb{R}}^\vee$  into 21 open regions. Seven of the regions comprise the avoidance locus  $\mathcal{A}_C$ . They are colored in Figure 2.10, and they represent the seven ways of bipartitioning the four ovals of  $C_{\mathbb{R}}$  by a straight line. The central blue region on the right is the convex body dual to the convex hull of  $C_{\mathbb{R}}$ , in our affine drawing on the left.

The number seven of colored regions seen in Figure 2.10 attains the following upper bound.

**Proposition 2.5.2** *Let  $C \subset \mathbb{P}^2$  be a smooth curve of even degree  $d$ . Up to closure, its avoidance locus  $\mathcal{A}_C$  is a union of  $m$  connected components in  $(\mathbb{P}^2)_{\mathbb{R}}^\vee \setminus C_{\mathbb{R}}^\vee$  where  $m$  is bounded above by*

$$(2.8) \quad \frac{9}{128}d^4 - \frac{9}{32}d^3 + \frac{15}{32}d^2 - \frac{3}{8}d + 1.$$

Moreover, each component can be regarded as a convex cone in  $\mathbb{R}^3$ .

**PROOF.** Any line intersects  $C$  in  $d$  points, counting multiplicity. Points in  $(\mathbb{P}^2)_{\mathbb{R}}^\vee \setminus C_{\mathbb{R}}^\vee$  correspond to real lines that intersect  $C$  transversally. The appearance or non-appearance of a real point in this intersection only changes by crossing the dual curve  $C_{\mathbb{R}}^\vee$ . Thus,  $\mathcal{A}_C \setminus C_{\mathbb{R}}^\vee$  is a union of connected components of  $(\mathbb{P}^2)_{\mathbb{R}}^\vee \setminus C_{\mathbb{R}}^\vee$ . The prefix “up to closure” is needed because  $\mathcal{A}_C$  also contains some points in  $C_{\mathbb{R}}^\vee$ , corresponding to real lines that do not meet  $C_{\mathbb{R}}$  but are tangent to  $C$  at complex points.

To prove the upper bound, we start with the Harnack’s inequality. It says that the real curve  $C_{\mathbb{R}}$  can have at most  $\binom{d-1}{2} + 1$  ovals in  $\mathbb{P}_{\mathbb{R}}^2$ . However, for our count we only care about the outermost ovals, i.e. those not contained inside any other oval. By a result of Arnold in [2], which is a more precise version of a classical inequality due to Petrovsky [69], the number of outermost ovals of the curve  $C_{\mathbb{R}}$  is at most

$$k = \frac{3}{8}d^2 - \frac{3}{4}d + 1.$$

If we pick a generic point in each oval, their configuration has  $\binom{k}{2} + 1$  bipartitions that can be realized by a straight line. Indeed, dually, this is the number of regions in the complement of a general arrangement



of  $k$  lines in the plane  $\mathbb{P}_{\mathbb{R}}^2$ . The quartic polynomial in (2.8) is simply  $\binom{k}{2} + 1$  with Petrovsky's expression for  $k$ .

It remains to check that this number is the desired upper bound. Indeed, every connected component of  $\mathcal{A}_C$  is uniquely labeled by a bipartition of the set of non-nested ovals. The number of such bipartitions that are realized by a straight line is bounded above by the said bipartitions of the points.

The set  $\mathcal{A}_C$  is the convex dual of the convex hull of  $C_{\mathbb{R}}$  in the affine space  $\mathbb{P}_{\mathbb{R}}^2 \setminus L$ , where  $L \in \mathcal{A}_C$ . Therefore each of its components is convex.  $\square$

For plane sextics, the upper bound in (2.8) evaluates to 46. In the following example we present a sextic that attains the bound.

**Example 2.5.3** Consider the following net of sextics where  $t$  and  $\epsilon$  are parameters:

$$\begin{aligned} F_{t,\epsilon} = & 60x^6 - 750x^5z - 111x^4y^2 + 1820x^4z^2 + 700x^3y^2z - 2250x^3z^3 \\ & + 20x^2y^4 - 1297x^2y^2z^2 + 960x^2z^4 - 56xy^4z + 1440xy^2z^3 - y^6 \\ & - 576y^2z^4 + t(x^3 + xz^2 - y^2z)^2 + \epsilon(x^2z^4 + y^2z^4 + z^6) \end{aligned}$$

For  $t_0 = -\frac{1645}{2} - 150\sqrt{34}$  and  $\epsilon = 0$ , the sextic  $F_{t_0,0}$  has 10 isolated real singular points:

$$\begin{aligned} (1 : \pm\sqrt{2} : 1), (2 : \pm\sqrt{10} : 1), (3 : \pm\sqrt{30} : 1), (4 : \pm 2\sqrt{17} : 1), \\ ((3 - \sqrt{34})/5 : 0 : 1), (0 : 0 : 1). \end{aligned}$$

No three of these 10 points lie on a line. For any sufficiently small  $\epsilon > 0$  and  $t$  sufficiently close to  $t_0$ , the sextic  $F_{t,\epsilon}$  is smooth with 10 small ovals arranged around the singular points of  $F_{t_0,0}$ . When these ovals are small enough, the avoidance locus will have the maximum number 46 of connected components, by the argument given in the proof of Proposition 2.5.2. We used the construction developed by Kunert and Scheiderer in [57] for this example.

In Example 2.5.1 and the proof of Proposition 2.5.2 we have seen the one to one correspondence between the components of the avoidance locus of a smooth curve  $C$  and bipartitions of all non-nested ovals in the real curve  $C_{\mathbb{R}}$  using lines in  $\mathbb{P}_{\mathbb{R}}^2$  that do not intersect  $C_{\mathbb{R}}$ . This correspondence suggests that in order to compute the avoidance locus in  $\mathbb{P}_{\mathbb{R}}^V$  we find the boundaries for moving any of such lines. In our algorithm for computing the avoidance locus  $\mathcal{A}_C$ , to be described in this section, we use bitangents to serve as the desired boundary lines.

Let  $C$  be a smooth plane curve of degree  $d$ . A *bitangent* of  $C$  is a line  $L$  in  $\mathbb{P}^2$  that is tangent to  $C$  at two points. Note that bitangents of  $C$  correspond to nodal singularities of the dual curve  $C^V$ . By the

Plücker formulas, the expected number of bitangents is

$$\frac{1}{2}(d-3)(d-2)d(d+3),$$

which evaluates to 324 for  $d = 6$ . A bitangent  $L$  is called *relevant* if the real part of the divisor  $L \cap C$  is an even divisor on the curve  $C$ . For generic curves  $C$ , this means that  $L$  has no real intersection points with  $C$  except possibly the two points of tangency. If these two points are real, then  $L$  corresponds to an extreme point of a convex connected component of  $\mathcal{A}_C$ . If  $L$  can be represented with a linear form with only real coefficients then we call it a *real* bitangent.

**Example 2.5.4** Let  $C$  be the smooth sextic that we represented for Type 8nd in Section 2.3. This curve has 324 distinct complex bitangents of which 124 are real. Of the real bitangents,

- 8 are tangent at non-real points and meet the curve in two more non-real points;
- 60 are tangent at real points and meet the curve in two more non-real points;
- 4 are tangent at non-real points and meet the curve in two more real points;
- 52 are tangent at real points and meet the curve in two more real points.

The last two families of bitangents intersect the real curve  $C_{\mathbb{R}}$  transversally at two of the intersection points. Therefore,  $C$  only has 68 real relevant bitangents. The curve  $C$  together with its 68 relevant bitangents is shown in Figure 2.11.

Due to Bézout's theorem, or simply from the formula above, curves of degrees less than four have no bitangents. From the Zeuthen classification [70, Table 1], among all 28 bitangent lines for a smooth quartic, the number of real ones only depends on the topological type. In higher degrees, when this is not the case, not much seems known. In the following conjecture we suggest the bound that we have observed experimentally. See Table 2.7.

**Conjecture 2.5.5** *The number of real bitangents of a smooth sextic in  $\mathbb{P}_{\mathbb{R}}^2$  ranges from 12 to 306. The lower bound is attained by curves in the following four types: empty, 1, 2, (11) and (hyp). The upper bound is attained by certain 11-oval curves of Gudkov-type (51)5.*

We now describe an algorithm to compute the avoidance locus  $\mathcal{A}_C$ .

**Remark 2.5.6** Let  $C$  be a smooth curve in  $\mathbb{P}_{\mathbb{R}}^2$  of degree  $d \geq 4$ . If  $C$  contains at least two non-nested ovals or has a non-nested oval which is not convex, then every connected component of the avoidance locus

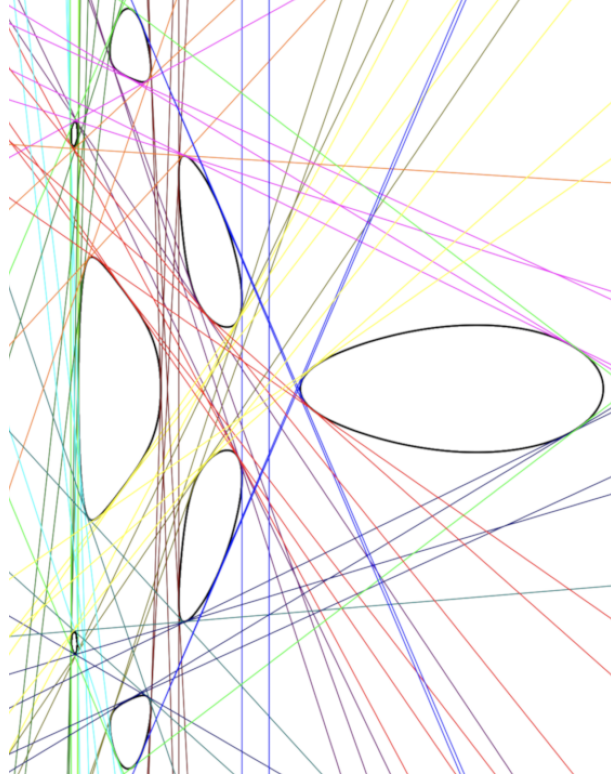


FIGURE 2.11. A sextic  $C$  of Type 8nd; the avoidance locus  $\mathcal{A}_C$  is represented by 68 real relevant bitangents.

$\mathcal{A}_C$  has a relevant bitangent in its closure. If  $C$  does not satisfy this hypothesis then  $\mathcal{A}_C$  is connected.

Assume that  $C$  satisfies the hypothesis in Remark 2.5.6. The avoidance locus can be represented as the connected components (cliques) of a graph  $\mathcal{G}_C$ . We construct the *avoidance graph*  $\mathcal{G}_C$  as follows.

**Algorithm 2.5.7** (Avoidance graph of a smooth plane curve)

**Input:**  $(f, d)$ , such that

- $d$  is an even integer.
- $f \in \mathbb{C}[x, y, z]$  is homogeneous of degree  $d$ .
- $C := V_{\mathbb{C}}(f)$  is smooth.

**Output:** The avoidance graph  $\mathcal{G}_C$  corresponding to  $C$ .

- 1: Let  $L = \{L_1, \dots, L_k\}$  be the set of all complex bitangents to the curve  $C$ , where  $k = \frac{1}{2}(d-3)(d-2)d(d+3)$ .
- 2: Set  $L_{\mathbb{R}} \subset L$  to be the subset consisting of all real bitangents.

- 3: Discard those bitangents that are not relevant from  $L_{\mathbb{R}}$  and call the remaining set  $V_{\mathcal{G}}$ .
- 4: Let  $E_{\mathcal{G}}$  be the set of all  $L_i L_j$  such that
  - $L_i, L_j \in V_{\mathcal{G}}$ ,
  - $(L_i + L_j) \cap C_{\mathbb{R}} = \emptyset$ ,
  - $\{t\tilde{L}_i + (1-t)\tilde{L}_j : 0 < t < 1\} \cap C_{\mathbb{R}}^{\vee} = \emptyset$ , where  $\tilde{L} \in \mathbb{P}_{\mathbb{R}}^{\vee}$  is the corresponding point to the line  $L \subset \mathbb{P}_{\mathbb{R}}^2$ .
- 5: **return** The graph  $\mathcal{G}_C = (V_{\mathcal{G}}, E_{\mathcal{G}})$  with vertex set  $V_{\mathcal{G}}$  and edges in  $E_{\mathcal{G}}$ .

We made a proof-of-concept implementation of this algorithm for the case of sextics. Its two main ingredients are computing the bitangents in step 1 and the dual curve in step 4.

To compute the bitangents in step 1, we employ the variety of binary sextics with two double roots. The prime ideal of this variety is defined by 13 forms of degree 7; see the row labeled 2211 in [58, Table 1]. Substituting the binary form  $f(x, y, -\frac{1}{w}(ux + vy))$  into that ideal, and clearing denominators, yields the ideal in  $\mathbb{Q}[u, v, w]$ . The zero set of this ideal consists of 324 points  $(u : v : w)$ , each corresponding to a bitangent  $ux + vy + wz = 0$ . Note that the sign of our linear forms representing the bitangents has to be chosen carefully.

For the computation of the dual curve we solve a linear system of equations in the  $\binom{30+2}{2} = 496$  coefficients of  $C^{\vee}$ . The equations are derived by projecting  $C$  from random points  $p \in \mathbb{P}^2$ . The ramification locus of this projection reveals (up to scaling) the binary form of degree 30 that defines  $C^{\vee} \cap p^{\perp}$ .

Finally, the graph  $\mathcal{G}_C$  is a disjoint union of cliques, one for each connected component of  $\mathcal{A}_C$ . This follows from Remark 2.5.6 and convexity of the connected components. Midpoints of the segments  $\{t\tilde{L}_i + (1-t)\tilde{L}_j : 0 < t < 1\}$ , appearing in step 4, furnish sample points in the components.

In Example 2.5.4, the avoidance graph  $\mathcal{G}_C$  is found to consist of 14 cliques: four  $K_6$ 's, five  $K_5$ 's, four  $K_4$ 's and one  $K_3$ . Hence  $\mathcal{A}_C$  consists of 14 convex components. One can see all the 14 ways to bipartition the 8 ovals in Figure 2.11 by lines that avoid  $C_{\mathbb{R}}$ .

Another important family of lines associated with a smooth plane curve  $C$  consists of flex lines. While the nodes on  $C^{\vee}$  correspond to bitangents of  $C$ , the cusps on  $C^{\vee}$  represent the *flex lines* of  $C$ . The number of *inflection points* is  $3d(d-2)$  for a general curve of degree  $d$ . A classical result due to Felix Klein states that at most one third of the complex inflection points of a real plane curve can be real. Brugallé and López de Medrano [8] proved, using tropical methods, that Klein's upper bound  $d(d-2)$  is attained for all  $d \geq 3$ . Hence, for smooth sextics, the number of real inflection points can be any even integer between 0 and 24. The distribution of the numbers of real bitangents

and real inflection points over the 64 rigid isotopy types is presented in Section 2.6.

By passing through the discriminant hypersurface, the numbers of real inflection points and bitangents of a sextic  $C$  often change. Although, they may also change within the same rigid isotopy type. In the space of all plane sextics, there are more hypersurfaces that all together with the discriminant provide necessary conditions for these changes. Each of such hypersurfaces is defined by one of the following properties:

- (222)  $C$  has a *tritangent line*, i.e. a line that is tangent to  $C$  in three distinct points.
- (321)  $C$  has a *flex-bitangent*, i.e. a line that meets  $C$  with multiplicity 3 in one point and is tangent at another point.
- (411)  $C$  has an *undulation point*, in which the tangent meets  $C$  with multiplicity at least 4.

If  $C$  is smooth then the total number of complex inflection points resp. bitangents drops below the bounds 72 resp. 324 in all above exceptional cases. Furthermore, the number of real inflection points or bitangents changes only when passing through the discriminant or one of these hypersurfaces. When generic sextics approach these hypersurfaces, three lines come together: three bitangents for a tritangent line (222), and two bitangents and a flex line for a flex-bitangent (321), a bitangent and two flex lines for an undulation point (411). We define the *bitangent discriminant* to be the Zariski closure of the set of smooth sextics in  $\mathbb{P}V = \mathbb{P}^{27}$  having fewer than 324 bitangent lines.

**Theorem 2.5.8** *Let  $\mathcal{T}$  be the Zariski closure in  $\mathbb{P}V = \mathbb{P}^{27}$  of the set of smooth sextics with a tritangent line and let  $\mathcal{F}$  be the locus of smooth sextics with a flex-bitangent. Then:*

- (1) *The loci  $\mathcal{T}$  and  $\mathcal{F}$  are irreducible hypersurfaces of degree 1224 and 306 respectively.*
- (2) *Their union  $\mathcal{B} = \mathcal{T} \cup \mathcal{F}$  is the bitangent discriminant.*

**PROOF.** The binary sextics with three double roots in  $\mathbb{R}[x, y]_6$  define an irreducible variety of codimension 3. (It is defined by 45 quartics [58, Table 1].) Let  $\mathcal{X}$  be the incidence variety of all pairs  $(L, f)$  in  $(\mathbb{P}^2)^\vee \times \mathbb{P}V$  where  $L$  is the dual of a tritangent line to  $V_{\mathbb{C}}(f) \subset \mathbb{P}^2$ . The locus  $\mathcal{T}$  is the projection of  $\mathcal{X}$  onto  $\mathbb{P}V$ . The intersection of  $\mathcal{X}$  with any subspace of the form  $\{L\} \times \mathbb{P}V$  for  $L \in (\mathbb{P}^2)^\vee$  has codimension 3 in  $\mathbb{P}V$ . Taking the union over all  $L$ , we conclude that  $\mathcal{T}$  has codimension 1. Since the projection of  $\mathcal{X}$  onto the first factor is surjective with irreducible fibers of constant dimension,  $\mathcal{X}$  is irreducible, hence so is  $\mathcal{T}$ . The same argument applies to  $\mathcal{F}$ . The degrees of the hypersurfaces  $\mathcal{F}$  and  $\mathcal{T}$  were computed for us by Israel Vainsencher with the

Maple package `schubert`. The relevant theory is described by Colley and Kennedy in [19]. This completes the proof of (1).

To prove (2), we start with the fact that any smooth deformation of a sextic in  $\mathcal{T}$  splits a tritangent into three bitangents. Similarly, for a sextic in  $\mathcal{F}$ , a flex-bitangent turns into two bitangents and a flex line. This shows that  $\mathcal{T}$  and  $\mathcal{F}$  are both contained in the bitangent discriminant. By degenerating the singularities of the dual picture in  $C^\vee$ , we can argue for the reverse.  $\square$

In Proposition 2.5.2 we proved that the number of connected components of the avoidance locus  $\mathcal{A}_C$ , where  $C$  is a smooth sextic, can not exceed 46. Moreover, throughout this section, we presented two examples of smooth sextics, for two extreme cases where  $\mathcal{A}_C$  has zero and 46 components. We now conclude this section with the following result on the avoidance loci of plane sextics.

**Corollary 2.5.9** *For any integer  $m$  between 0 and 46, there exists a smooth sextic  $C$  in  $\mathbb{P}_{\mathbb{R}}^2$  whose avoidance locus  $\mathcal{A}_C$  comprises exactly  $m$  convex connected components.*

**PROOF.** We start with one of the 64 components in the complement of the discriminant and there we pick two smooth sextics whose avoidance locus has 0 and 46 number of connected components. By using the bitangent discriminant, we prove that along a path connecting these two sextics, any integer between 0 and 46 is realizable: Let  $f_1$  be a sextic of Type 10nd whose avoidance locus has 46 components, as in Example 2.5.3. Let  $f_0$  be a sextic of Type 10nd with empty avoidance locus, for instance

$$f_0 = (20x^2 - (y+10z)^2 + z^2)(21y^2 - (x-10z)^2 + z^2)(20(x-5z+y)^2 - (y+10z)^2 + z^2) + z^6.$$

The real picture of such a curve is shown in Figure 2.12. Let  $U$  be the connected component of  $\mathbb{P}_{\mathbb{R}}^{27} \setminus \Delta$  that contains both  $f_0$  and  $f_1$ . Consider the bitangent discriminant  $\mathcal{B}$  of Theorem 2.5.8. There is an open dense subset  $\mathcal{B}_0$  of  $\mathcal{B}$ , whose points represent curves with a single tritangent line or a single flex-bitangent. The exceptional locus  $Z = \mathcal{B} \setminus \mathcal{B}_0$  has codimension at least 2 in  $\mathbb{P}_{\mathbb{R}}^{27}$ , hence  $V = U \setminus Z$  is path-connected. Fix a path  $\gamma: [0, 1] \rightarrow V$  with  $\gamma(0) = f_0$ ,  $\gamma(1) = f_1$ . Let  $\{\gamma(t_1), \dots, \gamma(t_k)\}$  be its intersection points with  $\mathcal{B}$ . Since  $\gamma(t_i)$  lies in  $\mathcal{B}_0$ , the number of connected components of the avoidance locus of  $V_{\mathbb{R}}(\gamma(t))$  cannot change by more than 1 in a neighborhood of  $t_i$ . Indeed, at a point where that number drops by one, exactly three relevant bitangents come together, giving a sextic with a single tritangent in  $\mathcal{B}_0$ . Therefore, along the path  $\gamma$  we cross sextics with any number of convex avoidance components between 0 and 46.  $\square$

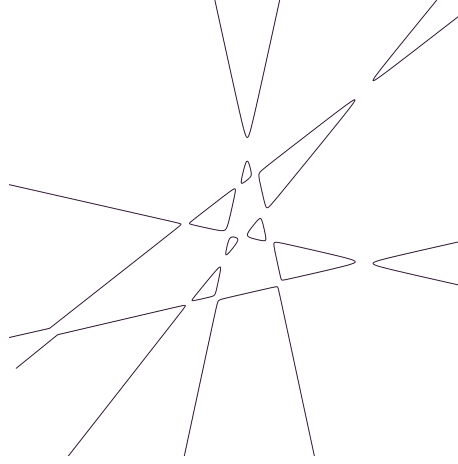


FIGURE 2.12. A smooth sextic with 10 ovals and empty avoidance locus

## 2.6. Reality questions for plane sextics

In this section we extend our experiments and we report on the numbers of real features associated with real sextics in  $\mathbb{P}_{\mathbb{R}}^2$ . The results are summarized in Table 2.7. Certified samples were drawn in the vicinity of each of our current 64 representatives, using the local exploration method that is described after Proposition 2.4.1.

Each row of Table 2.7 has five entries: the name of the rigid isotopy type, numbers of real inflection points, numbers of real eigenvectors, numbers of real bitangents, and one real rank. The numbers are ranges of integers that were observed in our experiments. For instance, for Type 1, which is the type with only one oval, we found numbers ranging between 12 and 56 of real bitangents among 324 complex ones. In some cases, all samples gave the same number of real solutions. For instance, all our Type (71) sextics had 108 real bitangents.

Type	Flex	Eigenvec	Bitang	Rank
0	0	3-31	12	3
1	0-12	3-31*	12-56	3
(11)	0-14	11-31*	12-66	10
2	0-8	5-31*	12-52	13
(21)	0-10	7-31*	16-86	14
(11)1	2-6	7-31*	20-66	15
3	0-8	7-31*	24-94	13
(hyp)	0-14	11-31*	12-52	13
(31)	2-10	19-31*	24-90	13
(21)1	0-6	11-31*	28-72	14
(11)2	0-4	11-31*	32-82	13
4	0-2	11-31*	36-54	11

(41)nd	14-16	21-31*	48-90	16
(41)d	12-14	27-31*	98-104	14
(31)1	2-8	15-31*	40-86	14
(21)2nd	10-16	17-31*	54-82	20
(21)2d	8-16	19-31*	60-70	17
(11)3	8-12	19-31*	48-94	14
5	2-10	19-31*	52-112	15
(51)	12-16	21-31*	54-64	14
(41)1	22	27-31*	90-104	14
(31)2	14-18	27-31*	126-130	14
(21)3	16	27-31*	112-116	14
(11)4	6-10	25-31*	76-106	15
6	10-12	23-31*	78-108	14
(61)	16	27-31*	78-88	14
(51)1nd	16	23-25	110-124	15
(51)1d	20-24	29	136	16
(41)2	16-20	29-31	126-128	14
(31)3nd	12	25-31*	124-148	15
(31)3d	20-22	29	132	16
(21)4	14-20	27-31*	138-142	15
(11)5nd	6-16	29-31*	116-122	16
(11)5d	8-16	25-31*	120-128	16
7	4-14	25-31*	96-124	14
(71)	20-24	29	108	16
(61)1	20-22	25	104-214	15
(51)2	22	25-31	226-228	15
(41)3	20	23-25	154-214	14
(31)4	22	21	162-214	14
(21)5	16-20	29-31	168	13
(11)6	12-14	27-31*	172-176	14
8	0-12	23-31*	124-142	13
(81)nd	18-22	23	122-196	14
(81)d	18-24	29	124-132	12
(71)1	14-18	21-31	104-240	13
(61)2	18-20	23-31	228-276	13
(51)3	22	25	192-254	13
(41)4nd	14-16	25	188-220	9
(41)4d	18	25	194-230	11
(31)5	20	25-31	198-260	13
(21)6	20	23-31	242-258	15
(11)7	14-16	29-31	216	14
9nd	8-16	25-31*	162-172	15
9 d	4-16	29-31*	156	15
(91)	18-22	23	124-236	13
(81)1	16-20	23-31	162-240	14



(51)4	20	27	232-234	10
(41)5	18-20	27-31	232	10
(11)8	14-18	25-31	142-210	13
10	0-24	21-31*	192	12
(91)1	18-22	25-31	200-284	14
(51)5	20-22	25-31	276-306	10
(11)9	16-20	25-31	174-250	14

TABLE 2.7. The results of our computational experiments on the reality of four major features associated to each rigid isotopy class of smooth plane sextics: inflection points, eigenvectors, bitangents and rank.

For the calculation of bitangents we applied numerical methods. This means that, for some instances, the number of real solutions might be undercounted. This can happen when two or more real bitangents lie very close to each other. Bitangents and their applications were discussed in detail in the previous section.

The column concerning the reality of *inflection points* is labeled by “Flex”. In the previous section we discussed that a smooth sextic  $V_{\mathbb{C}}(f) \subset \mathbb{P}^2$  has  $72 = 3 \cdot 6 \cdot 4$  complex inflection points. They are computed as the solutions of the equations

$$f(x, y, z) = \det \begin{bmatrix} \frac{\partial^2 f}{\partial x^2} & \frac{\partial^2 f}{\partial x \partial y} & \frac{\partial^2 f}{\partial x \partial z} \\ \frac{\partial^2 f}{\partial x \partial y} & \frac{\partial^2 f}{\partial y^2} & \frac{\partial^2 f}{\partial y \partial z} \\ \frac{\partial^2 f}{\partial x \partial z} & \frac{\partial^2 f}{\partial y \partial z} & \frac{\partial^2 f}{\partial z^2} \end{bmatrix} = 0.$$

Due to Felix Klein, Brugallé and López de Medrano [8], for a general sextic in  $\mathbb{P}_{\mathbb{R}}^2$ , the number of real inflection points is an even integer between 0 and 24. The data stored in our table comes from an empirical distribution on the 64 rigid isotopy types. Note that  $a - b$  in this column means all even integers  $k$  such that  $a \leq k \leq b$  are observed as the number of real inflection points of a sextic with the corresponding type.

We now give the definitions needed to understand the columns labeled by “Eigenvect” and “Rank” in Table 2.7, namely, we define the *eigenvector* and *rank* of a plane curve. These two columns pertain to the study of tensors in multilinear algebra. Here we identify the space  $\mathbb{R}[x, y, z]_6$  of ternary sextics with the space of symmetric tensors of format  $3 \times 3 \times 3 \times 3 \times 3 \times 3$ . Such a symmetric tensor  $f$  has 28 distinct entries, and these are the coefficients  $c_{ijk}$  of the general sextic (2.4).

A vector  $v = (v_1, v_2, v_3) \in \mathbb{C}^3$  is an *eigenvector* of  $f$  if  $v$  is parallel to the gradient of  $f$  at  $v$ . Therefore, every eigenvector is a solution to

$$(2.9) \quad \text{rank} \begin{bmatrix} v_1 & v_2 & v_3 \\ \frac{\partial f}{\partial x}(v) & \frac{\partial f}{\partial y}(v) & \frac{\partial f}{\partial z}(v) \end{bmatrix} = 1$$

in  $\mathbb{P}_{\mathbb{C}}^2$ . Following [1, Theorem 2.1], a general ternary form  $f$  of degree  $d$  has  $d^2 - d + 1$  eigenvectors. Those vectors are the critical points of restricting  $f$  on the unit sphere  $\mathbb{S}^2 = \{(x, y, z) \in \mathbb{R}^3 : x^2 + y^2 + z^2 = 1\}$ . Since  $f$  attains a minimum and a maximum on  $\mathbb{S}^2$ , the number of real eigenvectors is at least 2. We note that the upper bound  $d^2 - d + 1$  is attained over  $\mathbb{R}$ . Anna Seigal and Bernd Sturmfels in [1, Theorem 6.1] showed that if  $f$  is a product of  $d$  general linear forms, then all its complex eigenvectors are real. Therefore, the number of real eigenvectors of a general ternary sextic is an odd integer between 3 and 31.

The column labeled “Eigenvec” shows the empirical distribution on the rigid isotopy types. For many rigid isotopy types we found instances that attain the maximal number 31 of real eigenvectors. Among them are the 35 types that have unions of six real lines in general position in their closure. These types are marked with an asterisk next to the number 31. We found these by perturbing each of the four combinatorial types of arrangements of six lines in general position in  $\mathbb{P}_{\mathbb{R}}^2$ . This search process resulted in 35 of the rigid isotopy types. This is the result stated in Proposition 2.4. The computation we described is the proof.

Maccioni in [63] proved that the number of real eigenvectors of a ternary form is bounded below by  $2\ell + 1$ , where  $\ell$  is the number of ovals. The result of our experiments in the third column of Table 2.7 confirms this theorem. Moreover, there are seven types where our computations prove the converse, namely that all values between this lower bound and the upper bound 31 are realized in these types.

For real inflection points and real eigenvectors we performed exact computations. That means, we are sure that all numbers listed in the table actually occur. However, we do not know whether there are more possible numbers.

Finally, we explain our data in the last column. The *rank*  $r$  of a ternary form  $f$  of degree  $d$  is the minimum number of summands in a representation

$$(2.10) \quad f(x, y, z) = \sum_{i=1}^r \lambda_i (a_i x + b_i y + c_i z)^d.$$

**Remark 2.6.1** Every tensor is a sum of rank one tensors. The smallest number of summands needed in such a representation is the *rank* of that tensor. This notion depends on the underlying field. Symmetric

tensors of rank 1 are a constant times powers of linear forms. This is the motivation for the definition above.

The computations for estimating the real rank are more delicate than the rest. Similar to the computation of bitangents, in this case also our results are accomplished numerically as the exact determination of the real rank of a sextic  $f$  is very difficult. The task is to decide the solvability over  $\mathbb{R}$  of the equations in the unknowns  $\lambda_i, a_i, b_i, c_i$  obtained by equating coefficients in (2.10). This computation is a challenge for both symbolic and numerical methods. There is no known method that is guaranteed to succeed in practice. If  $f$  is a generic sextic in  $\mathbb{R}[x, y, z]_6$  then the complex rank of  $f$  is 10, and the real rank of  $f$  is an integer between 10 and 19. This was shown in [66, Proposition 6.3]. We expect that 19 is not a tight upper bound for the real rank.

A standard package for tensors, that is widely used in the engineering community is the software `tensorlab` [83]. This program furnishes a local optimization method for the following problem: given  $f$  and  $r$ , find a sextic  $f^*$  of rank  $r$  that is closest to  $f$ , with respect to the Euclidean distance on the tensor space  $(\mathbb{R}^3)^{\otimes 6}$ . If the output  $f^*$  is very close to the input  $f$ , we can be confident that  $f$  has real rank  $\leq r$ . If  $f^*$  is far from  $f$ , even after many tries with different starting parameters, then we believe that  $f$  has real rank  $\geq r + 1$ .

We found the software `tensorlab` the best existing tool for our rank experiments, however, it does not furnish any guarantees. To increase our accuracy, we needed to rerun the same instance many times to achieve a lower bound on the real rank. Obtaining these numbers with high confidence proved to be difficult. We had considerable help from Anna Seigal and Emanuele Ventura in carrying this out. Most puzzling is the real rank 20 we found for our representative of type (21)2nd, as this seems to contradict [66, Proposition 6.3]. This is either an error arising in our numerical method, or the sextic lies on some exceptional locus.

This could be an interesting future project at the interface of numerics and real algebraic geometry to do the same calculation for a larger sample of sextics in each rigid isotopy class. The guiding problem is to find the maximal generic real rank among sextics. The following question that yet has remained unanswered underscores the challenge.

**Problem.** In [66, Example 6.7], it is shown that the real rank of the monomial  $x^2y^2z^2$  is either 11, 12 or 13. Verify the correct rank.

Our experimental data in this section needs further improvement, however, each entry in Table 2.7 can be also regarded as a conjecture. For example, we conjecture that smooth sextics with topological types (71) and (21)5 have 108 and 168 real bitangents, respectively.

## 2.7. Connections to K3 surfaces

In our final section of this chapter we discuss implications for real K3 surfaces and their connections to plane sextics. In particular we show how to construct quartic surfaces in  $\mathbb{P}_{\mathbb{R}}^3$  with prescribed topology. An *algebraic surface* is the zero locus of a polynomial equation in  $\mathbb{P}_{\mathbb{C}}^3$ . A *quartic surface* is an algebraic surface of degree four. i.e. the defining equation is a homogeneous polynomial of degree four in four unknowns. Two basic models of algebraic K3 surfaces are quartic surfaces in  $\mathbb{P}^3$  and double-covers of  $\mathbb{P}^2$  branched at a sextic curve. We start with briefly explaining a well-known example for such a surface. See [42] for details.

Let  $K \subset \mathbb{P}^3$  be a quartic surface with a node  $p$ . Let  $K'$  be the blow-up of  $K$  at  $p$ . There is a two-to-one projection from  $K'$  to  $\mathbb{P}^2$ . The ramification locus of this double cover is a plane curve  $C$  of degree six, and all the nodes of  $K$  which are not  $p$  map to the nodes of  $C$ . One can also check that there is a “reverse direction” to this process.

By the genus degree formula, the maximum number of nodes on a plane curve  $C$  of degree six is 15. This is attained when  $C$  is the union of six lines intersecting in pairwise distinct points. Therefore a quartic surface has at most 16 nodes. Quartic surfaces attaining this bound are called *Kummer surfaces*. They were first discovered by Ernst Eduard Kummer in his geometrical studies with applications to ray systems and ballistics, following the work of William Rowan Hamilton. Figure 2.13 shows a Kummer surface and the corresponding plane sextic where all of the complex nodes are real.

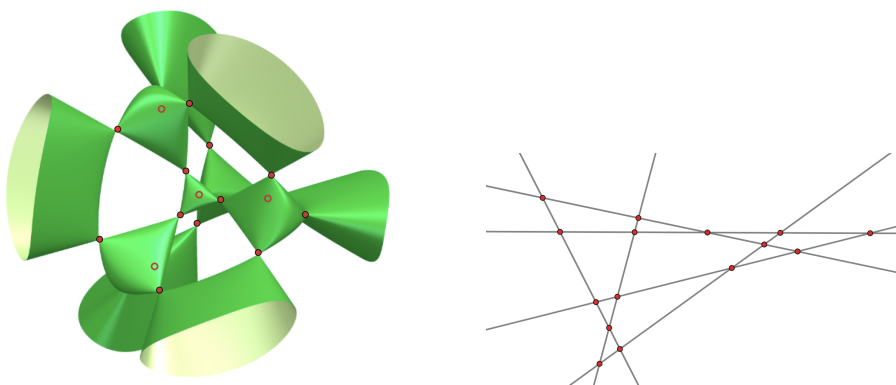


FIGURE 2.13. A Kummer surface with 16 real nodes and the corresponding plane sextic

In a similar manner, each of our ternary sextics in Section 2.3 represents a K3 surface over  $\mathbb{Q}$ . Suppose we can write  $f = v_3^2 - v_2v_4$  where  $v_i$  is a homogeneous polynomial of degree  $i$  in  $x, y, z$ . Then  $F = v_2w^2 + 2v_3w + v_4$  is a quartic in four variables that realizes the K3

surface with one singular point at  $(0 : 0 : 0 : 1)$ . Blowing up that singular point gives the K3 surface encoded by  $f$ . Perturbing the coefficients of  $F$  gives a smooth quartic surface with similar properties.

As the relevance between reality of nodes on a Kummer surface and the corresponding plane sextic suggests, the real topology of the surface  $V_{\mathbb{R}}(F)$  is determined by the topological type of the real curve  $V_{\mathbb{R}}(f)$  and its sign behavior. By perturbing  $F$  to a polynomial  $\tilde{F}$ , we can obtain a smooth quartic surface whose real part  $V_{\mathbb{R}}(\tilde{F})$  has the desired topology. See [82] for details.

In Section 2.3 we have shown that many of the 64 types can be constructed by adding a positive sextic to the product of a plane quartic and a plane conic. For such types, the sextic has the desired form  $f = v_3^2 - v_2v_4$ . The resulting quartic  $F$  can be expressed with reasonably small integer coefficients.

Let  $S \subset \mathbb{P}^3$  be a smooth K3 surface. Its real part  $S_{\mathbb{R}} \subset \mathbb{P}_{\mathbb{R}}^3$  is an orientable surface with at most one connected component. Unless  $S_{\mathbb{R}}$  is the union of two tori, it has non-positive Euler characteristic and therefore it is determined (up to homeomorphism) by its total Betti number and its Euler characteristic. If  $S_{\mathbb{R}}$  is nonempty, by Smith-Thom inequality its total Betti number ranges between 2 and 24, and according to the Comessatti inequalities its Euler characteristic ranges between  $-18$  and  $20$ . There are 64 possible combinations of these two numbers; they are displayed in [80, Table (3.3), page 189]. All these 64 possibilities can be realized as a quartic surface in  $\mathbb{P}^3$ . These topological classification was studied by Utkin [82]. The isotopic and rigid isotopic classifications are due to Kharlamov [47, 49]. We refer to Silhol's book [80, Section VIII.4] for proofs and further information.

We now conclude this section by presenting two explicit quartic surfaces that realize the minimal and the maximal Euler characteristic. The following example for the minimal case arises from a plane sextic with ten empty ovals.

**Example 2.7.1** Let  $\bar{F} \in \mathbb{C}[x, y, z, w]_4$  be defined as

$$\begin{aligned} \bar{F} = & 100w^4 - 12500w^2x^2 + 104x^4 - 12500w^2y^2 + 1640x^2y^2 + 1550y^4 \\ & + 12500w^2yz - 75x^2yz - 1552y^3z + 9375w^2z^2 - 487x^2z^2 \\ & - 1533y^2z^2 + 354yz^3 + 314z^4. \end{aligned}$$

The variety  $V_{\mathbb{C}}(\bar{F}) \subset \mathbb{P}^3$  is smooth and its real locus  $V_{\mathbb{R}}(\bar{F})$  is a connected orientable surface of genus 10. The Euler characteristic of that surface is  $-18$ . This is the smallest possible Euler characteristic for a real K3 surface. To construct the quartic  $\tilde{F}$  from a sextic  $f$  of the form

$f = v_3^2 - v_2v_4$ , we set

$$\begin{aligned} v_2 &= -4x^2 - y^2 + 2yz + 3z^2, \\ v_3 &= 10^{-3}z^3, \\ v_4 &= 33001x^4 + 131227x^2y^2 + 30980y^4 - 11842x^2yz - 62072y^3z \\ &\quad - 155986x^2z^2 - 122652y^2z^2 + 56672yz^3 + 100672z^4. \end{aligned}$$

The plane sextic  $V_{\mathbb{C}}(f)$  is smooth and the real part  $V_{\mathbb{R}}(f)$  has Type 10. These informations we easily obtained by using our code `SexticClassifier`. The quartic

$$F = v_2w^2 + 2v_3w + v_4$$

has a node at  $(0 : 0 : 0 : 1)$ . The curve  $V_{\mathbb{C}}(f)$  is the ramification locus of the projection from this node. To smoothening the singular surface  $V_{\mathbb{C}}(F)$  we make a small perturbation. For sufficiently small  $\epsilon$ , for example  $\epsilon = 10^{-10}$ , the K3 surface defined by  $\tilde{F} = F + \epsilon w^4$  has the desired properties. Now we use the techniques discussed in Section 2.3 for polishing the polynomials by improving integer coefficients and to obtain  $\bar{F}$  from  $\tilde{F}$ .

Finally, we dedicate our last example which is the closing of this chapter to our favorite algebraic geometer Karl Rohn. He was a professor at the University of Leipzig from 1904 until 1920 and his inspiring article [75] was our motivation for this project.

**Example 2.7.2** Let  $G \in \mathbb{C}[x_0, x_1, x_2, x_3]_4$  be defined as

$$G = \tau(s_1^2 - 6s_2)^2 + (s_1^2 - 4s_2)^2 - 64s_4,$$

where  $s_i$  is the  $i$ th elementary symmetric polynomial in  $x_0, \dots, x_3$ , i.e.

$$\begin{aligned} s_1 &= x_0 + x_1 + x_2 + x_3, \\ s_2 &= x_0x_1 + x_0x_2 + x_0x_3 + x_1x_2 + x_1x_3 + x_2x_3, \\ s_4 &= x_0x_1x_2x_3, \end{aligned}$$

and  $\tau = (16\sqrt{10} - 20)/135$ . This quartic is Rohn's imaginary symmetroid in [75, §9]. The variety of this nonnegative form  $V_{\mathbb{C}}(G) \subset \mathbb{P}^3$  is exactly ten points with real coordinates. Subtracting a positive definite form multiplied with a small positive scalar gives a quartic surface with ten connected components. The surface  $V_{\mathbb{R}}(\bar{G})$  is the disjoint union of ten spheres, so it has Euler characteristic 20. To represent this instance we use the techniques in Section 2.4 and construct

$$\bar{G} = 6s_1^4 - 53s_1^2s_2 + 120s_2^2 - 320s_4.$$

which has nicer integer coefficients.

So far, we have explored the topological and rigid isotopy classifications of smooth plane sextics. We gave an exact computation for the discriminant and we constructed an example for each rigid isotopy type of plane sextics. Using our representative polynomials together

with the software that we developed to identify the topological type of a given sextic curve, we ran many experiments. Tables 2.2 to 2.6 show the results of our probabilistic studies and Table 2.7 summarizes our computational data on the reality of some key features associated to the real part of a plane sextic. Algorithm 2.5.7 constructs the avoidance locus of a plane curve from its real bitangents. We found an upper bound for the number of connected components of the avoidance locus of a plane curve, and we proved that for plane sextics, any number between zero and this upper bound is realizable. These two results appear in Proposition 2.5.2 and Corollary 2.5.9, respectively. Finally, we finished our discussion about plane sextics with briefly explaining their connections to K3 surfaces. We are now ready to move on to three-dimensional projective space and explore space sextics and their real features.

## CHAPTER 3

### Real Space Sextics and their Tritangents

In this chapter, we present a computational study of canonical curves of genus 4 over the field  $\mathbb{R}$  of real numbers. Such a curve  $C$ , provided it is smooth and non-hyperelliptic, is the complete intersection in  $\mathbb{P}^3$  of a unique surface  $Q$  of degree two and a (non-unique) surface  $K$  of degree three. Conversely, any smooth complete intersection of a quadric and a cubic in  $\mathbb{P}^3$  is a genus 4 curve. The degree of  $C = Q \cap K$  is six: any plane in  $\mathbb{P}^3$  meets  $C$  in six complex points, counting multiplicity. We refer to such a curve  $C$  as a *space sextic*.

We denote the canonical divisor class of the smooth curve  $C$  by  $\kappa_C$ . A *theta characteristic* of  $C$  is a divisor class  $\theta$  such that  $2\theta = \kappa_C$ . A theta characteristic is *odd* if  $\dim H^0(C, \theta)$  is odd and is *even* otherwise. An even theta characteristic is said to be *vanishing* if  $\dim H^0(C, \theta) > 0$ .

For a smooth proper surface  $X$ , we use the terminology of *intersection pairing*, *exceptional curve*, and *blow-up/blow-down* from [39, Chapter V]. A *del Pezzo surface  $X$  of degree 1* is a smooth sextic surface in  $\mathbb{P}(1 : 1 : 2 : 3)$  with weighted coordinates  $(u : v : w : r)$  of the form

$$X_{\mathcal{P}}: \lambda r^2 = f_0 w^3 + f_2(u, v) w^2 + f_4(u, v) w + f_6(u, v),$$

where each  $f_d$  is homogeneous polynomial of degree  $d$  and  $\lambda, f_0 \in k$  are nonzero. Without loss of generality, one may always assume that  $\lambda = f_0 = 1$ .

Since  $C$  is a smooth space sextic, it has exactly 120 odd theta characteristics and there is no theta characteristic  $\theta$  such that  $\dim H^0(C, \theta) > 2$  (as  $\dim H^0(C, 2\theta) = 4$ ). In particular, each odd theta characteristic  $\theta$  has a unique effective representative which we will refer to as  $D_\theta$ . Since  $C$  is its own canonical model, by definition we have that  $2D_\theta$  is cut out by linear form which we will denote  $l_\theta$ . Let  $\theta$  be an odd theta characteristic of  $C$ . We call the zero locus  $H_\theta := V(l_\theta) \subseteq \mathbb{P}^3$  the *tritangent plane* associated to  $\theta$ . Any plane  $H \subseteq \mathbb{P}^3$  of this form is called a *tritangent plane* of  $C$  or *tritangent* for short.

Note that we exclude from consideration planes which are tangent to  $C$  at 3 points (counted with multiplicity) but do not arise from odd theta characteristics. If the unique quadric  $Q_C$  containing  $C$  is smooth then every plane tangent to  $C$  at 3 points is a tritangent plane in the sense of our definition above [38, Theorem 2.2]. However, if  $Q$  is singular, then the curve  $C$  has infinitely many tritangents. We can see this as follows. Any plane  $H$  tangent to  $Q$  contains the singular point



of  $Q$ , and it is tangent to  $Q$  at every point in the line  $H \cap Q$ . Since the intersection of  $H$  and  $C$  is contained in  $Q$ , the plane  $H$  is tangent to  $C$  at every point in  $C \cap H$ . These planes do not correspond to odd theta characteristics.

In what follows we focus on the case when the quadric surface  $Q$  containing the space sextic  $C$  is singular. A tritangent is *real* if it is defined by a linear form with real coefficients. A real tritangent is *totally real* if it touches the curve  $C$  at three distinct real points.

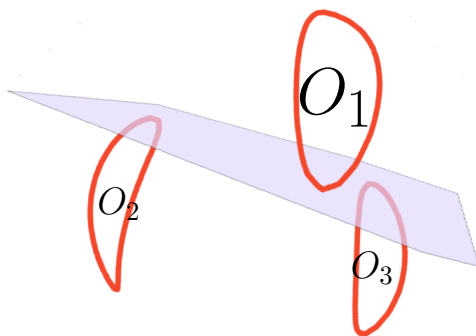


FIGURE 3.1. Totally real tritangent of a curve with three ovals. The plane touches  $O_1$  on one side and  $O_2, O_3$  on the other.

A space sextic  $C$  has at most five ovals [38, §3], since the maximum number of ovals is the genus of  $C$  plus one. By [38, Proposition 3.1], all 120 tritangents of  $C$  are real if and only if the number of ovals of  $C$  attains this upper bound. A heuristic argument suggests that at least  $80 = \binom{5}{3} \times 8$  of the 120 real tritangents are totally real, since eight planes can touch three ovals as in Figure 3.1. The analogous fact for genus three curves is true: a plane quartic with four ovals has 28 real bitangents, of which at least  $24 = \binom{4}{2} \times 4$  are totally real. The situation is more complicated in genus 4, as seen in Figure 3.2.

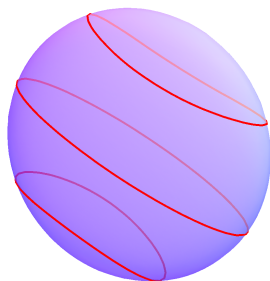


FIGURE 3.2. No tritangent touches all three ovals of this sextic curve on the smooth quartic.

In 1928, Emch [26, §49] asked whether there exists a space sextic with all of its 120 tritangent planes totally real. He exhibited a curve suspected to attain the bound 120. However, ninety years later, Harris and Len [38, Theorem 3.2] showed that only 108 of the tritangents of Emch's curve are totally real. In [38, Question 3.3] they reiterated the question whether 120 totally real tritangents are possible. Our Example 3.3.1 answers that question affirmatively.

**Theorem 3.1** *The number of totally real tritangents of a space sextic with five ovals can be any integer between 84 and 120. Each of these numbers is realized by an open semialgebraic set of such curves.*

This chapter is organized as follows. In Section 3.1 we construct space sextics associated with del Pezzo surfaces of degree one. These curves lie on a singular quadric  $Q$  and are obtained by blowing up eight points in the plane. This construction has the advantage of producing 120 rational tritangents when the points are rational. In Section 3.2 we construct these 120 planes and we explain a method to decide which are totally real depending on the configuration of the eight points. In Section 3.3 we present a set of eight points with integer coordinates which gives rise to a space sextic with 120 totally real tritangents. This solves the long lasting problem by Emch. In the same section, we also prove Theorem 3.1.

In Section 3.4 we extend this construction to real curves obtained from complex configurations in  $\mathbb{P}^2$  that are invariant under complex conjugation. Theorem 3.4.1 summarizes what we found about these special space sextics. In Section 3.5 we turn to arbitrary space sextics, where  $Q$  is now generally smooth, and we show how to compute the 120 tritangents of  $C = Q \cap K$  directly from the equations defining  $Q$  and  $K$ . Section 3.6 offers a study of the discriminants associated with our polynomial system, and Section 3.7 sketches some directions for future research. Finally, the scripts used throughout this chapter are available at [55].

### 3.1. Space sextics from del Pezzo surfaces of degree 1

We shall employ the classical construction of space sextics from del Pezzo surfaces of degree one. We describe this construction below and direct the reader to [23, §8] or [53, §2] for further details. Any space sextic  $C$  that is obtained from this construction is special: the quadric  $Q$  that contains  $C$  is singular. See also [52], where these curves  $C$  are referred to as *uniquely trigonal genus 4 curves*.

These curves are special as the unique quadric containing it is singular. Nevertheless, the construction remains a valuable source of space sextics as many interesting qualities of them are both computationally and conceptually much more accessible compared to the generic

case. In Proposition 4.4.1 we show that any space sextic on a singular quadric arises this way. Moreover, we describe special algorithms which compute the 120 tritangents.

Fix a configuration  $\mathcal{P} := \{P_1, \dots, P_8\} \subseteq \mathbb{P}^2$  of eight points in  $\mathbb{P}_{\mathbb{R}}^2$ . We may assume that  $\mathcal{P}$  is sufficiently generic to allow for the choices to be made below. Additionally, genericity of  $\mathcal{P}$  ensures that the resulting space sextic  $C$  is a smooth curve in  $\mathbb{P}^3$ . For practical computations we always choose points  $P_i$  whose coordinates are in the field  $\mathbb{Q}$  of rational numbers. This ensures that each object arising in our computations is defined over  $\mathbb{Q}$ .

First, note that the space of plane cubics through  $\mathcal{P}$  has dimension  $10 - 8 = 2$ . Let  $\{u, v\}$  be any basis of it. Next, observe that the space of plane sextics vanishing doubly on  $\mathcal{P}$  has dimension  $28 - 8 \cdot 3 = 4$ . It is spanned by  $\{u^2, uv, v^2, w\}$  for some sextic  $w$ . Further, the space of plane nonics vanishing triply on  $\mathcal{P}$  has dimension  $55 - 8 \cdot 6 = 7$ . It is spanned by  $\{u^3, u^2v, uv^2, v^3, uw, vw, r\}$  for some nonic  $r$ . This defines a rational map

$$\begin{aligned} \psi: \quad \mathbb{P}^2 &\dashrightarrow \mathbb{P}(1:1:2:3) \\ (x:y:z) &\longmapsto (u(x,y,z):v(x,y,z):w(x,y,z):r(x,y,z)). \end{aligned}$$

The closure of the image of  $\psi$  is cut out by a single equation of degree six. As it turns out, we can say a lot about the image of  $\psi$  [64, Remark 24.4.2].

**Proposition 3.1.1** *The image of  $\psi$  is a del Pezzo surface of degree 1.*

Henceforth, we let  $X_{\mathcal{P}} := \overline{\text{Im}(\psi)}$ . By abuse notation we label the coordinates of  $\mathbb{P}(1:1:2:3)$  by  $u, v, w, r$  (respectively, with respect to weights). After a linear change of coordinates we can write the defining equation of  $X_{\mathcal{P}}$  in  $\mathbb{P}(1:1:2:3)$  as

$$X_{\mathcal{P}}: r^2 = w^3 + f_2(u, v) \cdot w^2 + f_4(u, v) \cdot w + f_6(u, v),$$

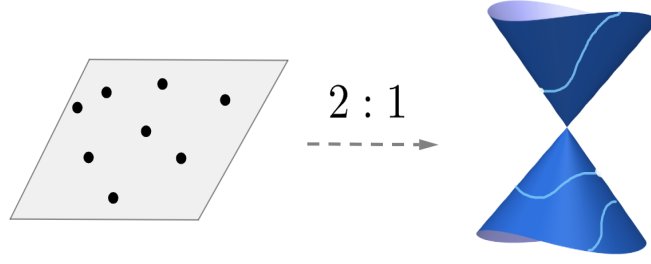
such that each  $f_2, f_4, f_6$  is homogeneous degree 2, 4, 6 respectively.

Now consider the projection  $\pi: \mathbb{P}(1:1:2:3) \rightarrow \mathbb{P}(1:1:2)$  onto its first three coordinates and an embedding  $\phi$  of  $\mathbb{P}(1:1:2)$  as a singular quadric in  $\mathbb{P}^3$ , which is illustrated in Figure 3.3.

The projection  $\pi$  is a generically 2-to-1 rational map branched along the curve  $C'$  of weighted degree six given by  $r = 0$ . The defining equation of  $C'$  in  $\mathbb{P}(1:1:2)$  is hence given by

$$(3.1) \quad C': \quad 0 = w^3 + f_2(u, v) \cdot w^2 + f_4(u, v) \cdot w + f_6(u, v).$$

The embedding  $\phi$  is an isomorphism between  $\mathbb{P}(1:1:2)$  and  $V(x_1^2 - x_0x_2) \subseteq \mathbb{P}^3$ , where  $(x_0:x_1:x_2:x_3)$  are the homogeneous coordinates of  $\mathbb{P}^3$ . The curve  $C := \phi(C')$  is therefore a space sextic which lies on a singular quadric.



$$\begin{array}{ccc}
 \mathbb{P}^2 & \xrightarrow{\psi} & \mathbb{P}(1:1:2:3) \supseteq X_{\mathcal{P}} := \psi(\mathbb{P}^2) \\
 \pi \downarrow & & \downarrow (u:v:w:r) \\
 & & (u:v:w) \\
 & & \downarrow \\
 & & \mathbb{P}(1:1:2) \supseteq C' := \text{BranchCurve}(\pi|_{X_{\mathcal{P}}}) \\
 \phi \downarrow & & \downarrow (u:v:w) \\
 & & (u^2:uv:v^2:w) \\
 & & \downarrow \\
 \mathbb{P}^3 & \supseteq & C
 \end{array}$$

FIGURE 3.3. The ramification locus of the 2-to-1 rational map  $\phi \circ \pi \circ \psi$  is the space sextic lying on a singular quadric.

### 3.2. Constructing the tritangents

Note that any tangent plane of the singular quadric  $V(x_1^2 - x_0x_2) \subseteq \mathbb{P}^3$  is tangent to the curve  $C$  at its points of intersection; the plane intersects the quadric in a double line passing through the node of the cone, which in turn intersects the cubic in three double points. However, because all intersection points lie on a line through the node of the cone, the tangent plane arises from an even theta characteristic rather than an odd theta characteristic, which is why we will disregard them in the context of this chapter.

**Proposition 3.2.1** *Let  $C$  be a space sextic curve on a singular quadric  $Q$ . Then any plane corresponding to an odd theta characteristic of  $C$  does not pass through the singularity of  $Q$ .*

**PROOF.** Let  $H$  be a plane passing through the node of  $Q$  such that  $H$  is tangent to  $C$  at each point in  $C \cap H$ . As  $H$  passes through the node of  $Q$ , we have that  $H \cap Q$  is the union of two lines which each meet  $C$  in three points. As each point in  $C \cap H$  has even multiplicity, the two lines must be coincident. But then the class of the divisor  $\frac{1}{2}(C \cap H)$  of  $C$  is the vanishing even theta characteristic.  $\square$

We derive 120 tritangents of our curve  $C$  in  $\mathbb{P}^3$  from the 240 exceptional curves on the del Pezzo surface  $X_{\mathcal{P}}$  (cf. Lemma 3.2.2). There is an order two automorphism  $\iota$  of  $X_{\mathcal{P}}$ , called the *Bertini involution*. The image of an exceptional curve  $e$  under the Bertini involution  $\iota$  is another exceptional curve  $e' = \iota(e)$ . If  $\varphi := \phi \circ \pi: X_{\mathcal{P}} \rightarrow V(x_0x_2 - x_1^2)$  is the 2-to-1 covering branched along  $C$ , then  $\varphi \circ \iota = \varphi$ . In particular,  $\varphi(e) = \varphi(e')$ . The intersection  $e \cap e'$  consists of three points on  $X_{\mathcal{P}}$ . Their image under  $\varphi$  is the triple of points at which the tritangent corresponding to  $\{e, e'\}$  touches  $C$ . We can thus decide whether a tritangent is totally real by checking whether the intersection  $e \cap e'$  in  $X_{\mathcal{P}}$  contains one or three real points. This intersection can be carried out in  $\mathbb{P}^2$ , as we shall explain next.

Recall that  $X_{\mathcal{P}}$  is the blow-up of  $\mathbb{P}^2$  at  $\mathcal{P}$ . By blowing down, we may view the eight exceptional fibers of the blow-up as the eight points of  $\mathcal{P}$ , and we may view the remaining 112 exceptional curves of  $X_{\mathcal{P}}$  as (possibly singular) curves in  $\mathbb{P}^2$ . We can determine the images of the exceptional curves in  $\mathbb{P}^2$  from [81, Table 1], as well as how they are matched into pairs  $\{e, e'\}$  via the Bertini involution. We named the following types after their degrees in  $\mathbb{P}^2$ .

8 pairs of type (0,6):

The exceptional fiber at one point  $P_i$  matches the sextic vanishing triply at  $P_i$  and doubly at the other seven points. The three components of the tangent cone of this sextic determine the three desired points on the branch curve  $C$ .

$\binom{8}{2} = 28$  pairs of type (2,5):

The line through  $P_i$  and  $P_j$  matches the quintic vanishing at all eight points and doubly at the six points in  $\mathcal{P} \setminus \{P_i, P_j\}$ . Their intersection in  $\mathbb{P}^2 \setminus \mathcal{P}$  consists of three complex points. Either one or three of them are real (see Figure 3.4).

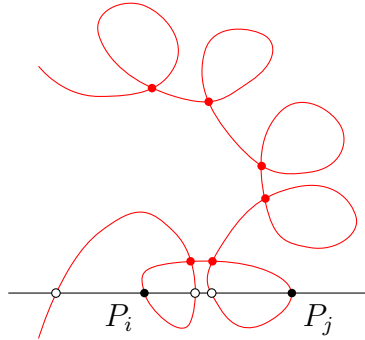


FIGURE 3.4. 28 lines pair with 28 rational quintics

$\binom{8}{3} = 56$  pairs of type (2,4):

The conic through  $P_{i_1}, \dots, P_{i_5}$  matches the quartic vanishing at  $\mathcal{P}$  and doubly at the three other points. Their intersection in  $\mathbb{P}^2 \setminus \mathcal{P}$  consists of three complex points (see Figure 3.5).

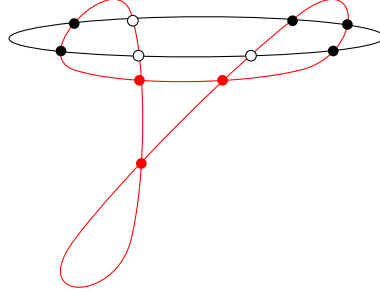


FIGURE 3.5. 56 conics pair with 56 rational quartics

$\binom{8}{2} = 28$  pairs of type (3,3):

For two points  $P_i$  and  $P_j$ , the cubic vanishing doubly at  $P_i$ , non-vanishing at  $P_j$ , and vanishing singly at  $\mathcal{P} \setminus \{P_i, P_j\}$  matches the cubic vanishing doubly at  $P_j$ , non-vanishing at  $P_i$ , and vanishing singly at  $\mathcal{P} \setminus \{P_i, P_j\}$ . Their intersection in  $\mathbb{P}^2 \setminus \mathcal{P}$  consists of three points in  $\mathbb{P}^2$  (see Figure 3.6).

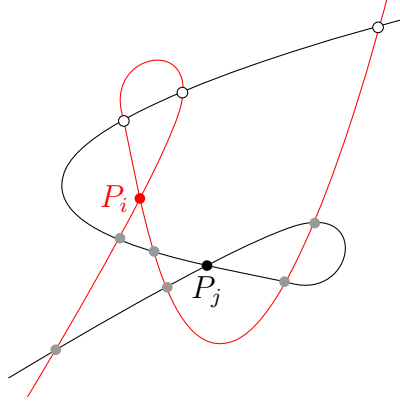


FIGURE 3.6.  $\mathcal{P}$  determines 28 pairs of rational cubics

The following lemma summarizes the reality issues on the del Pezzo surface  $X_{\mathcal{P}}$  that arises from the constructions in  $\mathbb{P}^2$  described above.

**Lemma 3.2.2** *Let  $\{e, e'\}$  be a pair of exceptional curves of type (0,6), (1,5), (2,4) or (3,3) contained in the del Pezzo surface  $X_{\mathcal{P}}$ . Then  $\varphi(e \cap e')$  spans a tritangent plane of the space sextic  $C$  in  $\mathbb{P}^3$ . That tritangent is totally real if and only if the intersection  $e \cap e'$  is real on  $X_{\mathcal{P}}$ .*

PROOF. Let  $-\kappa$  be the anticanonical divisor class of  $X_{\mathcal{P}}$ . Then  $-\kappa$  and  $-2\kappa$  are ample but not very ample. The class  $-3\kappa$  is very ample, and its linear system embeds  $X_{\mathcal{P}}$  into  $\mathbb{P}^6$ . Consider the sequence of maps  $\mathbb{P}^2 \dashrightarrow X_{\mathcal{P}} \rightarrow V(x_0x_2 - x_1^2) \subset \mathbb{P}^3$ . The first map is the blow-up  $\psi$ , which is birational. The second map is the 2-1 morphism  $\varphi$  given by the linear system  $| -2\kappa |$ . The second map takes the 240 exceptional curves in pairs  $\{e, e'\}$  onto the 120 hyperplane sections of  $V(x_0x_2 - x_1^2)$  defined by the tritangent planes of  $C$ .

The pairs are as indicated above, since their classes add up to  $-2\kappa$  by [81, Table 1]. Intersection points of the pairs of curves on  $X_{\mathcal{P}}$  become singular points of the intersection curves on  $V(x_0x_2 - x_1^2)$ , so the planes are tangent at those points. The tritangent being totally real means that these three points have real coordinates.  $\square$

### 3.3. 120 totally real tritangents

In this section, we present a concrete instance (Example 3.3.1) that we found of a space sextic for which all 120 complex tritangents are totally real. This corrects a mistake by Emch [26, §49] in 1928 and answers the follow up question [38, Question 3.3] by Harris and Len.

Following [53, Example 2.5], we parametrize the singular quadric  $Q$  as  $\{(1 : t : t^2 : W)\}$ . This represents  $C$  by a polynomial in two unknowns  $(t, W)$  that has Newton polygon  $\text{conv}\{(0, 0), (6, 0), (0, 3)\}$ :

$$(3.2) \quad C : t^6 + c_1t^5 + c_2t^4W + c_3t^4 + c_4t^3W + c_5t^2W^2 + c_6t^3 + c_7t^2W + c_8tW^2 + c_9W^3 + c_{10}t^2 + c_{11}tW + c_{12}W^2 + c_{13}t + c_{14}W + c_{15}.$$

In our computations, the del Pezzo surface  $X_{\mathcal{P}}$  is represented by  $(\mathbb{P}^2, \mathcal{P})$ . For each of the triples of points described above, we can compute their images in  $V(x_0x_2 - x_1^2) \subset \mathbb{P}^3$  using Gröbner-based elimination. These triples are the contact points of the corresponding tritangent plane of  $C$ . We may choose an affine open subset of  $V(x_0x_2 - x_1^2)$ , isomorphic to  $\mathbb{A}^2$ , containing these three points. The intersection of a plane in  $\mathbb{P}^3$  with the singular quadric  $Q$  is represented on this open subset by a plane curve with Newton polygon  $\text{conv}\{(0, 0), (2, 0), (0, 1)\}$ . We normalize this as follows:

$$(3.3) \quad \text{tritangent planes:} \quad t^2 + \alpha_1t + \alpha_2 + \alpha_3W.$$

The upper bound in Theorem 3.1 is attained in the following example.

**Example 3.3.1** Consider the following configuration of eight points:

$$\mathcal{P} = \{ (1:0:0), (0:1:0), (0:0:1), (1:1:1), (10:11:1), \\ (27:2:17), (-19:11:-12), (-15:-19:20) \} \subset \mathbb{P}_{\mathbb{R}}^2.$$

The resulting space sextic  $C$  in  $V(x_0x_2 - x_1^2)$  has 120 totally real tritangents. We prove this by computing the pairs of special curves in  $\mathbb{P}^2$  and by computing their triples of intersection points as described

above. For each of the  $112 = 28_{(1,5)} + 56_{(2,4)} + 28_{(3,3)}$  pairs of curves as above, we found that all three intersection points are real. We verified that the remaining eight tritangents of  $C$  are also totally real by computing the tangent cones of the special sextics in item 8.

We now convert the curve  $C$  to the format in (3.2). From that we can recover the pair  $(Q, K)$  defining the canonical model of  $C$ , for the independent verification in Example 3.5.1. We start by computing the cubics  $u, v$ . They are minimal generators of the ideal  $I := \bigcap_{i=1}^8 \mathfrak{m}_{P_i}$ , where  $\mathfrak{m}_{P_i}$  denotes the maximal ideal corresponding to the point  $P_i$ :

$$\begin{aligned} u &= 7151648400xy^2 - 434820164119x^2z + 354394201544xyz \\ &\quad - 38806821565y^2z + 692107405715xz^2 - 580026269975yz^2, \\ v &= 14303296800x^2y - 782195108453x^2z + 613370275528xyz - \\ &\quad 49450554755y^2z + 1245021817105xz^2 - 1041049726225yz^2. \end{aligned}$$

Next, we compute the sextic  $w$ . It is the element of lowest degree in  $I^{(2)} \setminus I^2$ , where  $I^{(2)}$  is the *symbolic square* of the ideal  $I$ . We find

$$\begin{aligned} w &= 175674063641748261863073581969689280x^4yz \\ &\quad + 11115515429554564750686439346701440x^3y^2z \\ &\quad - 445819563363162103552629662552521920x^2y^3z \\ &\quad + 264167833624792096768707005238371200xy^4z \\ &\quad - 20036962656454818365487885637968107x^4z^2 \\ &\quad - 294913066878605444782558855953184976x^3yz^2 \\ &\quad - 44062271090476792370117994521819642x^2y^2z^2 \\ &\quad + 755657199632193956412295956477085200xy^3z^2 \\ &\quad - 416363969347671237983809688854251675y^4z^2 \\ &\quad + 32905512814926710254817331888615230x^3z^3 \\ &\quad + 28993156637165570509985808089578930x^2yz^3 \\ &\quad + 40808451826702177753226924348677890xy^2z^3 \\ &\quad - 78682528595564243828185219353313650y^3z^3 \\ &\quad - 1745283730188673093290045100489475x^2z^4 \\ &\quad - 5237850029165498581303629066909850xyz^4 \\ &\quad - 2460237915794525755410066318259875y^2z^4. \end{aligned}$$

The curve  $C$  is defined by the generator of the principal ideal

$$\left( (\langle \det J(u, v, w) \rangle + \text{Minors}_{2 \times 2} \begin{pmatrix} u^2 & uv & v^2 & w \\ 1 & t & t^2 & W \end{pmatrix}) : \langle u, v \rangle^2 \right) \cap \mathbb{Q}[t, W],$$

where  $J(u, v, w)$  is the Jacobian matrix of the map  $(x, y, z) \mapsto (u, v, w)$ . The determinant of  $J(u, v, w)$  gives the singular model of the branch curve in  $\mathbb{P}^2$  and the  $2 \times 2$  minors determine its image in the singular quadric in  $\mathbb{P}^3$ . In our case, the generator of the principal ideal is in the



form of (3.2), and explicitly is given by

$$\begin{aligned}
C : & 22070179871476654215734436981460373192064947078797748209t^6 \\
& + 5585831392725719195345163470516310362705889042844010328t^5 \\
& + 14175569812724447393500233789877848531491265t^4W \\
& - 447718078603500717216424896040737869157828321607704039864t^4 \\
& - 86567655386571901223236593151698362962027440t^3W \\
& + 57114529769698357624742306475t^2W^2 \\
& + 474302309016648096934423520799618219755274954155075926592t^3 \\
& + 192856342071229007723481356183461213738057680t^2W \\
& - 194302706043604453258752959400tW^2 - 26371599148125W^3 \\
& + 2341397816853864817617847981162945070584483528261510775184t^2 \\
& - 183528856281941126263893376861009344326329920tW \\
& + 164969244105921949388612135400W^2 \\
& - 5390258693970772695117811943833419754488807920338145746560t \\
& + 61550499069700173478724063089387654812308400W \\
& + 3193966974265623365398753846860968247266969720956505401600.
\end{aligned}$$

We next compute each of the 120 tritangent planes explicitly, in the format (3.3). For instance, the tritangent that arises from the line spanned by the points  $(10:11:1)$  and  $(27:2:17)$  in  $\mathcal{P}$  is found to be

$$\begin{aligned}
& 345059077005W - 153208173277626716984179949t^2 \\
& + 277165925195542929496239488t - 2613400142391424482367340.
\end{aligned}$$

We now have a list of 120 such polynomials. Each of these intersects the curve  $C$  in three complex points with multiplicity two in the  $(t, W)$ -plane. All of these complex points are found to be real.

Now we present an example which attains our lower bound in Theorem 3.1.

**Example 3.3.2** A similar computation verifies that the following configuration of eight points gives 84 totally real tritangents:

$$\begin{aligned}
\mathcal{P} = \{ & (-12 : 9 : 11), (7 : -5 : -7), (1 : 3 : 3), (2 : 2 : -1), \\
& (-2 : 2 : 1), (1 : 3 : 1), (3 : 3 : 2), (8 : -8 : -7) \} \subset \mathbb{P}_{\mathbb{R}}^2.
\end{aligned}$$

**PROOF OF THEOREM 3.1.** The 120 tritangent planes arising from the construction above correspond to the odd theta characteristics of  $C$ . They are tritangent to  $C$  but they do not pass through the singular point  $(0 : 0 : 0 : 1)$  of the quadric  $V(x_0x_2 - x_1^2)$  in  $\mathbb{P}^3$ . Each such tritangent is an isolated regular solution to the polynomial equations that define the tritangents of  $C$ . These equations are described explicitly as the tritangent ideal in Section 4. We may perturb the equation  $x_0x_2 - x_1^2$  to obtain a new curve  $C'$ . By the Implicit Function Theorem, for each tritangent  $H$  of  $C$  there is a nearby tritangent plane  $H'$  of  $C'$ . Moreover, if the perturbation is sufficiently small and the three points of  $C \cap H$  are real and distinct, then  $C' \cap H'$  also consists of three distinct real points. Conversely, if two points of  $C \cap H$  are distinct and

complex conjugate, then two points of  $C' \cap H'$  will also be distinct and complex conjugate.

Hence, if our blow-up construction gives  $m$  totally real tritangents for some  $m \leq 120$  then that same number of real solutions persists throughout some open semialgebraic subset in the space  $\mathbb{P}_{\mathbb{R}}^9 \times \mathbb{P}_{\mathbb{R}}^{19}$  of pairs  $(Q, K)$  of a real quadric and a real cubic in  $\mathbb{P}^3$ .

Examples 3.3.2 and 3.3.1 exhibit configurations with  $m = 84$  and  $m = 120$ . Every integer  $m$  between these two values can be realized as well. We verified that assertion computationally, by constructing a configuration  $\mathcal{P}$  in  $\mathbb{P}_{\mathbb{Q}}^2$  for every integer between 84 and 120.  $\square$

**Remark 3.3.3** It may be possible to prove by hand that every integer  $m$  between 84 and 120 is realizable. The idea is to connect the two extreme configurations with a general semialgebraic path in  $\mathbb{P}_{\mathbb{R}}^9 \times \mathbb{P}_{\mathbb{R}}^{19}$ . That path crosses the *tritangent discriminant*  $\Delta_2$  (cf. Section 5) transversally. At such a crossing point, precisely one of the 120 configurations marked (0,6), (1,5), (2,4) or (3,3) fails to have its three intersection points distinct. This means that the number of real triples changes by exactly one. So, the number of totally real tritangents of the associated space sextic changes by exactly one. This is not yet a proof because the path might cross the discriminant  $\Delta_1$ .

### 3.4. Space sextics with fewer ovals

In Section 3.1 we started with eight points in the real projective plane  $\mathbb{P}_{\mathbb{R}}^2$ . Here we generalize by taking a configuration  $\mathcal{P}$  in the complex projective plane  $\mathbb{P}_{\mathbb{C}}^2$  that is invariant under complex conjugation. This also defines a real curve  $C$  in  $V(x_0x_2 - x_1^2) \subset \mathbb{P}_{\mathbb{R}}^3$ . To be precise, for  $s \in \{1, 2, 3, 4, 5\}$ , let  $\mathcal{P}$  consist of  $2s - 2$  real points and  $5 - s$  complex conjugate pairs. Such a configuration of eight points defines a real del Pezzo surface  $X_{\mathcal{P}}$ . Additionally, the map  $\mathbb{P}^2 \dashrightarrow \mathbb{P}^3$  in Figure 3.3 and its branch curve  $C$  are defined over  $\mathbb{R}$ . The space sextic  $C$  has  $s$  ovals and it is not of dividing type when  $s \leq 4$ . By, [38, Proposition 3.1], the number of real tritangents of  $C$  equals  $2^{s+2}$ . For curves which come from the construction in Section 3.1, we can derive this number by examining how complex conjugation acts on the special curves in  $\mathbb{P}_{\mathbb{C}}^2$  we had associated with the point configuration  $\mathcal{P}$ . We follow our notation from Section 3.2.

$8_{(0,6)}$ : The exceptional fiber over a point  $P_i$  defines a real tritangent if and only if the point  $P_i$  itself is real.

$28_{(1,5)}$ : This tritangent is real if and only if the pair  $\{P_i, P_j\}$  is real, i.e. either  $P_i$  and  $P_j$  are both real, or  $P_j$  is the conjugate of  $P_i$ . Among the 28 pairs, the number of real pairs is thus  $4 = 0 + 4$ ,  $4 = \binom{2}{2} + 3$ ,  $8 = \binom{4}{2} + 2$  and  $16 = \binom{6}{2} + 1$  for  $s = 1, 2, 3, 4$ .

$56_{(2,4)}$ : This tritangent is real if and only if the triple of singular points in the quartic is real. This happens if either the three points are real, or there is one real point and a conjugate pair. Among the 56 triples, the number of real triples is thus **0**, **6** =  $0 + 2 \cdot 3$ , **12** =  $\binom{4}{3} + 4 \cdot 2$ , **26** =  $\binom{6}{3} + 6 \cdot 1$  for  $s = 1, 2, 3, 4$ .

$28_{(3,3)}$ : In this case, the tritangent is real if and only if the two cubics are conjugate, and this happens if and only if the pair  $\{P_i, P_j\}$  is real. Hence the count is **4**, **4**, **8**, **16**, as in the case 28.

For each value of  $s \in \{1, 2, 3, 4\}$ , if we add up the respective four numbers then we obtain  $2^{s+2}$ . For instance, for  $s = 3$ , the analysis above shows that  $4 + 8 + 12 + 8 = 32$  of the 120 tritangents are real.

We wish to know how many of these  $2^{s+2}$  real tritangents can be totally real, as  $\mathcal{P}$  ranges over the various types of real configurations. Our investigations led to the findings summarized in Theorem 3.4.1.

**Theorem 3.4.1** *The third row in Table 3.1 lists the ranges of currently known values for the number of totally real tritangents of real space sextics  $C$  that are constructed by blowing up eight points in  $\mathbb{P}^2$ :*

<i>s ovals</i>	1	2	3	4	5
<i>real</i>	8	16	32	64	120
<i>totally real</i>	$[0, 8]$	$[1, 15]$	$[10, 32]$	$[35, 63]$	$[84, 120]$

TABLE 3.1. Real and totally real tritangents of a space sextic  $C$  on a singular quadric  $Q$ , according to number of ovals of  $C$ .

The following examples exhibit some lower and upper bounds.

**Example 3.4.2** ( $s = 1$ ) Let  $\mathcal{P}$  be the following configuration in  $\mathbb{P}_{\mathbb{C}}^2$ :

$$\begin{array}{ll}
 P_1 = & (i : 1 - i : 0) & P_2 = \overline{P_1} \\
 P_3 = & (2 - i : -3 - i : 3 + i) & P_4 = \overline{P_3} \\
 P_5 = & (2 - i : 1 - i : -2 - i) & P_6 = \overline{P_5} \\
 P_7 = & (4i : -i : 4) & P_8 = \overline{P_7}
 \end{array}$$

The curve  $C$  consists of only one oval in  $\mathbb{P}_{\mathbb{R}}^3$ . One checks that **none** of the eight real tritangents of  $C$  is totally real, i.e. no plane is tangent to  $C$  at three real points. On the other hand, for the following configuration, **all** eight real tritangents are totally real:

$$\begin{array}{ll}
 P_1 = & (i : 0 : 1) & P_2 = \overline{P_1} \\
 P_3 = & (1 - 3i : -3 + 2i : 1) & P_4 = \overline{P_3} \\
 P_5 = & (0 : 2 + 3i : -3 - 2i) & P_6 = \overline{P_5} \\
 P_7 = & (4i : -3 + 4i : 1 + i) & P_8 = \overline{P_7}
 \end{array}$$

**Example 3.4.3** ( $s = 2$ ) We fix the following configuration  $\mathcal{P}$  of two real points and three pairs of complex conjugate points in  $\mathbb{P}^2$ .

$$\begin{array}{ll} P_1 = & (1 : -2i : 2i) & P_2 = \overline{P_1} \\ P_3 = & (1 : 3 + 2i : -3i) & P_4 = \overline{P_3} \\ P_5 = & (1 + 2i : 4 + 2i : -4 + i) & P_6 = \overline{P_5} \\ P_7 = & (1 : 0 : -1) & P_8 = (0 : 4 : 1) \end{array}$$

The associated curve  $C$  has two ovals. Of its 16 real tritangents, **exactly one** is totally real. By a random search, we found examples where up to 15 of the real tritangents of the curve  $C$  are totally real. At present, we have not found any  $\mathcal{P}$  where the associated curve has either 0 or 16 totally real tritangents.

Figure 3.7 shows the empirical distribution we observed for  $s = 3$  (left) and  $s = 4$  (right). The respective ranges are  $[10, 32]$  and  $[35, 63]$ .

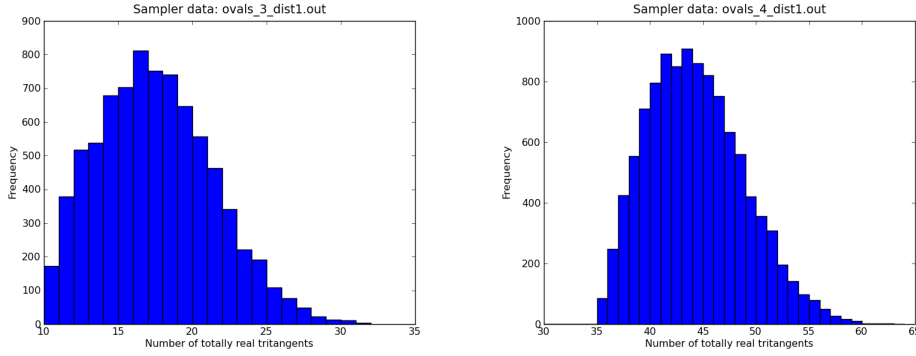


FIGURE 3.7. Count of totally real tritangents for  $s = 3$  and  $s = 4$ .

**Example 3.4.4** ( $s = 3$ ) The following configuration  $\mathcal{P}$  gives a space sextic  $C$  with three ovals that has 32 totally real tritangents:

$$\begin{array}{l} P_1 = (-204813760 - 55982740i : 452442430 + 319792532i : 1), \quad P_2 = \overline{P_1} \\ P_3 = (252002303 - 508295920i : 418802957 + 255990940i : 1), \quad P_4 = \overline{P_3} \\ P_5 = (420794066 : 346448315 : 1), \quad P_6 = (64527687 : 183049780 : 1), \\ P_7 = (410335352 : 364471450 : -1), \quad P_8 = (-210806629 : -146613813 : 1). \end{array}$$

### 3.5. Solving the tritangent equations

In Sections 3.1 to 3.4, we studied space sextics  $C$  lying on a singular quadric surface  $Q$ . By perturbing these, we obtained generic space sextics with many different numbers of totally real tritangents. However, not all numbers between 0 and 120 were attained by this method. To

remedy this, we considered arbitrary space sextics  $C = Q \cap K$ , defined by a random quadric  $Q$  and a random cubic  $K$ .

However, we found the problem of computing the tritangents directly from  $(Q, K)$  to be quite challenging. We conjecture that all integers between 0 and 120 can be realized by the totally real tritangents of some space sextic.

In spite of the very recent research ([40],[56]) on expanding Table 3.1 and finding the possible bounds, there are open cases remain to be realized or shown to be impossible: 64 real tritangents with all 64 totally real and 120 real tritangents with 80 - 83 totally real tritangents.

In what follows we describe a method – and its implementation – for computing the 120 tritangents directly from the homogeneous polynomials of degree two resp. three in  $x_0, x_1, x_2, x_3$  that define the quadric  $Q$  resp. the cubic  $K$ . In Section 4.2 of our next chapter we present an algorithmic version of this method for the case where the quadric is smooth, together with an algorithm to compute the corresponding *Steiner system*. We now introduce four unknowns  $u_0, u_1, u_2, u_3$  that serve as coordinates on the space  $(\mathbb{P}^3)^\vee$  of planes:

$$(3.4) \quad H : u_0x_0 + u_1x_1 + u_2x_2 + u_3x_3 = 0.$$

For generic real values of the  $u_i$ , the intersection  $Q \cap K \cap H = C \cap H$  consists of six distinct complex points in  $\mathbb{P}^3$ . We are interested in the special cases when these six points become three double points. We seek to find the *tritangent ideal*  $\mathcal{I}_C$ , consisting of polynomials in  $u_0, u_1, u_2, u_3$  that vanish at those  $H$  that are tritangent planes of  $C$ .

We fix the projective space  $\mathbb{P}^6$  whose points are the binary sextics

$$f = a_0t_0^6 + a_1t_0^5t_1 + a_2t_0^4t_1^2 + a_3t_0^3t_1^3 + a_4t_0^2t_1^4 + a_5t_0t_1^5 + a_6t_1^6.$$

Inside that  $\mathbb{P}^6$  we consider the threefold of squares of binary cubics:

$$(3.5) \quad f = (b_0t_0^3 + b_1t_0^2t_1 + b_2t_0t_1^2 + b_3t_1^3)^2.$$

The defining prime ideal of that threefold is minimally generated by 45 quartics in  $a_0, a_1, a_2, a_3, a_4, a_5, a_6$ . This is revealed by the row labeled  $\lambda = (2, 2, 2)$  in [58, Table 1]. Computing these 45 quartics is a task of elimination, which we carried out in a preprocessing step.

Consider now a specific instance  $(Q, K)$ , defining  $C = Q \cap K$ . We then transform the above 45 quartics in  $a_0, \dots, a_6$  into higher degree equations in  $u_0, \dots, u_3$ . This is done by projecting  $C \cap H$  onto a line. This gives a univariate polynomial of degree six whose seven coefficients are polynomials of degree 12 in  $u_0, u_1, u_2, u_3$ . We replace  $a_0, \dots, a_6$  by these polynomials. Theoretically, it suffices to project onto a single generic line. Practically, we had more success with multiple (possibly degenerate) projections onto the coordinate axes, and gathering the resulting systems of 45 equations each.

To be more precise, fix one of the 12 ordered pairs  $(x_i, x_j)$ . First, solve the equation (3.4) for  $x_i$ , substitute into the equations of  $Q$  and  $K$ , and clear denominators. Next, eliminate  $x_j$  from the resulting ternary quadric and cubic. The result is a binary sextic  $f$  in the two unknowns  $\{x_0, x_1, x_2, x_3\} \setminus \{x_i, x_j\}$  whose coefficients  $a_0, \dots, a_6$  are expressions of degree 12 in  $u_0, \dots, u_3$ . We substitute these expressions into the 45 quartics precomputed above. This results in 45 polynomials of degree 48 in  $u_0, \dots, u_3$  that lie in the tritangent ideal  $\mathcal{I}_C$ . Repeating this elimination process for the other 11 pairs  $(x_i, x_j)$ , we obtain additional polynomials in  $\mathcal{I}_C$ . Altogether, we have now enough polynomials of degree 48 to generate  $\mathcal{I}_C$  on any desired affine open subset in the dual  $(\mathbb{P}^3)^\vee$  of planes in  $\mathbb{P}^3$ . The homogeneous ideal  $\mathcal{I}_C$  is radical and it has 120 zeros in  $(\mathbb{P}^3)^\vee$ .

To compute these zeros, we restrict ourselves to an open chart, say  $U = \{u_3 \neq 0\} \simeq \mathbb{C}^3$ . The resulting system (with  $u_3 = 1$ ) is grossly over-constrained, with up to  $12 \times 45$  equations in the three unknowns  $u_0, u_1, u_2$ . We compute a lexicographic Gröbner bases, using `fglm` [28], as our ideal is zero-dimensional. For generic instances  $(Q, K)$ , the lexicographic Gröbner basis has the shape

$$(3.6) \quad \{u_1 - p_1(u_3), u_2 - p_2(u_3), p_3(u_3)\},$$

where  $\deg(p_3) = 120$  and  $\deg(p_1) = \deg(p_2) = 119$ . For degenerate  $(Q, K)$  we proceed with a triangular decomposition.

We implemented this method in `MAGMA` [6]. The Gröbner basis computation was very hard to carry out. It took several days to finish for Example 3.5.2. The output had coefficients of size  $\sim 10^{680}$ .

We applied our implementation to several curves  $C$ , some from configurations  $\mathcal{P} \subset \mathbb{P}_{\mathbb{Q}}^2$ , and some from general instances  $(Q, K)$ .

The first case is used as a tool for independent verification, e.g. for Example 3.3.1. Here,  $p_3$  decomposes into linear factors over  $\mathbb{Q}$ . Each factor yields a rational tritangent, for which we compute the three (double) points in  $H \cap C$  symbolically. To check whether one or three are real, we again project onto a line. This yields a univariate rational polynomial of degree 6. We can test whether it is the square of a cubic with positive discriminant. More generally, any non-linear factor with only real roots also allows us to continue our computations symbolically over an algebraic field extension.

In the second case, the univariate polynomial  $p_3$  is typically irreducible over  $\mathbb{Q}$ , and we solve (3.6) numerically. We compute all real tritangents  $H$  and their intersections  $H \cap C$ . Based on the resulting numerical data, we decide which  $H$  are totally real. Complex zeroes are also counted, to attest that there are indeed 120 solutions. This certifies that the chosen open chart  $U$  was indeed generic.

**Example 3.5.1** The polynomial  $C(t, W)$  in Example 3.3.1 translates into a cubic  $K(x_0, x_1, x_2, x_3)$  which is unique modulo the quadric  $Q = x_0x_2 - x_1^2$ . We apply the algorithm above to the instance  $(Q, K)$  with  $U = \{u_3 \neq 0\}$ . The result verifies that all 120 tritangents are rational and totally real. Interestingly, two of the 120 tritangents have a coordinate that is zero. These two special planes are

$$\begin{aligned} 0 = & 666727858907928630542805134887161895157u_0 \\ & -371406861222752391050720128495402169926u_1 \\ & -13148859997292971155483015u_3 \end{aligned}$$

and

$$\begin{aligned} 0 = & 7984878906436628716387308745543788472u_1 \\ & -4446108899575055719305582305633616071u_2 \\ & +10689705055237706452395u_3. \end{aligned}$$

**Example 3.5.2** The curve  $C = Q \cap K$  in [38, §3] is given by

$$\begin{aligned} Q &= x_0^2 + x_1^2 + x_2^2 - 25x_3^2 \\ K &= (x_0 + \sqrt{3}x_3)(x_0 - \sqrt{3}x_1 - 3x_3)(x_0 + \sqrt{3}x_1 - 3x_3) - 2x_3^3. \end{aligned}$$

It has five ovals, so all tritangents are real. Our computation shows that there are only 108 distinct tritangents. Twelve are solutions of multiplicity two in the ideal  $I_C$ , and none of the tritangents are rational. This verifies [38, Theorem 3.2]. Figure 3.8 shows three tritangents, meeting 3, 2 and 1 ovals of the red curve respectively.

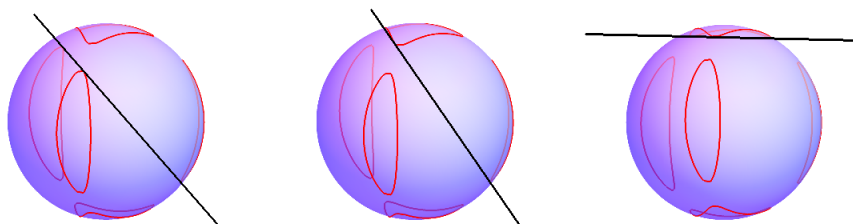


FIGURE 3.8. The curve in Example 3.5.2 has 108 totally real tritangents

In [38, Question 3.3], Harris and Len asked whether this example can be replaced by one with 120 distinct totally real tritangents. Our computations in Examples 3.3.1 and 3.5.1 establish the affirmative answer. However, we do not yet know whether all integers between 0 and 120 are possible for the number of totally real tritangents.

### 3.6. Discriminants

In this chapter we consider two parameter spaces for space sextics. First, there is the space  $\mathbb{P}_{\mathbb{R}}^9 \times \mathbb{P}_{\mathbb{R}}^{19}$  of pairs  $(Q, K)$  consisting of a real quadric and a real cubic in  $\mathbb{P}^3$ . The regions for which the number of real tritangents remains constant partitions  $\mathbb{P}_{\mathbb{R}}^9 \times \mathbb{P}_{\mathbb{R}}^{19}$  into open strata. This stratification is refined by regions for which the number of totally real tritangents remains constant. We are interested in the discriminantal hypersurfaces that separate these strata.

Second, there is the space  $(\mathbb{P}_{\mathbb{R}}^2)^8$  of configurations  $\mathcal{P}$  of eight labeled points in the plane. This space works for any fixed value of  $s$  in  $\{1, 2, 3, 4, 5\}$ , representing configurations of  $2s - 2$  real points and  $5 - s$  complex conjugate pairs. For simplicity of exposition we focus on the fully real case  $s = 5$ . In any case, the number of real tritangents is fixed, and we care about the open strata in  $(\mathbb{P}_{\mathbb{R}}^2)^8$  in which the number of totally real tritangents is constant. Again, we seek to describe the discriminantal hypersurface, but now in  $(\mathbb{P}^2)^8$ .

For  $\mathcal{P} \in (\mathbb{P}^2)^8$ , denote the associated space sextic by  $C_{\mathcal{P}}$ . Let  $\Sigma$  denote the locus of configurations in  $(\mathbb{P}^2)^8$  which are not in general position. We define the *tritangent discriminant locus* by

$$Y = \overline{\left\{ \mathcal{P} \in (\mathbb{P}^2)^8 \setminus \Sigma : \begin{array}{l} C_{\mathcal{P}} \text{ has a tritangent} \\ \text{with contact} \\ \text{order at least 4 at some} \\ \text{point} \end{array} \right\}},$$

where the over-line denotes the Zariski closure.

**Lemma 3.6.1** *Every irreducible component of  $Y$  is a hypersurface.*

PROOF. Let  $\mathcal{P}_0 \in Y \setminus \Sigma$ , and fix local coordinates  $\bar{p} = (p_1, \dots, p_{16})$  for a neighborhood  $\mathcal{U}$  of  $\mathcal{P}_0 = \bar{p}_0$  in  $(\mathbb{P}^2)^8$ . The bivariate equation (3.2) that represents  $C_0$  is the specialization at  $\bar{p}_0$  of a general equation

$$(3.7) \quad C : c(t, W) = t^6 + d_1(\bar{p})t^5 + d_2(\bar{p})t^4W + \dots + d_{15}(\bar{p}),$$

where the coefficients  $d_i(\bar{p})$  are rational functions regular at  $p_0$ . Let  $H_0$  be a tritangent plane to  $C_0$  with a contact point of order at least 4. Then  $H_0$  is either the tritangent associated to a point in  $\mathcal{P}_0$  or associated to one of the patterns in Figure 3.4, 3.5 or 3.6. Either way, we see that  $H_0$  is obtained by specializing an equation of the form

$$(3.8) \quad H : h(t, W) = t^2 + e_1(\bar{p})t + e_2(\bar{p}) + e_3(\bar{p})W,$$

where the coefficients  $e_i(\bar{p})$  are rational functions regular at  $\bar{p}_0$ .

The resultant of  $c(t, W)$  and  $h(t, W)$  with respect to  $W$  is a polynomial  $f(t)$  of degree 6 whose coefficients are rational functions in  $\bar{p}$ . Note that  $H$  is a tritangent plane to  $C$ , so  $f = g^2$  as in (3.5). The



roots of the cubic  $g$  correspond to the contact points of  $H$  with  $C$ . In particular,  $H_{\bar{p}}$  has a point of contact with  $C_{\bar{p}}$  of order at least 4 precisely when the discriminant of  $g$  is zero. Since the coefficients of  $g$  are rational functions in  $\bar{p}$ , regular at  $\bar{p}_0$ , this means that a neighborhood of  $\mathcal{P}_0$  in  $Y$  has codimension 1 in  $\mathcal{U}$ . This implies that every irreducible component of  $Y$  has codimension 1.  $\square$

The following theorem describes these irreducible components:

**Theorem 3.6.2** *The tritangent discriminant locus  $Y$  is the union of  $120 = 8_{(0,6)} + 28_{(1,5)} + 56_{(2,4)} + 28_{(3,3)}$  irreducible hypersurfaces in  $(\mathbb{P}^2)^8$ , one for each point in  $\mathcal{P}$  and each pattern in Figures 3.4, 3.5 and 3.6. The 8 components of type  $(0,6)$  have total degree 306, namely 54 in the point corresponding to the exceptional curve and 36 in the other seven points. The 28 components of type  $(1,5)$  have total degree 216, namely 18 in each of the two points on the line and 30 for the six on the quintic. The 56 components of type  $(2,4)$  have total degree 162, namely 18 in each of the five points on the conic and 24 for the three on the quartic. The 28 components of type  $(3,3)$  have total degree 144, namely 18 in each of the eight points.*

We prove Theorem 3.6.2 computationally. In order to do so, it is convenient to make the following observation. Let  $Y = V(f)$  with  $f$  a  $\mathbb{Z}^8$ -homogeneous polynomial of  $\mathbb{Z}^8$ -degree  $(d_1, \dots, d_8)$ . We scale  $f$  so that its coefficients are relatively prime integers. For a prime  $p$ , let  $f_p$  denote the reduction of  $f$  modulo  $p$ . If  $p$  is large, then

$$Y_p = V(f_p) \subset (\mathbb{P}_{\mathbb{F}_p}^2)^8$$

has the same  $\mathbb{Z}^8$ -degree as  $Y$ . We can thus calculate  $(d_1, \dots, d_8)$  by using Gröbner bases over a large finite field  $\mathbb{F}_p$ .

Let  $k = \mathbb{F}_p$  be the field with  $p = 10^6 + 3$  elements and  $k^{\text{al}}$  its algebraic closure. Let  $S = \mathbb{P}_k^1$  and let  $R = k[a, b]$  be the coordinate ring of  $S$ . Let  $\mathbb{P}_R^2 := \text{Proj } R[x, y, z]$  be the projective plane over  $R$ . If  $X$  is some family, its specialization to  $(a : b) \in S$  is denoted  $X_{(a:b)}$ .

We use the following configuration of eight points in  $\mathbb{P}_R^2$ :

$$\mathcal{P} = \{ (24 : -23 : 57), (11 : 25 : -27), (-30 : 29 : 79), (14 : -23 : 26), \\ (43 : 92 : 61), (-34 : 81 : 7), (88 : 29 : 69), (a : b : 0) \} \subset \mathbb{P}_{\mathbb{R}}^2.$$

Then  $\mathcal{P}$  is in general position for generic  $a, b$ . Let  $\mathcal{U}$  be the open subset of  $S$  parameterizing specializations in general position. The following result concerns generic specializations. We omit the proof.

**Proposition 3.6.3** *There exists a pair of ternary cubics  $u, v \in R[x, y, z]$ , a ternary sextic  $w \in R[x, y, z]$ , bivariate polynomials  $c, h \in R[t, W]$  as in (3.7) and (3.8), and an explicitly computable finite set  $X \subset S(k^{\text{al}})$  such that, whenever  $(a : b) \in \mathcal{U} \setminus X$ , the following hold:*

- (a) *The specializations  $u_{(a:b)}, v_{(a:b)}$  span the space of cubics passing through all eight points in  $\mathcal{P}_{(a:b)}$ .*
- (b) *The specializations  $u_{(a:b)}^2, uv_{(a:b)}, v_{(a:b)}^2, w_{(a:b)}$  span the space of sextics vanishing doubly at each point in  $\mathcal{P}_{(a:b)}$ .*
- (c) *The specialization  $\{c_{(a:b)}(t, W) = 0\}$  is a smooth genus 4 curve  $C_{a:b}$  lying on a singular quadric surface.*
- (d) *The specialization  $\{h_{(a:b)}(t, W) = 0\}$  is a tritangent plane to  $C_{(a:b)}$  where the coefficient of  $W$  is nonzero.*
- (e) *For any  $(a : b) \in X$ , the curve  $C_{(a:b)}$  is smooth, genus 4, and none of the tritangent planes have a point of contact order larger than 4.*

We now derive Theorem 3.6.2 from Proposition 3.6.3. The degree  $d_8$  of  $Y$  in the last point  $P_8$  is computed by restricting to the slice

$$\{(24 : -23 : 57)\} \times \{(11 : 25 : -27)\} \times \dots \times \{(88 : 29 : 69)\} \times \mathbb{P}^2.$$

This restriction of  $Y$  is a curve of degree  $d_8$  in  $\mathbb{P}^2$ . We compute this degree as the number of points in the intersection with the line

$$S = \{(a : b : c) \in \mathbb{P}^2 : c = 0\}.$$

The same argument works also for each irreducible component of  $Y$ . These components correspond to the various tritangent patterns, marked (0,6), (1,5), (2,4) and (3,3). We perform this computation for each pattern over  $\mathbb{F}_p$ , and we obtain the numbers stated in Theorem 3.6.2.

We now turn to the canonical representation of arbitrary space sextics  $C = Q \cap K$ , namely by pairs  $(Q, K)$  in  $\mathbb{P}^9 \times \mathbb{P}^{19}$ . We shall identify three irreducible hypersurfaces in  $\mathbb{P}^9 \times \mathbb{P}^{19}$  that serve as discriminants for different scenarios of how  $C$  can degenerate. For each hypersurface, we shall determine its *bidegree*  $(\alpha, \beta)$ . Here  $\alpha$  is the degree of its defining polynomial in the coefficients of  $Q$ , and  $\beta$  is the degree of its defining polynomial in the coefficients of  $K$ .

First, there is the classical discriminant  $\Delta_1$ , which parametrizes all pairs  $(Q, K)$  such the curve  $C = Q \cap K$  is singular. This is an irreducible hypersurface in  $\mathbb{P}^9 \times \mathbb{P}^{19}$ , revisited recently in [12]. The general points of  $\Delta_1$  are irreducible curves  $C$  of arithmetic genus 4 that have one simple node, so the geometric genus of  $C$  is 3. The discriminant  $\Delta_1$  specifies the wall to be crossed when the number of real tritangents changes as  $(Q, K)$  moves throughout  $\mathbb{P}_{\mathbb{R}}^9 \times \mathbb{P}_{\mathbb{R}}^{19}$ .

Second, there is the wall to be crossed when the number of totally real tritangents changes. The discriminant  $\Delta_2$  comprises space sextics with a tritangent  $H$  that is degenerate, in the sense that  $H$  is tangent at one point and doubly tangent at another point of  $C$ . For real pairs  $(C, H)$ , such a point of double tangency deforms into two contact points of a tritangent  $H_\epsilon$  at a nearby curve  $C_\epsilon$ , and this pair is either real or complex conjugate. On the hypersurface in  $\mathbb{P}^9 \times \mathbb{P}^{19}$  where  $Q$  is singular, the locus  $\Delta_2$  is the image of the discriminant with 120 components in Theorem 3.6.3 under the map that takes a configuration  $\mathcal{P} \in (\mathbb{P}^2)^8$  to its associated curve  $C_{\mathcal{P}}$ .

Our third discriminant  $\Delta_3$  parametrizes pairs  $(Q, K)$  such that the curve  $C = Q \cap K$  has two distinct tritangents that share a common contact point on  $C$ . In other words, the curve  $C$  has a point whose tangent line is contained in two tritangent planes. The discriminant  $\Delta_3$  furnishes an embedded realization of the *common contact locus* that was studied in the dissertation of Emre Sertöz [79, §2.4].

The following theorem was found with the help of Gavril Farkas and Emre Sertöz. The numbers are derived from results in [27, 79].

**Theorem 3.6.4** *The discriminantal loci  $\Delta_1$ ,  $\Delta_2$  and  $\Delta_3$  are irreducible and reduced hypersurfaces in  $\mathbb{P}^9 \times \mathbb{P}^{19}$ . Their bidegrees are*

$$\begin{aligned} \text{bidegree}(\Delta_1) &= (33, 34), \\ \text{bidegree}(\Delta_2) &= (744, 592), \\ \text{bidegree}(\Delta_3) &= (8862, 5236). \end{aligned}$$

PROOF. Consider the discriminant  $\Delta_1$  for curves in  $\mathbb{P}^3$  that are intersections of two surfaces of degree  $d$  and  $e$ . It has bidegree

$$(e(3d^2 + 2de + e^2 - 8d - 4e + 6), d(3e^2 + 2de + d^2 - 8e - 4d + 6)).$$

This can be found in many sources, including [12, Proposition 3]. For  $d = 2$  and  $e = 3$  we obtain  $\text{bidegree}(\Delta_1) = (33, 34)$ , as desired.

To determine the other two bidegrees, we employ known facts from the enumerative geometry of  $\overline{\mathcal{M}}_4$ , the moduli space of stable curves of genus 4. The Picard group  $\text{Pic}(\overline{\mathcal{M}}_4)$  is generated by four classes  $\lambda, \delta_0, \delta_1, \delta_2$ . Here  $\lambda$  is the *Hodge class*, and the  $\delta_i$  are classes of irreducible divisors in the boundary  $\overline{\mathcal{M}}_4 \setminus \mathcal{M}_4$ . They represent:

- $\delta_0$ : a genus 3 curve that self-intersects at one point;
- $\delta_1$ : a genus 1 curve intersects a genus 3 curve at one point;
- $\delta_2$ : two genus 2 curves intersect at one point.

Our discriminants  $\Delta_i$  are the inverse images of known irreducible divisors in the moduli space under the rational map  $\mathbb{P}^9 \times \mathbb{P}^{19} \dashrightarrow \overline{\mathcal{M}}_4$ .

First,  $\Delta_2$  is the pull-back of the divisor  $D_4 \subset \overline{\mathcal{M}}_4$  of curves with degenerate odd spin structures. From [27, Theorem 0.5]:

$$(3.9) \quad [D_4] = 1440\lambda - 152\delta_0 - \alpha\delta_1 - \beta\delta_2 \quad \text{for some } \alpha, \beta \in \mathbb{N}.$$

For any curve  $\gamma \in \overline{\mathcal{M}}_4$ , the sum  $\sum_{i=0}^2 \gamma \cdot \delta_i$  counts points on  $\gamma$  whose associated curve is singular. Write  $h$  resp.  $v$  for the curve  $\gamma$  that represents *line*  $\times$  *point* resp. *point*  $\times$  *line* in  $\mathbb{P}^9 \times \mathbb{P}^{19}$ . We saw

$$(h \cdot \delta_0, v \cdot \delta_0) = \text{bidegree}(\Delta_1) = (33, 34).$$

Moreover, it can be shown that

$$h \cdot \lambda = v \cdot \lambda = 4 \quad \text{and} \quad h \cdot \delta_i = v \cdot \delta_i = 0 \quad \text{for } i = 1, 2.$$

This implies the assertion about the bidegree of our discriminant:

$$\text{bidegree}(\Delta_2) = (h \cdot [D_4], v \cdot [D_4]) = (1440 \cdot 4 - 152 \cdot 33, 1440 \cdot 4 - 152 \cdot 34).$$

Similarly,  $\Delta_3$  is the pull-back of the *common contact divisor*  $Q_4 \subset \overline{\mathcal{M}}_4$  studied by Sertöz. It follows from [79, Theorem II.2.43] that

$$(3.10) \quad [Q_4] = 32130\lambda - 3626\delta_0 - \alpha\delta_1 - \beta\delta_2 \quad \text{for some } \alpha, \beta \in \mathbb{N}.$$

Replacing (3.9) with (3.10) in our argument, we find that  $\text{bidegree}(\Delta_3)$  is

$$(h \cdot [Q_4], v \cdot [Q_4]) = (32130 \cdot 4 - 3626 \cdot 33, 32130 \cdot 4 - 3626 \cdot 34).$$

This completes our derivation of the bidegrees in Theorem 3.6.4.

The irreducibility of the loci  $\Delta_i$  is shown by a standard double-projection argument. One marks the relevant special point(s) on  $C$ . Then  $\Delta_i$  becomes a family of linear spaces of fixed dimension.  $\square$

### 3.7. What next?

In this chapter, we initiated the computational study of totally real tritangents of space sextics in  $\mathbb{P}^3$ . These objects are important in algebraic geometry because they represent odd theta characteristics of canonical curves of genus 4. We developed systematic tools for constructing curves all of whose tritangents are defined over algebraic extensions of  $\mathbb{Q}$ , and we used this to answer the longstanding question whether the upper bound of 120 totally real tritangent planes can be attained. We argued that computing the tritangents directly from the representation  $C = Q \cap K$  is hard, and we characterized the discriminants for these polynomial systems.

Working on these problems led us to many natural directions to be explored next. In the following list, so far much progress is made on Question (2) in [40] and [56]. There are at most 120 facets in the convex hull of a space sextic  $C$  in  $\mathbb{R}^3$ . These form a ruled surface of degree 54, by [72, Theorem 2.1]. In [56], apart from expanding Table 3.1, Kummer shows that the maximal number of facets in the convex

hull of  $C$  is 8. Finally, we propose the following ten specific problems for further study.

- (1) Decide whether every integer between 0 and 120 is realizable.
- (2) Determine the correct upper and lower bounds in Table 3.1. In particular, is 84 the lower bound for curves with five ovals?
- (3) A smooth quadric  $Q$  is either an ellipsoid or a hyperboloid. Degtyarev and Zvonilov [22] characterized the topological types of real space sextics on these surfaces. What are the possible numbers of totally real tritangents for their types?
- (4) What does [22] tell us about space sextics on a singular quadric  $Q$ ? Which types arise on  $Q$ , how do they deform to those on a hyperboloid, and what does this imply for tritangents?
- (5) Given a space sextic  $C$  whose quadric  $Q$  is singular, how to best compute a configuration  $\mathcal{P} \in (\mathbb{P}^2)^8$  such that  $C = C_{\mathcal{P}}$ ? Our idea is to design an algorithm based on the constructions described in [52, Proposition 4.8 and Remark 4.12].
- (6) Let  $C_{\mathcal{P}}$  be the space sextic of a configuration  $\mathcal{P} \in (\mathbb{P}^2)^8$ . How to see the ovals of  $C_{\mathcal{P}}$  in  $\mathbb{P}^2$ ? For each tritangent as in Figure 3.4, 3.5 or 3.6, how to see the number of ovals it touches?
- (7) Design a custom-tailored *homotopy algorithm* for numerically computing the 120 tritangents from the pair  $(Q, K)$ .
- (8) The *tropical limit* of a space sextic has 15 classes of tritangents, each of size eight [38, Theorem 5.2]. This is realized classically by a  $K_{3,3}$ -curve, obtained by taking  $K$  as three planes tangent to a smooth quadric  $Q$ . How many totally real tritangents are possible in the vicinity of  $(Q, K)$  in  $\mathbb{P}_{\mathbb{R}}^9 \times \mathbb{P}_{\mathbb{R}}^{19}$ ?
- (9) The 28 bitangents of a plane quartic are the off-diagonal entries of a symmetric  $8 \times 8$ -matrix, known as the *bitangent matrix* [21]. How to generalize this to genus 4? Is there such a canonical matrix (or tensor) for the 120 tritangents?
- (10)\* Lehavi [60] shows that a general space sextic  $C$  can be reconstructed from its 120 tritangents. How to do this in practice?

(★) In the next chapter, we answer the last problem.

## CHAPTER 4

### Tritangents and Their Space Sextics

Space sextic curves offer a rich example for understanding the various geometric features of non-planar algebraic curves. Several questions for plane curves have natural analogues for curves in arbitrary projective spaces. An important direction of inquiry is the study of hyperplanes that have a special intersection with the curve. In this chapter, we focus on the tritangents of  $C$ , planes in  $\mathbb{P}^3$  which are tangent to  $C$  at every point of intersection with  $C$ . They reflect important intrinsic facts about the curve as well as important details about the extrinsic geometry.

For instance, the tritangents arise from effective representatives of the theta characteristics. As such, they provide insight into the Jacobian variety and over the complex numbers yield important information regarding values of theta functions. Conversely, any principally polarized abelian variety  $A$  of dimension 4 defines 120 planes in  $\mathbb{P}^3$  via its theta functions. If  $A$  is the Jacobian of a non-hyperelliptic genus 4 curve, these 120 planes are the tritangents of its canonical model [17]. On the extrinsic side of geometry, Caporaso and Sernesi [13] have proven that over the complex numbers the theta characteristics determine the curve uniquely.

The history of reconstructing a curve from its theta hyperplanes starts in the 19th and early 20th century. For the non-hyperelliptic genus 3 curves, Aronhold [3] and Coble [18] provided methods and formulas for the reconstruction from certain ordered subsets of the 28 theta hyperplanes. In this case, the curve is a plane quartic and the hyperplanes are bitangents, lines that are tangent to the curve at two points. Also see [23, sections 6.1.2 and 6.2.2] for details.

More recently, several mathematicians including Lehavi [59], Caporaso and Sernesi [13], worked on the generalization of this problem in terms of dropping the order requirement on the theta hyperplanes and extending to higher genus curves. In 2014, Lehavi [60] explained how over the complex numbers the tritangents can be used to recover the curve for generic space sextics on smooth quadrics.

In this chapter we present several algorithms related to space sextic curves and their tritangents. In Section 4.2 we give an algorithm to compute the tritangents of space sextics on smooth quadrics and their Steiner systems; see Algorithms 4.2.1 and 4.2.2.

For computing sextic curves which arise from a construction involving del Pezzo surfaces of degree 1 and their tritangents, we rely on methods in the first three sections of the previous chapter. In Section 4.3, we compute the corresponding Steiner system for this case. In Section 4.4, we show that these curves are exactly the ones lying on singular quadrics and answer the last question of the previous chapter by presenting the inverse of that construction. In other words, given the space sextic, we find the corresponding eight points in the plane. see Algorithm 4.4.7.

Finally, in Section 4.5 we state a minor correction of [60, Theorem 2] and extend [60, Theorem 1 and 2] to space sextics on singular quadrics and over more general fields. Using them, we explain how to reconstruct space sextics from their tritangents, see Algorithms 4.5.5 and 4.5.10, for generic curves on smooth quadrics and generic curves on singular quadrics. Moreover, we allow fields with positive characteristics, provided that it is sufficiently high. All algorithms have been implemented in MAGMA [6] and are available on <https://software.mis.mpg.de>.

One of the greatest challenges in working with tritangents of space sextics symbolically, especially over fields of characteristic 0, is that the field over which all of their equations are defined is monstrous. To be precise, if  $C$  is a generic curve defined over  $\mathbb{Q}$ , then its 120 tritangents are defined over an algebraic extension of  $\mathbb{Q}$  of degree  $\# \mathrm{Sp}(8, \mathbb{F}_2) = 47377612800$ . This is critical for the reconstruction algorithms, as their correctness hinge on the existence of a single successful example. This is where space sextics from del Pezzo surfaces of degree 1 come in. For them we have a reliable method of constructing space sextics with 120 rational tritangents.

Most of the objects and notations are defined in the previous chapter. In the following section we introduce the new objects to be used throughout this chapter. For further details see [23, Section 5.4.2]. Also, some notation will closely follow that of [60].

**Convention 4.1** For the remainder of this chapter, fix a base field  $k$  of characteristic not equal to 2. In Sections 4.2 and 4.5 we assume for convenience that  $k$  is algebraically closed.

Moreover, let  $\mathbb{P}^3$  denote the projective 3-space over  $k$  and let  $C \subseteq \mathbb{P}^3$  be a smooth curve of degree 6, or equivalently a canonical model of a non-hyperelliptic curve of genus 4. We can write the curve as an intersection of a unique quadric surface  $Q_C$  and a suitable cubic surface, neither of which are necessarily smooth.

### 4.1. Steiner systems and syzygetic quadruples

Let  $J(C)$  be the Jacobian variety of  $C$  and let  $J(C)[2]$  be its 2-torsion points. For any  $\alpha \in J(C)[2] \setminus \{0\}$ , we define the *Steiner complex* associated to  $\alpha$  by

$$\Sigma_{C,\alpha} := \left\{ \{\theta, \theta + \alpha\} : \begin{array}{l} 2\theta = \kappa_C \text{ and} \\ \dim H^0(C, \theta) = \dim H^0(C, \theta + \alpha) \equiv 1 \pmod{2} \end{array} \right\},$$

where  $\theta$  is a theta characteristic of  $C$ ; or equivalently, for the corresponding linear forms

$$\mathcal{S}_{C,\alpha} := \{\{l_\theta, l_{\theta+\alpha}\} : \{\theta, \theta + \alpha\} \in \Sigma_{C,\alpha}\}.$$

We call the set

$$\mathcal{S}_C := \{\mathcal{S}_{C,\alpha} : \alpha \in J(C)[2] \setminus \{0\}\}$$

the *Steiner system* associated to  $C$ .

We call four theta characteristics  $\theta_1, \dots, \theta_4$  *syzygetic* if  $\sum_{i=1}^4 D_{\theta_i}$  is cut out by a quadric in  $\mathbb{P}^3$ . This means that there exists a quadric  $V(q) \subseteq \mathbb{P}^3$  such that  $C \cap (\bigcup_{i=1}^4 H_i) = C \cap V(q^2)$ . We call the linear forms  $l_1, \dots, l_4$  *syzygetic* if they arise from syzygetic odd theta characteristics.

Note that if  $\theta_1, \dots, \theta_4$  are odd theta characteristics of  $C$  such that  $Y := C \cap (\bigcup_{i=1}^4 H_i)$  consists of 12 points of multiplicity 1, then  $\theta_1, \dots, \theta_4$  are syzygetic if and only if there exists a quadric  $Q'$  which is not  $Q_C$  passing through the 12 points of  $Y$ .

**Remark 4.1.1** There are exactly 255 non-trivial 2-torsion points  $\alpha \in J(C)[2] \setminus \{0\}$ . On the other hand, the 120 tritangents yield precisely  $\binom{120}{2} = 7140$  pairs  $\{l_{\theta_1}, l_{\theta_2}\}$ . Intriguingly, the 7140 pairs can be split evenly into 255 blocks, each block containing exactly 28 pairs, such that

- the union of any two pairs inside a block is syzygetic,
- the union of any two pairs in two distinct blocks is not syzygetic,
- the intersection of any two pairs inside a block is empty.

These blocks are the Steiner complexes  $\Sigma_{C,\alpha}$  in our definition above. See [23, Section 5.4.2] for further explanations.

In general combinatorics a Steiner system with parameters  $(t, k, n)$  is an  $n$ -element set together with a set of  $k$ -element subsets called blocks, such that each  $t$ -element subset is contained in exactly one block. If we forget the pairings in our Steiner complexes  $\mathcal{S}_{C,\alpha}$  and simply consider them as subsets of cardinality 56, then our Steiner



system  $\mathcal{S}_C$  would be a specific instance of a general Steiner system with parameters  $(t, k, n) = (2, 56, 120)$ .

#### 4.2. Space sextics on smooth quadrics

In this section we give a full description of the algorithm appearing in Section 3.5 for calculating the 120 tritangents of a space sextic that lies on a smooth quadric. Moreover, we provide an algorithm for calculating its Steiner system.

If  $C \subseteq \mathbb{P}^3$  lies on a smooth quadric, it suffices to compute all planes which are tangent at their points of intersection since there are no vanishing theta characteristics. In theory, this can be done by intersecting  $C$  with a parametrized plane and forcing its projection onto a single generic line to be three double points. In practice, it is often sufficient and generally much more efficient to project onto all coordinate axes instead.

**Algorithm 4.2.1** (Tritangents of space sextics on smooth quadrics)

**Input:**  $(f, g)$ , where

- $f, g \in k[\mathbf{x}] := k[x_0, \dots, x_3]$  homogeneous of degrees 2, 3,
- $V(f)$  smooth,
- $C := V(f) \cap V(g)$  a space sextic.

**Output:**  $\{l_\theta : \theta \text{ odd theta characteristic of } C\} \subseteq k[\mathbf{x}]$ .

- 1: Denote by  $\mathbb{P}k[t_0, t_1]_6$  the space of homogeneous sextic polynomials in  $k[t_0, t_1]$ . Let  $V(J) \subseteq \mathbb{P}k[t_0, t_1]_6$  be the threefold of perfect squares whose ideal  $J \subseteq k[a_0, \dots, a_6]$  is minimally generated by 45 quartics; see [58, Table 1]

$$\begin{array}{ccc} \mathbb{P}k[t_0, t_1]_6 & \xrightarrow[\cup \cup]{\cong} & \mathbb{P}^6 \\ a_0 t_0^6 + \dots + a_6 t_1^6 \mapsto (a_0 : \dots : a_6) & & \\ \cup \cup & & \cup \cup \\ \{(b_0 t_0^3 + \dots + b_3 t_1^3)^2 : (b_0 : \dots : b_3) \in \mathbb{P}^3\} & \xrightarrow{\cong} & V(J) \end{array}$$

- 2: Consider the defining linear form of a parametrized plane in  $k[\mathbf{x}]$

$$u_0 x_0 + \dots + u_3 x_3 \in k[\mathbf{u}^{\pm 1}][\mathbf{x}] := k[u_0^{\pm 1}, \dots, u_3^{\pm 1}][x_0, \dots, x_3].$$

- 3: **for**  $i, j \in \{0, \dots, 3\}$ ,  $i \neq j$  **do**

- 4: Let  $f_i, g_i$  be the images of  $f, g$  under the substitution map

$$k[\mathbf{u}^{\pm 1}][\mathbf{x}] \longrightarrow k[\mathbf{u}^{\pm 1}][x_j, x_k, x_l], \quad x_i \longmapsto \frac{-u_j x_j - u_k x_k - u_l x_l}{u_i},$$

where  $\{i, j, k, l\} = \{0, \dots, 3\}$ .

- 5: Compute the following resultant which is a homogeneous sextic in  $x_k, x_l$

$$\sum_{\mu=0}^6 c_\mu \cdot x_k^{6-\mu} x_l^\mu := \text{Res}(f_i, g_i, x_j) \in k[\mathbf{u}^{\pm 1}][x_k, x_l].$$

- 6: Let  $I_{ij}$  denote the image of  $J$  under the substitution map

$$k[a_0, \dots, a_6] \longrightarrow k[\mathbf{u}^{\pm 1}], \quad a_\mu \longmapsto c_\mu.$$

- 7: Set  $I := \sum_{i,j} I_{ij}$  and compute the 120 points in  $V(I)$ .

- 8: **return**  $\{z_0x_0 + \dots + z_3x_3 : (z_0 : \dots : z_3) \in V(I)\}$ .

A simple way to obtain the Steiner system from the set of linear forms is to exploit the fact that they form a Steiner system in the combinatorial sense; see Remark 4.1.1. Algorithm 4.2.2 simply enumerates through all pairs of linear forms, grouping those together which are syzygetic.

**Algorithm 4.2.2** (Steiner system via syzygetic relations)

**Input:**  $(f, g, T)$ , where

- $f, g \in k[\mathbf{x}]$  homogeneous of degrees 2, 3,
- $V(f)$  smooth,
- $C := V(f) \cap V(g)$  a space sextic,
- $T = \{l_\theta : \theta \text{ odd theta characteristic of } C\} \subseteq k[\mathbf{x}]$ .

**Output:**  $\mathcal{S}_C$ , the Steiner system associated to  $C$ .

- 1: Initialize  $\mathcal{S}_C := \emptyset$ .
- 2: **for**  $\{l_1, l_2\} \subseteq T$  with  $l_1 \neq l_2$  **do**
- 3:   **if**  $\exists S \in \mathcal{S}_C \exists \{l_3, l_4\} \in \Sigma : l_1, \dots, l_4 \text{ syzygetic}$  **then**
- 4:     Set  $S := S \cup \{\{l_1, l_2\}\}$ .
- 5:   **else**
- 6:     Set  $S := \{\{l_1, l_2\}\}$  and  $\mathcal{S}_C := \mathcal{S}_C \cup \{S\}$ .
- 7: **return**  $\mathcal{S}_C$ .

**Remark 4.2.3** The bottleneck in Algorithm 4.2.2 is deciding whether four linear forms  $l_1, \dots, l_4$  are syzygetic in Step 3. This can be done in several ways depending on what is viable. One straightforward option would be to compute whether the intersection  $C \cap (\bigcup_{i=1}^4 V(l_i))$ , as a divisor of  $C$ , is linearly equivalent to  $2\kappa_C$  using the MAGMA intrinsic `IsLinearlyEquivalent`.

**Remark 4.2.4** Note that Algorithm 4.2.2 can also be applied ad verbum to space sextics on singular quadrics. Algorithm 4.2.1 has a straightforward generalization:

For a sextic on a singular quadric, the ideal  $I$  in Step 7 will be positive dimensional. It will contain infinitely many tangent planes of the singular quadric that contain the singularity; see Proposition 3.2.1. This positive dimensional component can be removed using saturation, leaving us with the desired 120 tritangents that are of interest to us.

When applied to space sextic curves that arise from the construction in Section 3.1, both Algorithm 4.2.1 and Algorithm 4.2.2 prove to be inferior to their more specialized counterparts in Section 3.1, which is why we generally advise against using them for space sextics on singular quadrics.

### 4.3. Space sextics on singular quadrics

We briefly review the construction of space sextics from del Pezzo surfaces of degree 1 and its tritangents from the previous chapter. For more details see Sections 3.1 to 3.3. Next, we use this construction to compute the corresponding Steiner system.

For a fixed configuration  $\mathcal{P} := \{P_1, \dots, P_8\} \subseteq \mathbb{P}^2$  of eight points, recall the following diagram from Figure 3.3:

$$\begin{array}{ccc}
 \mathbb{P}^2 & \xrightarrow{\psi} & \mathbb{P}(1:1:2:3) \supseteq X_{\mathcal{P}} := \psi(\mathbb{P}^2) \\
 \pi \downarrow & & \downarrow (u:v:w:r) \\
 & & \downarrow (u:v:w) \\
 & & \mathbb{P}(1:1:2) \supseteq C' := \text{BranchCurve}(\pi|_{X_{\mathcal{P}}}) \\
 \phi \downarrow & & \downarrow (u:v:w) \\
 & & \downarrow (u^2:uv:v^2:w) \\
 \mathbb{P}^3 & \supseteq & C
 \end{array}$$

where the map  $\psi$  is the blow-up of  $\mathbb{P}^2$  at  $\mathcal{P}$ . The image of  $\psi$  is a del Pezzo surface of degree 1 with the following defining equation

$$X_{\mathcal{P}}: r^2 = w^3 + f_2(u, v) \cdot w^2 + f_4(u, v) \cdot w + f_6(u, v),$$

in the weighted projective space  $\mathbb{P}(1:1:2:3)$ , such that each  $f_2, f_4, f_6$  is homogeneous degree 2, 4, 6 respectively. Note that we obtain an elliptic curve on  $X$  by specializing  $t = 0$ , which will be important in Section 4.4.

The ramification locus of the projection  $\pi$  is  $C'$ . The defining equation of the branch curve  $C'$  in  $\mathbb{P}(1:1:2)$  is

$$C': \quad 0 = w^3 + f_2(u, v) \cdot w^2 + f_4(u, v) \cdot w + f_6(u, v).$$

Finally the space sextic  $C \subseteq \mathbb{P}^3$  is the image of  $C'$  under the embedding  $\phi$ , i.e.  $C = \phi(C')$ .

We observed that the 120 tritangents of  $C$  have a natural description in the framework of our construction. Recall that  $l_\theta$  is the linear form corresponding to the odd theta characteristic  $\theta$ . If  $H_\theta := V(l_\theta)$  is a tritangent of  $C$ , then  $\phi^{-1}(H_\theta)$  is a curve in  $\mathbb{P}(1 : 1 : 2)$  of weighted degree 2 tangent to  $C'$  at 3 points (counting multiplicity). We call  $\phi^{-1}(H_\theta)$  a *tritangent curve* of  $C'$ .

Every tritangent curve of  $C'$  is the image of exactly two exceptional curves  $(e, e')$  on the del Pezzo surface  $X$  under  $\pi$ , which are conjugate under the Bertini involution of  $X$ . We differentiate between the following types of tritangents, which are named after the degrees of  $\overline{\psi^{-1}e}, \overline{\psi^{-1}e'} \subseteq \mathbb{P}^2$ . The 120 tritangents (120 tritangent curves) are 8, 28, 56, and 28 tritangents (tritangent curves) of type  $(0, 6)$ ,  $(1, 5)$ ,  $(2, 4)$ , and  $(3, 3)$  respectively.

**Example 4.3.1** Consider the configuration  $\mathcal{P} = \{P_1, \dots, P_8\} \subseteq \mathbb{P}\mathbb{Z}^3$  of the following 8 points as in 3.3.1:

$$\begin{aligned} P_1 &= (1:0:0), & P_2 &= (0:1:0), \\ P_3 &= (0:0:1), & P_4 &= (1:1:1), \\ P_5 &= (10:11:1), & P_6 &= (19:-11:12), \\ P_7 &= (15:19:-20), & P_8 &= (27:2:17). \end{aligned}$$

One can verify that the points in  $\mathcal{P} \subseteq \mathbb{P}\mathbb{Q}^3$  are in general position, which also implies that the points in  $\overline{\mathcal{P}} \subseteq \mathbb{P}\mathbb{F}_p^3$  remain in general position for all but finitely many primes  $p$ . For instance, for  $p = 97$  they stay in general position, while for  $p = 5$  we have  $\overline{P}_2 = \overline{P}_5 \in \mathbb{P}\mathbb{F}_5^3$ .

From now on, consider the base field  $k := \mathbb{F}_{97}$ . We compute two linearly independent cubics  $u, v$  that vanish on  $\mathcal{P}$  and a sextic  $w$  not divisible by  $u$  or  $v$ , vanishing doubly on  $\mathcal{P}$ . Our implementation gives

$$\begin{aligned} u &= x_0x_1^2 + 33x_0^2x_2 + 74x_0x_1x_2 + 77x_1^2x_2 + 47x_0x_2^2 + 59x_1x_2^2, \\ v &= x_0^2x_1 + 86x_0^2x_2 + 57x_0x_1x_2 + 35x_1^2x_2 + 15x_1x_2^2, \\ w &= x_0^4x_1x_2 + 72x_0^3x_1^2x_2 + 68x_0^2x_1^3x_2 + 55x_0x_1^4x_2 + 67x_0^4x_2^2 \\ &\quad + 78x_0^3x_1x_2^2 + 11x_0^2x_1^2x_2^2 + 18x_0x_1^3x_2^2 + 43x_1^4x_2^2 + 23x_0^2x_1x_2^3 \\ &\quad + 55x_0x_1^2x_2^3 + 64x_1^3x_2^3 + 7x_0^2x_2^4 + 96x_0x_1x_2^4 + 21x_1^2x_2^4. \end{aligned}$$

This results in the following space sextic  $C \subseteq \mathbb{P}^3$ , which can be verified to be smooth:

$$C: \begin{cases} 0 = x_1^2 - x_0x_2, \\ 0 = 94x_0^3 + 88x_0^2x_1 + 27x_0^2x_2 + 16x_0x_1x_2 + 82x_0x_2^2 + 72x_1x_2^2 \\ \quad + 73x_2^3 + 18x_0^2x_3 + 17x_0x_1x_3 + 84x_0x_2x_3 + 43x_1x_2x_3 \\ \quad + 37x_2^2x_3 + 63x_0x_2^2 + 64x_1x_2^2 + 63x_2x_3^2 + 74x_3^3. \end{cases}$$

Let  $h_{12}$  and  $h_{34}$  be the lines through the points  $P_1, P_2$  and  $P_3, P_4$  respectively and let  $h_{125}$  and  $h_{345}$  be the conics through the points  $\mathcal{P} \setminus \{P_1, P_2, P_5\}$  and  $\mathcal{P} \setminus \{P_3, P_4, P_5\}$  respectively. They are given by

$$\begin{aligned} h_{12} &= x_2, & h_{125} &= 19x_0^2 + 58x_0x_1 + 65x_1^2 + 21x_0x_2 + 31x_1x_2, \\ h_{34} &= x_0 - x_1, & h_{345} &= 3x_0x_1 + 89x_0x_2 + 3x_1x_2 + 42x_2^2. \end{aligned}$$

Their images in  $\mathcal{P}^3$  are cut out by the following polynomials and one can verify that each of them intersect  $C$  in three double points:

$$\begin{aligned} l_{12} &= x_3, & l_{125} &= x_0 + 52x_1 + 23x_2 + 87x_3, \\ l_{34} &= x_0 + 70x_1 + 8x_2 + 43x_3, & l_{345} &= x_0 + 71x_1 + 65x_2 + 94x_3. \end{aligned}$$

**Constructing the Steiner system:** Let  $P_1, \dots, P_8$  be eight points in  $\mathbb{P}^2$  in general position, let  $X_{\mathcal{P}}$  be the del Pezzo surface of degree 1 obtained by blowing up  $\mathbb{P}^2$  at  $\{P_1, \dots, P_8\}$ , and let  $C$  the space sextic arising from  $X_{\mathcal{P}}$ . The Steiner system of  $C$  can be much more efficiently constructed than for a generic space sextic by making use of the initial eight points in  $\mathbb{P}^2$ :

We label each tritangent by a subset of  $\{1, \dots, 9\}$  depending on their types as follows:

$$L(H) := \begin{cases} \{1, \dots, 8\} \setminus \{i\} & \text{if } H \text{ is of type } (0, 6), \\ \{1, \dots, 8, 9\} \setminus \{i, j\} & \text{if } H \text{ is of type } (1, 5), \\ \{i, j, k\} & \text{if } H \text{ is of type } (2, 4), \\ \{i, j, 9\} & \text{if } H \text{ is of type } (3, 3), \end{cases}$$

where for each type  $i, j, k$  are as in Figure 4.1.

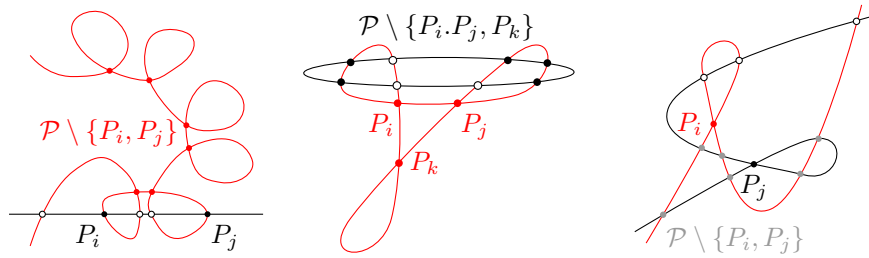


FIGURE 4.1. We use pairs of exceptional curves to construct the Steiner system.

Given four theta characteristics  $\theta_1, \dots, \theta_4$  and their tritangents  $H_1, \dots, H_4$ , we then have

$$\theta_1, \dots, \theta_4 \text{ syzygetic} \iff L(H_1) \Delta \dots \Delta L(H_4) = \emptyset.$$

The fact that the Steiner system of  $C$  can be constructed purely combinatorially is rooted in a classical connection between theta characteristics of  $C$  and quadratic forms over  $J(C)[2]$  [23, Section 5]:

The 256 points in  $J(C)[2]$  together with the Weil-pairing can be regarded as a symplectic vector space over  $\mathbb{F}_2$  of dimension 8. The space of quadratic forms of  $J(C)[2]$ , which we denote by  $\mathcal{Q}(J(C)[2])$ , is a homogeneous space of  $J(C)[2]$ . The disjoint union  $J(C)[2] \amalg \mathcal{Q}(J(C)[2])$  has the natural structure of an  $\mathbb{F}_2$ -vector space of dimension 9. Each quadratic form corresponds to a theta characteristic of  $C$ .

Let  $\text{res}_C: \text{Pic}(X) \rightarrow \text{Pic}(C)$  be the natural restriction and set  $v_i := \text{res}_C(e_i + \kappa_{X_{\mathcal{P}}})$ , where  $e_1, \dots, e_8$  are the eight exceptional divisors of  $X_{\mathcal{P}}$  corresponding to the eight points  $P_1, \dots, P_8$  under the blow-down map. We may construct an Aronhold basis  $B$  of  $J(C)[2] \amalg \mathcal{Q}(J(C)[2])$  from the set  $\{v_1, \dots, v_8, \text{res}_C(-\kappa_{X_{\mathcal{P}}})\} \subseteq \text{Pic}(C)$  via [73, Theorem II A1.1.]. The labeling of a tritangent plane stated above can be understood in terms of the  $B$ -coordinates of the corresponding odd theta characteristic, viewed as an element of  $J(C)[2] \amalg \mathcal{Q}(J(C)[2])$ . For further details, see [14, Section 1.1.4].

Under this correspondence, the eight exceptional divisors on  $X_{\mathcal{P}}$ , together with its anticanonical divisor, give rise to a special basis of  $J(C)[2] \amalg \mathcal{Q}(J(C)[2])$  called an Aronhold basis [73, Theorem II A1.1.]. The labeling of the tritangents defined above come from linear expressions of the corresponding quadratic forms in terms of the Aronhold basis. We refer to [14, Section 1.1.4] for the details of obtaining the Aronhold basis giving this particular labeling and its relation with being syzygetic.

**Example 4.3.2** Consider again the curve  $C \subseteq \mathbb{PF}_{97}^3$  and its four tritangents from Example 4.3.1. Their labels are:

$$\begin{aligned} L(V(l_{12})) &= \{3, 4, 5, 6, 7, 8, 9\}, & L(V(l_{125})) &= \{1, 2, 5\}. \\ L(V(l_{34})) &= \{1, 2, 5, 6, 7, 8, 9\}, & L(V(l_{345})) &= \{3, 4, 5\}. \end{aligned}$$

They have an empty symmetric difference and are therefore syzygetic. Indeed, one can verify that there exists a quadric which is not  $V(x_1^2 - x_0x_2)$  that vanishes on all 12 contact points of the tritangents with  $C$ .

#### 4.4. Reconstruction of eight points from space sextics

Given a space sextic curve  $C$  in  $\mathbb{P}^3$  which comes from blowing up the plane at eight points, we will construct some collection of 8 points in  $\mathbb{P}^2$  such that the construction applied to these 8 points gives a space sextic isomorphic to  $C$ . If a del Pezzo surface  $X$  of degree 1 has 8 pairwise orthogonal exceptional curves defined over  $k$ , then the blow-down of  $X$  along these 8 curves is isomorphic to  $\mathbb{P}^2$  [64, Theorem 24.4.iii]. The

8 exceptional curves mark 8 points in the plane. Since this is true of any collection of 8 pairwise orthogonal exceptional curves of  $X$ , we see that the set of 8 points in the plane which construct the branch curve of  $X$  is not unique, even up to linear transformations. The goal of our algorithm is to find one such set.

Over an algebraically closed field of characteristic not 2, a space sextic curve  $C$  arises from a del Pezzo surface of degree 1 if and only if the unique quadric in  $\mathbb{P}^3$  containing  $C$  is singular [64, Theorem 24.4.iii]. However, when  $k$  is not algebraically closed the situation is slightly more complicated. Nevertheless, our implementation is able to detect when a curve comes from eight  $k$ -rational points in the plane. Our method of detection and recovery uses the 120 tritangents given as input. By assuming that the 120 odd theta characteristics are defined over  $k$ , we can return to the simplicity of the algebraically closed case.

**Proposition 4.4.1** *Then a space sextic curve  $C$  defined over  $k$  arises from a del Pezzo surface of degree 1 if and only if the unique quadric in  $\mathbb{P}^3$  containing  $C$  is singular and all 120 odd theta characteristics are defined over  $k$ .*

PROOF. The forward direction is entirely classical. For the reverse, let  $Q$  be the singular quadric containing  $C$ . As  $C$  is smooth, we must have that  $Q$  is a quadric cone. We claim that  $Q$  is isomorphic over  $k$  to the weighted projective space  $\mathbb{P}(1:1:2)$ . Let  $H$  be any tritangent plane of  $C$  corresponding to an odd theta characteristic and let  $D := \frac{1}{2}(H \cap C)$ . By Proposition 3.2.1,  $H$  does not pass through the singularity of  $Q$ , so  $Q \cap H$  is a plane conic and  $D$  is an odd degree divisor on  $Q \cap H$ . Thus, we have that  $\mathbb{P}^1 \cong Q \cap H$ .

Since  $Q \cap H \subseteq H$  is a plane conic with a  $k$ -rational point, we may change coordinates so that  $H = V(x_3)$  and such that  $H \cap Q = V(x_3, x_1^2 - x_0x_2)$ . That is,  $Q$  is isomorphic to the standard quadric cone. Since  $C$  lies on a standard quadric cone, we have that  $C$  lies on a degree 1 del Pezzo surface  $X$ . Moreover, as all 120 tritangents of  $C$  are defined over  $k$ , there is a quadratic twist of  $X$  such that all 240 exceptional curves are defined over  $k$ . The proposition now follows from [64, Theorem 24.4].  $\square$

**Remark 4.4.2** Note that the construction of the space sextics from del Pezzo surfaces of degree 1 as in [54, Section 2] considers slightly more general configurations of 8 points in  $\mathbb{P}^2$ . Specifically, it was only required that the set of eight points be  $\text{Gal}(\bar{\mathbb{Q}}/\mathbb{Q})$ -invariant in order to construct a space sextic defined over  $\mathbb{Q}$ . For the sake of simplifying our implementation we do not consider this general setting.

We are now ready to provide an algorithm that for a given space sextic on a singular quadric, computes eight points in the plane, the

blow-up of which returns the same space sextic. First we present an overview of the steps.

**The reconstruction algorithm:** The algorithm proceeds along the following general steps:

- (i) Compute a degree 1 del Pezzo surface  $X$  as in Figure 3.3.
- (ii) Determine the 240 exceptional curves on  $X$ , possibly requiring a quadratic twisting of  $X$ .
- (iii) Identify 8 pairwise orthogonal curves defined over  $k$ .
- (iv) Identify a genus 1 curve  $E \subseteq X$  defined over  $k$ , and intersect it with the 8 exceptional curves to obtain 8 points.
- (v) Construct a particular embedding of  $E$  into  $\mathbb{P}^2$  with the properties expected of the blow-down of  $E$  along 8 pairwise orthogonal exceptional curves.

We shall assume that our curve  $C$  is given as the intersection of a cubic  $V(f)$  and the quadric  $V(x_1^2 - x_0x_2)$  in  $\mathbb{P}^3$  with coordinates  $(x_0:x_1:x_2:x_3)$ . Note that up to linear transformation any singular quadric with a smooth  $k$ -rational point is the one we have specified. We assume that we are given the 120 tritangent planes as linear forms  $\{\ell_1, \dots, \ell_{120}\}$  with coefficients in  $k$ . Finally, we use the existence of the maps in Figure 3.3 where  $C$  would be our given curve. As before, we will denote the coordinates of  $\mathbb{P}(1:1:2)$  and  $\mathbb{P}(1:1:2:3)$  by  $(u:v:w)$  and  $(u:v:w:r)$  respectively and let  $\pi$  be the usual projection.

To accomplish Steps (i) and (ii), we compute the pullback of the curve and the tritangent planes to  $\mathbb{P}(1:1:2)$  to set an equation for the del Pezzo surface  $X$  of degree 1. More precisely, let  $F$  be the pullback of  $f$  under the map  $\phi$  and  $h_i$  be the pullback of  $l_i$  under the map  $\phi$  for  $i = 1, \dots, 120$ . We may normalize  $F$  and the  $h_i$  so that the leading coefficient in  $w$  is 1. We choose  $\lambda \in k^\times$  such that

$$\text{Res}(h_1(u, v, w), \lambda F(u, v, w), w) \in k[u, v]$$

is a square over  $k$ . We set

$$r^2 - \lambda F(u, v, w)$$

to be the defining equation of a del Pezzo surface  $X$  in  $\mathbb{P}(1:1:2:3)$ . By definition,  $\phi$  maps the branch curve of the projection  $\pi|_X$  to  $C$ . Thus,  $X$  is exactly the same surface occurring in Section 4.3 up to isomorphism over  $\bar{k}$ . The choice of  $\lambda$  merely selects the unique quadratic twist such that the pair of exceptional curves over the tritangent curve defined by  $h_1$  is split over  $k$ .



**Lemma 4.4.3** *With the notation of the preceding paragraph, the subvariety*

$$V(r^2 - \lambda F(u, v, w), h_i(u, v, w)) \subseteq X$$

*is the union of two Bertini-conjugate exceptional curves  $e_{2i-1}$ ,  $e_{2i}$ . The curves are individually defined over  $k$  and are explicitly given by*

$$e_{2i-1}, e_{2i} := V\left(h_i(u, v, w), r \pm \sqrt{\text{Res}(h_i(u, v, w), \lambda F(u, v, w), w)}\right).$$

PROOF. From Section 4.3 we have that the image under  $\pi$  of any exceptional curve is a tritangent curve and every tritangent curve arises in this way. The first statement of the lemma follows immediately.

If  $C$  arose from blowing up eight  $k$ -rational points in the plane, then all of the exceptional curves on some quadratic twist of  $X$  must be defined over  $k$ . Since we have already chosen a twist where one pair of exceptional curves is split over  $k$ , all of them must be so.

All that remains to be shown is the correctness of the defining equations. We have defined  $h_i$  to be in the defining ideal of the tritangent curve, so the scheme

$$V(h_i(u, v, w), r^2 - \text{Res}(h_i(u, v, w), \lambda F(u, v, w), w))$$

must lie over the tritangent curve defined by  $h_i$ . Next, we see that

$$X \cap V(h_i(u, v, w)) = V(r^2 - \lambda F(u, v, w), h_i(u, v, w))$$

is reducible, with the two components defined over  $k$  corresponding to the two exceptional curves over  $V(h_i(u, v, w)) \subseteq \mathbb{P}(1:1:2)$ . Note  $h_i(u, v, w)$  is a degree 1 polynomial in  $w$  and both  $h_i$  and  $F$  are monic due to the normalization, so the resultant is really just the evaluation of  $\lambda F$  at  $-h_i(u, v, 0)$ . In particular, the resultant is a square and

$$X \cap V(h_i(u, v, w)) = V(r^2 - \lambda F(u, v, -h_i(u, v, 0)), h_i(u, v, w)).$$

The polynomial  $r^2 - \lambda F(u, v, -h_i(u, v, 0))$  factors over  $k$ , giving the two components.  $\square$

For Step (iii), we compute the Gram matrix for the intersection pairing on the lattice generated by the exceptional curves using Gröbner bases. We use the fact that the Weyl group of  $E_8$  acts via isometry on the lattice generated by the exceptional curves to optimize the process of searching for a collection of 8 pairwise orthogonal curves.

Step (iv) and (v) of our algorithm identify the eight points using the geometry of genus 1 curves, allowing us to avoid an expensive blow-down computation. Step (iv) turns out to be rather easy; the genus 1 curve  $E$  is obtained by specializing  $v = 0$ . To indirectly compute the blow-down of this genus 1 curve, we use the following lemma.

**Lemma 4.4.4** *Let  $E$  be a plane cubic curve and let  $p_1, p_2, p_3 \in E(\bar{k})$  be three collinear points. Then the embedding of  $E$  into  $\mathbb{P}^2$  is the unique embedding with  $p_1, p_2, p_3$  collinear, up to  $\text{Aut}(\mathbb{P}^2)$ .*

PROOF. Let  $D := p_1 + p_2 + p_3$  and let  $\gamma: E \rightarrow \mathbb{P}^2$  be an embedding. Since  $D$  is a hyperplane section of this embedding, we have that  $\gamma$  factors into  $|D|: E \rightarrow \mathbb{P}^2$ . There is exactly one complete linear system containing  $D$ , so we are done.  $\square$

The blow-down of the genus 1 curve  $E$  will be a plane curve of arithmetic genus 1, which is to say, a plane cubic curve. It suffices for us to identify three points on  $E$  which are collinear in the blow-down to identify the correct embedding into  $\mathbb{P}^2$  given by the blow-down. Crucially, *the eight intersection points of  $E$  with the set of eight pairwise orthogonal exceptional curves are the points where  $E$  meets the eight exceptional points of the blow-up in  $\mathbb{P}^2$* . In order to identify three collinear points on  $E$ , we use a “trivial” lemma, which states that the effective divisors in the hyperplane class correspond to hyperplanes.

**Lemma 4.4.5** *Let  $X$  be the degree 1 del Pezzo surface obtained from blowing up  $\{P_1, \dots, P_8\}$ . Let  $E \subseteq \mathbb{P}^2$  be a plane cubic curve passing through the eight points, let  $\text{res}_E: \text{Pic}(X) \rightarrow \text{Pic}(E)$  be the natural restriction, and let  $\ell \in \text{Pic}(X)$  be the hyperplane class on  $X$ . Then the effective representatives of the divisor class  $\text{res}_E(\ell)$  are exactly the divisors of  $E$  defined by lines in  $\mathbb{P}^2$ .*

PROOF. By definition, a representative of the class  $\ell$  is the strict transform of a line in  $\mathbb{P}^2$  not passing through any of the eight points of the blow up. The result extends to all effective representatives of  $\text{res}_E(\ell)$  via linear equivalence.  $\square$

An appropriate curve  $E$ , divisor  $D$ , and class  $\ell$  can be identified using only  $X$  and the exceptional curves of  $X$ . The class  $\ell \in \text{Pic}(X)$  is uniquely identified by its intersection numbers [64, Corollary 25.1.1]; it is the unique divisor class such that  $\ell^2 = 1$ ,  $\ell \cdot e_i = 0$ , and (redundantly)  $\ell \cdot (-\kappa_X) = 3$ . To find a representative, we use the following lemma.

**Lemma 4.4.6** *Let  $e'_1, e'_2$  be a pair of orthogonal exceptional curves of  $X$ . There exists an exceptional curve  $e$  such that  $\ell = [e + (e'_1 + e'_2)]$ .*

PROOF. Note that  $X$  is the blow-up of  $\mathbb{P}^2$  at  $\{P_1, \dots, P_8\}$ . The strict transform of the line through  $\{P_1, P_2\}$  is an exceptional curve  $e$ . Thus the pullback of the line through  $\{P_1, P_2\}$  by the blow-down, as a divisor of  $X$ , is  $e + (e'_1 + e'_2)$ .  $\square$

We are now equipped with all needed for presenting Algorithm 4.4.7.

**Algorithm 4.4.7** (Reconstruction of 8 points from space sextics)

**Input:**  $(f, \{l_1, \dots, l_{120}\})$ , where

- $f \in k[x_0, \dots, x_3]$  homogeneous of degrees 3 such that  $C := V(f) \cap V(x_1^2 - x_0x_2)$  space sextic,
- $\{l_1, \dots, l_{120}\}$  is a list of 120 tritangent plane to  $C$ .

**Output:**  $\mathcal{P} \subseteq \mathbb{P}^2$ , a set of 8 points such that the del Pezzo surface of degree 1 obtained by blowing up  $\mathbb{P}^2$  at  $\mathcal{P}$  has branch curve isomorphic to  $C$ .

- 1: Set  $F(u, v, w) := f(s^2, st, t^2, w)$  to be the pullback of  $f$  under the map  $\phi$ .
- 2: Set  $h_i := \ell_i(s^2, st, t^2, w)$  to be the pullback of linear form  $\ell_i$  under the map  $\phi$ .
- 3: Normalize  $F$  and  $h_1, \dots, h_{120}$ .
- 4: Choose  $\lambda \in k^\times$  such that  $\text{Res}(h_1(u, v, w), \lambda F(u, v, w), w) \in k[u, v]$  is a square.
- 5: Set the defining equation of the del Pezzo surface  $X$  to be  $r^2 - \lambda F(u, v, w)$ .
- 6: Set the pair of exceptional curves corresponding to the  $i$ -th tritangent,

$$e_{2i-1}, e_{2i} := V\left(h_i(u, v, w), r \pm \sqrt{\text{Res}(h_i(u, v, w), \lambda F(u, v, w), w)}\right).$$

- 7: Compute the Gram matrix  $M := (\deg(e_i \cap e_j))_{1 \leq i \neq j \leq 240}$ , where the diagonal entries are set to  $-1$ .
- 8: Determine a collection  $\{e'_i\}$  of eight pairwise orthogonal exceptional curves by computing an  $8 \times 8$  principal submatrix  $B$  of  $M$  such that  $-B$  is the identity matrix.
- 9: Construct the elliptic curve  $E$  on  $X$  by setting  $v = 0$  and set  $p_i := E \cap e'_i$ .
- 10: Identify the unique exceptional curve  $e$  such that

$$\deg(e \cap e'_j) = \begin{cases} 1 & \text{if } j = 1, 2, \\ 0 & \text{otherwise.} \end{cases}$$

- 11: Compute  $H^0(E, \mathcal{O}_E(D))$ , where  $D := (e \cap E) + p_1 + p_2$  is a divisor on  $E$ .
- 12: **return** The images of  $p_1, \dots, p_8$  under the map defined by  $H^0(E, \mathcal{O}_E(D))$ .

**Remark 4.4.8** One challenging step in Algorithm 4.4.7 that we deliberately avoided expanding on is the computation of  $H^0(E, \mathcal{O}_E(D))$  in Step 11, since most computer algebra systems have existing commands for it. For example, in our MAGMA implementation we use the intrinsic command `DivisorMap`.

**Example 4.4.9** We apply our algorithm to the space sextic curve obtained in Example 4.3.1. We recall that the defining equations of the space sextic  $C$  are:

$$\begin{aligned} q &= x_1^2 - x_0x_2, \\ f &= 94x_0^3 + 88x_0^2x_1 + 27x_0^2x_2 + 16x_0x_1x_2 + 82x_0x_2^2 + 72x_1x_2^2 + 73x_2^3 \\ &\quad + 18x_0^2x_3 + 17x_0x_1x_3 + 84x_0x_2x_3 + 43x_1x_2x_3 + 37x_2^2x_3 + 63x_0x_3^2 \\ &\quad + 64x_1x_3^2 + 63x_2x_3^2 + 74x_3^3. \end{aligned}$$

The defining equation of the del Pezzo surface  $X$  in  $\mathbb{P}(1:1:2:3)$  with coordinates  $(u:t:w:r)$  constructed in Algorithm 4.4.7 is

$$\begin{aligned} X: \quad -r^2 &= 2u^6 + 6u^5v + 79u^4v^2 + 54u^3v^3 + 10u^2v^4 + 49uv^5 + 16v^6 + 85u^4w \\ &\quad + 21u^3vw + 41u^2v^2w + 36uv^3w + 40v^4w + 55u^2w^2 + 22uvw^2 \\ &\quad + 55v^2w^2 + 80w^3. \end{aligned}$$

Algorithm 4.4.7 computes some set of eight pairwise orthogonal exceptional curves. Below are the defining equations in  $\mathbb{P}(1:1:2:3)$ .

$$\begin{aligned} e_1: \begin{cases} w = 61u^2 + 19uv + 83v^2, \\ r = 82u^3 + 44u^2v + 23uv^2 + 75v^3, \end{cases} & e_2: \begin{cases} w = 41u^2 + 9uv + 81v^2, \\ r = 23u^3 + 13u^2v + 14uv^2 + 37v^3, \end{cases} \\ e_3: \begin{cases} w = 45u^2 + 36uv + 90v^2, \\ r = 54u^2v + 18uv^2 + 13v^3, \end{cases} & e_4: \begin{cases} w = 4u^2 + 8uv + 93v^2, \\ r = 43u^3 + 5u^2v + 22uv^2 + 58v^3, \end{cases} \\ e_5: \begin{cases} w = 26u^2 + 57uv + 77v^2, \\ r = 68u^3 + 55u^2v + 30uv^2 + 95v^3, \end{cases} & e_6: \begin{cases} w = -u^2 + 22uv + 66v^2, \\ r = 81u^3 + 41u^2v + 20uv^2 + 5v^3, \end{cases} \\ e_7: \begin{cases} w = -u^2 + 69uv + 27v^2, \\ r = 16u^3 + 41u^2v + 16uv^2 + 13v^3, \end{cases} & e_8: \begin{cases} w = uv + 67v^2, \\ r = 32u^3 + 40u^2v + 66uv^2 + 24v^3. \end{cases} \end{aligned}$$

The genus 1 curve  $E \subseteq X$  is defined by the common zero set of  $v$  and the defining equation of  $X$ . Finally, the resulting eight points  $P' = \{P'_1, \dots, P'_8\}$  are

$$\begin{aligned} P'_1 &= (35:48:1), & P'_2 &= (41:1:0), \\ P'_3 &= (41:91:1), & P'_4 &= (61:1:0), \\ P'_5 &= (11:14:1), & P'_6 &= (27:95:1), \\ P'_7 &= (52:80:1), & P'_8 &= (88:68:1). \end{aligned}$$

Notice that the eight points  $\mathcal{P}'$  are not the same as the original collection of eight points  $\mathcal{P}$  in Example 4.3.1. The difference potentially arises due to choice made at Step (8) and linear transformations of  $\mathbb{P}^2$ . In this case the linear transformation given by the following matrix maps  $P'_i$  to  $P_i$  for  $i = 1, \dots, 8$ :

$$\begin{pmatrix} 34 & 61 & 39 \\ 27 & 3 & 75 \\ 34 & 61 & 53 \end{pmatrix}.$$

#### 4.5. Steiner systems to space sextics

In this section, we extend Lehavi's methods [60] for reconstructing space sextics from their Steiner system to space sextics on singular quadrics and to space sextics over more general fields. We detail their implementation in MAGMA and, as a consequence, obtain a simplified proof of Lehavi's results.

The method is naturally divided in two parts: the reconstruction of the unique quadric surface containing the curve and the reconstruction of a cubic surface which cuts out the curve on the quadric.

**Reconstructing the unique quadric.** For the reconstruction of the quadric, we briefly recall the notation in [60, Section 1].

**Definition 4.5.1** Let  $V_C := H^0(\mathcal{O}_{|\kappa_C|^*}(2))$  be the vector space of degree 2 forms on the canonical  $\mathbb{P}^3$  containing  $C$ .

For all  $\alpha \in J(C)[2] \setminus \{0\}$  and all  $\{\theta, \theta + \alpha\} \in \Sigma_{C,\alpha}$ , let  $q_{\theta, \theta + \alpha} := l_\theta \cdot l_{\theta + \alpha} \in V_C$  be the quadric form cutting out the two tri-tangent planes corresponding to  $\theta$  and  $\theta + \alpha$ .

For all  $\alpha \in J(C)[2] \setminus \{0\}$ , let  $V_{C,\alpha} \subseteq V_C$  be defined as in the following diagram:

$$\begin{array}{ccc} V_C = H^0(\mathcal{O}_{|\kappa_C|^*}(2)) & \supseteq & p^{-1}iH^0(\mathcal{O}_{|\kappa_C+\alpha|^*}(2)) =: V_{C,\alpha} \\ \downarrow p & & \\ H^0(2\kappa_C) & \xleftarrow{i} & H^0(\mathcal{O}_{|\kappa_C+\alpha|^*}(2)) \end{array}$$

where, if we view the elements of  $H^0(2\kappa_C)$  as effective representatives of  $2\kappa_C$ , the projection  $p: V_C \rightarrow H^0(2\kappa_C)$  maps a quadric  $Q$  to

$$p(Q) = \begin{cases} V(Q) \cap C & \text{if } \dim(V(Q) \cap C) = 0, \\ 0 & \text{otherwise.} \end{cases}$$

We have that  $H^0(\kappa_C + \alpha)$  is canonically isomorphic to  $H^0(\mathcal{O}_{|\kappa_C+\alpha|^*}(1))$  by definition. Thus, we define  $i$  to be the composition

$$i: H^0(\mathcal{O}_{|\kappa_C+\alpha|^*}(2)) \cong \text{Sym}^2 H^0(\kappa_C + \alpha) \longrightarrow H^0(2(\kappa_C + \alpha)) \cong H^0(2\kappa_C)$$

of canonically determined morphisms.

The results below are helpful for understanding Lehami's theorem and its simplified proof.

**Lemma 4.5.2** *For all  $\alpha \in J(C)[2] \setminus \{0\}$  and all  $\{\theta, \theta + \alpha\} \in \Sigma_{C,\alpha}$  we have  $q_{\theta, \theta + \alpha} \in V_{C,\alpha}$ . Additionally,  $q_C$  is trivially contained in  $V_{C,\alpha}$ .*

PROOF. We may write the 2-torsion class  $\alpha$  as

$$\frac{1}{2}(\mathcal{Z}(\ell_\theta) \cap C - \mathcal{Z}(\ell_{\theta+\alpha}) \cap C).$$

It is then clear that both  $\ell_\theta$  and  $\ell_{\theta+\alpha}$  cut out effective representatives of  $\kappa_C + \alpha$ . Since the sum of two effective representatives of  $\kappa_C + \alpha$  is certainly contained in the image of  $i$ , we are done with the first claim. The second claim is trivial.  $\square$

One of the pillars in Lehami's arguments is following semicontinuity statement [60, Corollary 7]. It can be derived from the classical semicontinuity theorem [39, Section III.12] and holds for any characteristic of  $k$ .

**Lemma 4.5.3** *Let  $\mathcal{V}/X$  be a vector bundle over a base  $X$  and let  $\mathcal{V}_1, \dots, \mathcal{V}_n$  be sub-bundles of  $\mathcal{V}$ . Then*

- (i) *the function  $\dim \langle \mathcal{V}_1|_x, \dots, \mathcal{V}_n|_x \rangle$  is lower semi-continuous on  $X$ ,*
- (ii) *the function  $\dim(\cap_{i=1}^n \mathcal{V}_i|_x)$  is upper semi-continuous on  $X$ .*

We will now state a generalization of Lehami's theorem for reconstructing the quadric for complex space sextics on smooth quadrics [60, Theorem 1]. The idea of the proof is remains the same.

**Theorem 4.5.4** *Let  $k$  be either of characteristic zero or of sufficiently high characteristic. Let  $C$  be a generic space sextic or a generic space sextic lying on a singular quadric over  $k$ . Then we have*

- (i)  $\mathbb{P}V_{C,\alpha} = \text{Span}(\{q_{\theta, \theta + \alpha} : \theta \in \Sigma_{C,\alpha}\})$  for all  $\alpha \in J(C)[2] \setminus \{0\}$ ,
- (ii)  $\bigcap_{\alpha \in J(C)[2] \setminus \{0\}} \mathbb{P}V_{C,\alpha} = \text{Span}\{q_C\}$ ,

where  $q_C$  denotes the unique quadric vanishing on  $C$ , up to scaling.

PROOF. We follow the strategy Lehami uses for proving [60, Theorem 1]. From Lemma 4.5.2 we immediately have the containments

$$\text{Span}\{q_{\theta, \theta + \alpha}\} \subseteq V_{C,\alpha} \quad \text{and} \quad \text{Span}\{q_C\} \subseteq \bigcap_{\alpha \in J(C)[2] \setminus \{0\}} V_{C,\alpha}.$$

For claim (i), each  $q_{\theta, \theta + \alpha}$  generates a rank 1 sub-bundle of  $V_{C,\alpha}$  over the family of smooth genus 4 curves  $C$  in  $\mathbb{P}^3$ . The dimension of their span is bounded by the dimension of  $V_{C,\alpha}$ . If we can demonstrate that  $\dim \text{Span}\{q_{\theta, \theta + \alpha}\} = \dim V_{C,\alpha}$  for a particular curve  $C$ , then via Lemma 4.5.3(i) the claim must be true for all curves in an open neighbourhood of  $C$ . In the proof of [60, Theorem 1] this is done by hand

with a pleasant but involved geometric argument, whereas we can simply use our implementation of Algorithm 4.5.5 as described in Example 4.5.6. In both cases the curve  $C$  is over  $k = \overline{\mathbb{Q}}$ , which shows the statement for both characteristic zero and sufficiently high characteristic (see the Spreading Out Theorem [71, Theorem 3.2.1]). Additionally, we consider a space sextic on a singular quadric in Example 4.5.6, which shows the statement for generic curves of that type.

The proof of the part (ii) is analogous, using Lemma 4.5.3(ii) instead.  $\square$

### Algorithm 4.5.5

**Input:**  $\mathcal{S}_C$ , the Steiner system of  $C$  as defined in Section 4.1.

**Output:**  $q_C$ , the unique quadric form vanishing on  $C$ .

1: Construct the subspaces

$$\mathbb{P}V_{C,\alpha} := \text{Span} \left( \{l_\theta \cdot l_{\theta+\alpha} : \{\theta, \theta+\alpha\} \in \mathcal{S}_{C,\alpha}\} \right) \text{ for all } \mathcal{S}_{C,\alpha} \in \mathcal{S}_C$$

2: Compute their one-dimensional intersection

$$\text{Span}\{q_C\} := \bigcap_{\mathcal{S}_{C,\alpha} \in \mathcal{S}_C} \mathbb{P}V_{C,\alpha}.$$

3: **return**  $q_C$ .

**Example 4.5.6** Consider again the curve  $C \subseteq \mathbb{P}\mathbb{F}_{97}^3$  and the four syzygetic tritangents  $l_{12}, l_{34}, l_{125}, l_{345}$  from Example 4.3.1. Then there exists exactly one  $\mathcal{S}_{C,\alpha} \in \mathcal{S}_C$  such that  $\{l_{12}, l_{34}\} \in \mathcal{S}_{C,\alpha}$ , for which we have  $\mathbb{P}V_{C,\alpha} \subseteq \mathbb{P}V_C$  given by the linear span

$$\mathbb{P}V_{C,\alpha} = \text{Lin} \left\{ \begin{array}{l} x_0^2 + 36 x_1 x_3, \\ x_1 x_2 + 84 x_1 x_3 + 32 x_2 x_3 + 68 x_3^2, \\ x_0 x_1 + 85 x_1 x_3 + 17 x_2 x_3 + 91 x_3^2, \\ x_2^2 + 10 x_1 x_3 + 94 x_2 x_3 + 27 x_3^2, \\ x_1^2 + 69 x_1 x_3 + 22 x_2 x_3 + 45 x_3^2, \\ x_0 x_3 + 39 x_1 x_3 + 34 x_2 x_3 + 38 x_3^2, \\ x_0 x_2 + 69 x_1 x_3 + 22 x_2 x_3 + 45 x_3^2 \end{array} \right\}.$$

One can easily see that  $x_1^2 - x_0 x_2 \in \mathbb{P}V_{C,\alpha}$ ; it is the difference of two of our generators above. Our implementation verifies that Theorem 4.5.4 (i) and (ii) hold for this particular curve. More generally, we can do the same for the curve  $C \subseteq \mathbb{P}\overline{\mathbb{Q}}^3$  obtained from the configuration  $\mathcal{P} \subseteq \mathbb{P}\mathbb{Q}^3$  in Example 4.3.1.

**Reconstructing a cubic:** Reconstructing a cubic from  $\mathcal{S}_C$  is a slightly more involved task. A *Cayley cubic* is an irreducible cubic surface in  $\mathbb{P}^3$  whose singular locus consists of 4 simple nodes in general position. If  $k$  is algebraically closed there is exactly one Cayley cubic up to linear transformations of  $\mathbb{P}^3$ . Lehavi's idea is to identify 4 nodes of a Cayley cubic containing  $C$ . [60, Theorem 2] allows us to identify the four nodes via an intersection theoretic argument. We state a corrected version here.

**Theorem 4.5.7** ([60, Theorem 2]) *Let  $\alpha \in J(C)[2] \setminus \{0\}$ . The four planes through each of the four triples of nodes of the Cayley cubic associated to  $\alpha$  are, set theoretically, the four intersection points in  $\mathbb{P}V_C$  of the six dimensional projective variety*

$$\mathbb{P}V\left(\left((V_C/V_{C,\alpha})^* \wedge (V_C/V_{C,\alpha})^*\right) \cdot S^2|\kappa_C|\right)$$

*and the 2nd Veronese image of  $|\kappa_C|$  in  $\mathbb{P}V_C$ . The “ $\cdot$ ” in the equation above denotes tensor contraction. Moreover, each of these four points have multiplicity 4 in the intersection.*

We provide some context for the statement of Theorem 4.5.7. To do so, it is helpful to consider the set up of [60, Lemma 14].

**Definition-Lemma 4.5.8** For any  $\alpha \in J(C)[2] \setminus \{0\}$ , consider the following multiplication map  $s$ , as well as the restriction of the projection onto the first coordinate on its preimage of  $\mathbb{P}V_{C,\alpha}$ :

$$\begin{array}{ccc} |\kappa_C| \times |\kappa_C| & \xrightarrow{s} & \mathbb{P}V_C \\ \cup & & \cup \\ X_\alpha := s^{-1}\mathbb{P}V_{C,\alpha} & \longrightarrow & \mathbb{P}V_{C,\alpha} \\ \downarrow & & \\ & & |\kappa_C| \end{array}$$

The two-dimensional fibers of the restricted projection lie over four points which represent four planes  $l_{1,\alpha}, \dots, l_{4,\alpha}$  intersecting triplewise in four points  $z_{1,\alpha}, \dots, z_{4,\alpha}$ . We define the *Cayley subspace* associated to  $\alpha$  by

$$\mathbb{P}W_{C,\alpha} := \text{Span} \left\{ \frac{\prod_{j=1}^4 l_{j,\alpha}}{l_{i,\alpha}} : 1 \leq i \leq 4 \right\} \oplus \text{Span}\{hq_C : \deg(h) = 1\}.$$

Generically, the first summand is the space of cubics with the nodes at  $z_{1,\alpha}, \dots, z_{4,\alpha}$  and the first summand contains the Cayley cubic associated to  $\alpha$ .



With the notation of Definition-Lemma 4.5.8, the planes through 3 nodes of the Cayley cubic are exactly the  $a \in |\kappa_C|$  such that the subvariety

$$\{x \in |\kappa_C| : v \cdot s(a, x) = 0 \text{ for all } v \in (V_C/V_{C,\alpha})^*\}$$

has dimension 2. For any  $v \in (V_C/V_{C,\alpha})^*$ , we now view  $v \cdot s(a, -) \in |\kappa_C|^*$  as an operator. As the null-spaces of these operators are identical, they are linearly dependent as vectors in  $|\kappa_C|^*$ . In particular, we have for any  $v, v' \in (V_C/V_{C,\alpha})^*$  that

$$(4.1) \quad v \cdot s(a, -) \wedge v' \cdot s(a, -) = \vec{0}.$$

In terms of a basis  $\{e_1, \dots, e_4\}$  for  $|\kappa_C|$ , we have that

$$(v \cdot s(a, e_1), \dots, v \cdot s(a, e_4)) \wedge (v' \cdot s(a, e_1), \dots, v' \cdot s(a, e_4)) = \vec{0}.$$

Or even more explicitly, that the  $2 \times 2$  minors of the matrix

$$\begin{bmatrix} v \cdot s(a, e_1) & \dots & v \cdot s(a, e_4) \\ v' \cdot s(a, e_1) & \dots & v' \cdot s(a, e_4) \end{bmatrix}$$

vanish. The variety defined in Theorem 4.5.7 is

$$V\left(\text{minors}_{2 \times 2} \begin{bmatrix} v \cdot s(a, e_1) & \dots & v \cdot s(a, e_4) \\ v' \cdot s(a, e_1) & \dots & v' \cdot s(a, e_4) \end{bmatrix} : v, v' \in (V_C/V_{C,\alpha})^*\right) \subseteq \mathbb{P}V_C$$

where  $\mathbb{P}V_C = S^2|\kappa_C|$  is endowed with tensor coordinates  $a \otimes b$ . A coordinate-free description is given by

$$V((V_C/V_{C,\alpha})^* \wedge (V_C/V_{C,\alpha})^* \cdot S^2|\kappa_C|) \subseteq V_C$$

which follows from Equation (4.1) since tensor contraction commutes with wedges.

If  $C = V(q_C, p_C)$  is a smooth space sextic, we have that the space  $I(C)_3$  of cubics containing  $C$  is 5-dimensional. It is spanned by the 4-dimensional subspace  $\text{Span}\{hq_C : \deg(h) = 1\}$  along with some irreducible cubic vanishing on  $C$ . Observe that the defining equation of any Cayley cubic containing  $C$  could serve as the additional cubic. Theorem 4.5.7 allows us to identify the four nodes of a Cayley cubic containing  $C$  but this is not quite enough information to recover the curve uniquely. However, a Cayley cubic containing  $C$  is (generically) contained in the space  $\mathbb{P}W_{C,\alpha}$ , so by using all  $\alpha \in J(C)[2] \setminus \{0\}$  we can recover the space of cubics containing  $C$ .

**Theorem 4.5.9** *Let  $C$  be a smooth space sextic, let  $\mathbb{PI}(C)_3$  be the four dimensional subspace of cubics in  $\mathbb{P}^3$  containing  $C$ , and let  $W_{C,\alpha}$  be as in Definition 4.5.8. Then*

(i) *If  $C$  is generic, we have  $\dim W_{C,\alpha} = 8$  for every  $\alpha \in J(C)[2] \setminus \{0\}$ .*

(ii) *If  $C$  is a generic member of the family of space sextics contained in a singular quadric, then  $\dim W_{C,\alpha} = 8$  for the  $\alpha \in J(C)[2] \setminus \{0\}$  not of the form  $\theta - \theta_0$ , where  $\theta$  is one of the 120 odd theta characteristics and  $\theta_0$  is the vanishing even theta characteristic.*

(iii) *Let  $C$  be as in case (i) or (ii) and let*

$$A := \{\alpha \in J(C)[2] \setminus \{0\} : \dim W_{C,\alpha} = 8\}.$$

*Then*

$$\mathbb{PI}(C)_3 = \bigcap_{\alpha \in A} \mathbb{PW}_{C,\alpha}.$$

The proof of Theorem 4.5.9 is similar to our proof of Theorem 4.5.4. We apply our implementation of Algorithm 4.5.10 to a specific example and, via semi-continuity, we obtain that the formula holds generically.

**Algorithm 4.5.10**

**Input:**  $(\mathcal{S}_C, q_C)$ , where

- $\mathcal{S}_C$ , the Steiner system as defined in Section 4.1,
- $q_C$ , the unique quadric form vanishing on  $C$ .

**Output:**  $p_C$ , a cubic form such that  $C = V(q_C) \cap V(p_C)$

- 1: We introduce the following coordinates on the homogeneous coordinate rings:

$$\begin{aligned} A(|\kappa_C| \times |\kappa_C|) &:= k[\mathbf{x}, \mathbf{y}] := k[x_0, x_1, x_2, x_3, y_0, y_1, y_2, y_3], \\ A(\mathbb{P}V_C) &:= k[\mathbf{z}] := k[z_{ij} : 0 \leq i \leq j \leq 3], \end{aligned}$$

so that the multiplication map  $s$  induces the homomorphism

$$s : A(\mathbb{P}V_C) \longrightarrow A(|\kappa_C| \times |\kappa_C|), \quad z_{ij} \longmapsto \begin{cases} x_i y_j & i = j, \\ x_i y_j + x_j y_i & i \neq j \end{cases}$$

and the projection map  $p$  induces the homomorphism

$$p : A(|\kappa_C| \times |\kappa_C|) \longrightarrow A(|\kappa_C|), \quad x_i \longmapsto x_i.$$

2: **for**  $\mathcal{S}_{C,\alpha} \in \mathcal{S}_C$  **do**

3: Construct the linear subspace  $\mathbb{P}V_{C,\alpha}$  as a subvariety of  $\mathbb{P}V_C$ :

$$\mathbb{P}V_{C,\alpha} := \text{Span} \left( \{l_\theta \cdot l_{\theta+\alpha} : \{l_\theta, l_{\theta+\alpha}\} \in \mathcal{S}_{C,\alpha}\} \right) \subseteq \mathbb{P}V_C \cong \mathbb{P}^{\{z_{ij}\}}.$$

Compute the linear generators  $F_{\mathbb{P}V_{C,\alpha}}$  of the defining ideal of  $\mathbb{P}V_{C,\alpha}$ .

4: Set  $F_{X_\alpha} := s(F_{\mathbb{P}V_{C,\alpha}}) \subseteq k[\mathbf{x}, \mathbf{y}]$ , so that  $X_\alpha = V(F_{X_\alpha})$ .

5: Let  $I_\alpha$  be the ideal generated  $F_{X_\alpha}$  and the  $2 \times 2$  minors of its Jacobian:

$$J_y F = \left( \frac{\partial f}{\partial y_j} \right)_{f \in F_{X_\alpha}, j=0, \dots, 3}.$$

6: Compute  $V(p^{-1}I_\alpha) =: \{l_{1,\alpha}, l_{2,\alpha}, l_{3,\alpha}, l_{4,\alpha}\} \subseteq |\kappa_C|$ .

7: Compute the four points  $\{z_{1,\alpha}, z_{2,\alpha}, z_{3,\alpha}, z_{4,\alpha}\} \subseteq |\kappa_C|^*$  which lie on exactly 3 of the planes in  $\{l_{1,\alpha}, l_{2,\alpha}, l_{3,\alpha}, l_{4,\alpha}\}$ .

8: Construct the set  $\mathcal{W}_{C,\alpha}$  of cubics in  $\mathbb{P}^3$  with nodes  $\{z_{1,\alpha}, z_{2,\alpha}, z_{3,\alpha}, z_{4,\alpha}\}$ .

9: Compute  $W_{C,\alpha} := \mathcal{W}_{C,\alpha} \oplus \text{Span}\{x_0 q_C, \dots, x_3 q_C\}$ .

10: Set  $A := \{\alpha \in J(C)[2] \setminus \{0\} : \dim W_{C,\alpha} = 8\}$ .

11: Compute the intersection

$$\text{PI}(C)_3 := \bigcap_{\alpha \in A} \mathbb{P}W_{C,\alpha}$$

and pick a  $p_C \in \text{PI}(C)_3$  such that the cubic  $V(p_C)$  does not contain the quadric  $V(q_C)$ .

12: **return**  $p_C$ .

**Example 4.5.11** Consider again the curve  $C$  from Example 4.3.1. For its  $\mathbb{P}V_{C,\alpha}$  in Example 4.5.6, we obtain the four points

$$\begin{aligned} \mathcal{Z}(p^{-1}I_\alpha) = & \left\{ \begin{array}{l} (4:76:7:1), \quad (a^{281863}:a^{394021}:a^{855207}:1), \\ (a^{736807}:a^{69925}:a^{526311}:1), \quad (a^{873223}:a^{800485}:a^{814599}:1) \end{array} \right\} \\ & \subseteq |\kappa_C|, \end{aligned}$$

where  $a \in \mathbb{F}_{973}$  is a generator of the multiplicative group of the finite field. The four nodes of the Cayley cubic are dual to the four points above, and are given by

$$\left\{ \begin{array}{l} (a^{691050}:a^{850020}:a^{167536}:1), \quad (a^{406794}:a^{311460}:a^{735568}:1), \\ (a^{214122}:a^{93444}:a^{161680}:1), \quad (43:25:72:1) \end{array} \right\} \subseteq |\kappa_C|^* = \mathbb{P}^3.$$

Under the reverse lexicographic order on the basis of the space of cubics,

$$\{x_0^3, x_0^2x_1, x_0x_1^2, x_1^3, x_0^2x_2, x_0x_1x_2, x_1^2x_2, x_0x_2^2, x_1x_2^2, x_2^3, \\ x_0^2x_3, x_0x_1x_3, x_1^2x_3, x_0x_2x_3, x_1x_2x_3, x_2^2x_3, x_0x_3^2, x_1x_3^2, x_2x_3^2, x_3^3\},$$

these four nodes yield

$$\mathbb{P}W_{C,\alpha} = \text{Lin} \left\{ \begin{array}{l} (1 \ 0 \ 0 \ 0 \ 0 \ 0 \ 0 \ 6 \ 29 \ 41 \ 38 \ 73 \ 0 \ 23 \ 58 \ 51 \ 68 \ 29 \ 51 \ 74), \\ (0 \ 1 \ 0 \ 0 \ 0 \ 0 \ 0 \ 3 \ 11 \ 34 \ 57 \ 79 \ 0 \ 38 \ 46 \ 92 \ 41 \ 34 \ 61 \ 88), \\ (0 \ 0 \ 1 \ 0 \ 0 \ 0 \ 0 \ 47 \ 72 \ 48 \ 42 \ 39 \ 0 \ 72 \ 8 \ 32 \ 93 \ 48 \ 85 \ 12), \\ (0 \ 0 \ 0 \ 1 \ 0 \ 0 \ 0 \ 3 \ 16 \ 2 \ 40 \ 8 \ 0 \ 85 \ 35 \ 90 \ 28 \ 69 \ 17 \ 15), \\ (0 \ 0 \ 0 \ 0 \ 1 \ 0 \ 0 \ 47 \ 72 \ 48 \ 42 \ 39 \ 0 \ 72 \ 8 \ 32 \ 93 \ 48 \ 85 \ 12), \\ (0 \ 0 \ 0 \ 0 \ 0 \ 1 \ 0 \ 3 \ 16 \ 2 \ 40 \ 8 \ 0 \ 85 \ 35 \ 90 \ 28 \ 69 \ 17 \ 15), \\ (0 \ 0 \ 0 \ 0 \ 0 \ 0 \ 1 \ 96 \ 0 \ 0 \ 0 \ 0 \ 0 \ 0 \ 0 \ 0 \ 0 \ 0 \ 0 \ 0), \\ (0 \ 0 \ 0 \ 0 \ 0 \ 0 \ 0 \ 0 \ 0 \ 0 \ 0 \ 0 \ 1 \ 96 \ 0 \ 0 \ 0 \ 0 \ 0 \ 0) \end{array} \right\}.$$

**Remark 4.5.12** For our example exhibiting Theorem 4.5.9(ii), it turns out that  $\dim W_{C,\alpha} = 7$  for every  $\alpha \in J(C)[2] \setminus \{0\}$  of the form  $\theta - \theta_0$ , with  $\theta$  one of the 120 odd theta characteristics and  $\theta_0$  the vanishing even theta characteristic. We anticipate that this is always the case.

**Conjecture 4.5.13** *Let  $C$  be a smooth space sextic contained in a singular quadric and let  $\alpha = \theta - \theta_0 \in J(C)[2] \setminus \{0\}$ , where  $\theta$  is one of the 120 odd theta characteristics and  $\theta_0$  the vanishing even theta characteristic. Then  $\dim W_{C,\alpha} = 7$ .*

Now we have completed our discussion on space sextics. We have given several algorithms: constructing a space sextic, its Steiner system and its 120 tritangents, in both cases where the sextic lies on a smooth or on a singular quadric surface. For the inverse direction: given a space sextic  $C$  that arises from a del Pezzo surface of degree one, Algorithm 4.4.7 returns a set of eight points such that blowing up the plane at those points gives rise to a space sextic isomorphic to  $C$ . Furthermore, we extended Leham's method for reconstructing a space sextic on a smooth quadric from its tritangents, to smooth sextics on singular quadrics and over more general fields. In the next chapter, we switch the gears and give an algebraic explanation of an optimization problem.

## CHAPTER 5

### The Algebraic Degree of the Fermat-Weber Point

The Weber problem is a geometric optimization problem that has a long history in the mathematical literature [51]. Given  $n$  fixed destination points  $\{(u_i, v_i)\}_{i=1}^n$  in the real plane with integer coordinates, find the optimal location of a single source point. In formula, determine

$$(5.1) \quad \min_{x,y} f(x,y) = \sum_{i=1}^n \sqrt{(x - u_i)^2 + (y - v_i)^2}.$$

The function  $f$  is strictly convex. Hence the solution of  $\frac{\partial f}{\partial x} = \frac{\partial f}{\partial y} = 0$  minimizes the function  $f$ . The unique minimum in (5.1) is called the *Fermat-Weber point* and denoted  $p^*$ .

Weber [86] was probably the first who formulated this problem in light of the location of a plant, with the objective of minimizing the sum of transportation costs from the plant to sources of the raw materials and to the market centers. The solution to this problem is simple to obtain for the special cases when  $n$  points lie on a straight line or form a regular  $n$ -gon. The case of  $n = 3$  was first formulated and thrown out as a challenge by Fermat as early as the 1600s. [51]. Cavalieri in 1647 proved that when three points form the vertices of a triangle with all the angles less than  $120^\circ$ , the minimizer point is the one that makes an angle of  $120^\circ$  with each side of the triangle. Heinen in 1834 completed the answer by showing that if the triangle has an angle of  $\geq 120^\circ$  then the minimizer is the vertex corresponding to the obtuse angle: see Figure 5.1.

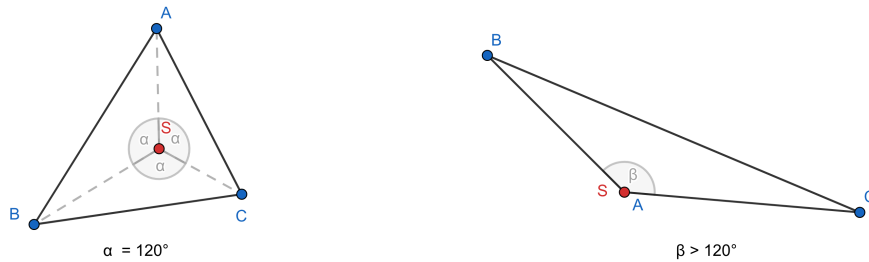


FIGURE 5.1. The red point minimizes the sum of Euclidean distances from three given points in the plane.

Fagnano in 1775 showed that for the case  $n = 4$ , if four given points form a convex quadrilateral the minimum solution point is the intersection of the diagonals of the quadrilateral, otherwise it is one of four points that is inside the convex hull of the three other points: see Figure 5.2. Chandrajit Bajaj in 1984 proved that in general, for the case of  $n = 5$  points, the Fermat-Weber point is the root of an irreducible polynomial of high degree and can not be obtained by straight-edge and compass constructions [4]. Furthermore, the Weber problem is not solvable by radicals over  $\mathbb{Q}$  for  $n \geq 5$ .

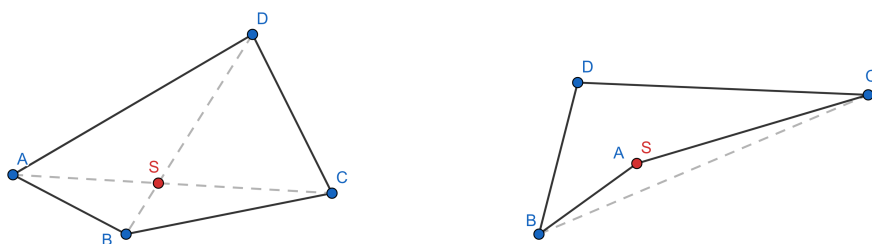


FIGURE 5.2. The red point minimizes the sum of Euclidean distances from four given points in the plane.

Jiawang Nie, Pablo A. Parrilo, and Bernd Sturmfels [67] define a  $n$ -ellipse with *foci*  $(u_i, v_i)$  and *radius*  $d$  to be the following set of points in the plane:

$$\{(x, y) \in \mathbb{R}^2 : \sum_{i=1}^n \sqrt{(x - u_i)^2 + (y - v_i)^2} = d\}.$$

The  $n$ -ellipse is the boundary of a convex set in the plane. For  $n = 1$  it is a circle, and for  $n = 2$  it is an ellipse. However, if  $n \geq 3$  the above set is not the vanishing set of an irreducible polynomial, and therefore, is not an algebraic curve anymore. The unique (up to sign) irreducible polynomial in unknowns  $x$  and  $y$  and with parameters  $d, u_1, v_1, \dots, u_n, v_n$  has degree  $2^n - \binom{n}{n/2} \delta_n$ , where  $\delta_n$  is 1 for even  $n$  and 0 for odd  $n$  [67]. The smallest  $d$ , such that the  $n$ -ellipse is non-empty defines the Fermat-Weber point. Nie, Parrilo, and Sturmfels ask for the algebraic degree of the Fermat-Weber point over the field of rational functions  $\mathbb{Q}(u_1, v_1, \dots, u_n, v_n)$ .

Now we formulate the problem more precisely. Let  $k$  be an arbitrary field and  $\bar{k}$  its algebraic closure, i.e. the smallest algebraically closed field containing  $k$ . The *minimal polynomial* of an element  $a \in \bar{k}$  over  $k$  is an irreducible monic polynomial with coefficients in  $k$ , having  $a$  as a root. The *algebraic degree* of  $a$  over  $k$  is the degree of its minimal polynomial over  $k$ . Let  $\{(u_i, v_i)\}_{i=1}^n$  be the set of  $n$  given points. In the nontrivial case  $n \geq 5$ , our interest is determining the algebraic

degree of the Fermat-Weber point  $p^*$  over the field of rational functions  $\mathbb{Q}(u_1, v_1, \dots, u_n, v_n)$ , where the *algebraic degree of a point* is defined to be the unique algebraic degree of its coordinates. Note that this degree is one for  $n = 4$  and is one or two for  $n = 3$ , depending on the configuration of three given points. The aim is to prove the following conjecture for the particular case  $d = 2$ :

**Conjecture 5.1** *For  $n$  general points in  $\mathbb{R}^d$  the algebraic degree of the Fermat-Weber point equals*

$$\sum_{i=2}^d 2^{n-i} \binom{n-1}{i} - 2 \binom{n-1}{n/2} \delta_n,$$

where  $\delta_n$  is zero for odd  $n$  and one for even  $n$ .

This formula which we explain in Section 5.1, first grew out of an informal discussion by Jean-Charles Faugère, Mohab Safey El Din, Bernd Sturmfels and Rekha Thomas at the Geometry and Optimization with Algebraic Methods workshop in 2015, in Berkeley. In Section 5.1 we give an algorithm that constructs the minimal polynomials of the coordinates of the Fermat-Weber point  $p^*$  and returns the algebraic degree of  $p^*$  over  $\mathbb{Q}(u_1, v_1, \dots, u_n, v_n)$ . Tracking the degree in all steps of the algorithm explains the conjecture above for the case where  $n$  points are in the real plane, i.e. for  $d = 2$ . Sections 5.2 and 5.3 contain the computation of the degree of the ideals appearing in the algorithm. The final ideal  $I_{p^*}$  is the defining ideal of  $p^*$ . Section 5.3 reports the computational results based on the calculation of the Fermat-Weber point for five to ten given points in SINGULAR and MACAULAY2.

### 5.1. Explaining the degree formula

Let  $\{(u_i, v_i)\}_{i=1}^n$  be the set of  $n$  points in the plane. The Fermat-Weber point is the minimizer point of the problem

$$\min_{x,y} f(x,y) = \sum_{i=1}^n \sqrt{(x - u_i)^2 + (y - v_i)^2}.$$

Define  $n$  distance functions

$$d_i = \sqrt{(x - u_i)^2 + (y - v_i)^2}.$$

Since we are interested in the unique solution of two partial derivatives

$$\frac{\partial f}{\partial x} = \sum_{i=1}^n \frac{(x - u_i)}{d_i}, \quad \text{and} \quad \frac{\partial f}{\partial y} = \sum_{i=1}^n \frac{(y - v_i)}{d_i},$$

we can form our desired polynomial system as follows:

$$\begin{cases} d_i^2 - (x - u_i)^2 - (y - v_i)^2 = 0, & \text{for } i = 1, \dots, n \\ \sum_{i=1}^n (x - u_i) \prod_{j \neq i} d_j = 0, \\ \sum_{i=1}^n (y - v_i) \prod_{j \neq i} d_j = 0. \end{cases}$$

This is a zero-dimensional system of polynomial equations in unknowns  $x, y, d_1, \dots, d_n$  and parameters  $u_1, v_1, \dots, u_n, v_n$ . However, we need to exclude the solutions where  $d_i = 0$  for some  $1 \leq i \leq n$ . The number of remaining solution points in  $\mathbb{C}$  is twice the algebraic degree of the Fermat-Weber point over  $\mathbb{Q}(u_1, v_1, \dots, u_n, v_n)$ . Note that if we choose our  $n$  points to be in general positions and have integer coordinates, we are indeed looking for the algebraic degree of the Fermat-Weber point over  $\mathbb{Q}$ . Now we give an algorithm to find the degree.

#### Algorithm 5.1.1

**Input:** A set  $\mathcal{P} = \{(u_i, v_i)\}_{i=1}^n$  of  $n$  given points in the plane with integer coordinates

**Output:** The algebraic degree of the Fermat-Weber point of the set  $\mathcal{P}$  over  $\mathbb{Q}$ .

- 1: Let  $R = \mathbb{Q}[x, y, d_1, \dots, d_n]$ , and define the ideal  $D := (D_x, D_y)$  where

$$D_x = \sum_{i=1}^n (x - u_i) \prod_{j \neq i} d_j, \quad D_y = \sum_{i=1}^n (y - v_i) \prod_{j \neq i} d_j.$$

- 2: Let  $d = \prod_{i=1}^n d_i$  and  $D^s = (D : (d)^\infty) \subset R$ .
- 3: Let  $I_i = D^s + (g_1, \dots, g_i) \subseteq R$  for  $1 \leq i \leq n$ , where

$$g_i = d_i^2 - (x - u_i)^2 - (y - v_i)^2.$$

- 4: Let  $I^s = (I_n : (d)^\infty)$ .
- 5: Let  $I_{p^*} = I^s \cap \mathbb{Q}[x, y]$ .
- 6: Eliminate  $\{y\}$  (resp.  $\{x\}$ ) from  $I_{p^*}$  and let  $h_x$  (resp.  $h_y$ ), be the unique generator of the resulting ideal.
- 7: **return**  $\deg(h_x)$  (resp.  $\deg(h_y)$ ).

**Remark 5.1.2** In the algorithm above, we could do the saturation of the ideals only once at step 4, but we break it in two steps, 2 and 4, for computational reasons.



**Convention 5.1.3** By the degree of an ideal  $I$  in a polynomial ring  $R$  we mean the degree of  $(I, z) \subset R[z]$  where  $(I, z)$  is the homogenization of the ideal  $I$  with respect to  $z$ . This is the degree of the scheme  $V(I)$ .

We are now ready to give an explanation for the formula in Conjecture 5.1, for the case  $d = 2$ : Proposition 5.2.8 at the end of the following section shows that the degree of the ideal  $D^s$  in step 2 is  $\binom{n}{2} + 1$ . Section 5.3 explains that for  $5 \leq n \leq 10$  the following results holds. The ideal  $I_n$  in step 3 is a zero dimensional ideal and has degree

$$\deg(I_n) = 2^{n-1} \cdot \left( \binom{n+1}{2} + 1 \right) - 4 \cdot \binom{n-1}{n/2} \delta_n,$$

where  $\delta_n$  is zero for odd  $n$  and one for even  $n$ . Saturating the ideal  $I_n$  by the ideal generated by  $d$ , drops the degree by  $n \cdot 2^n$ , and therefore,

$$\deg(I^s) = 2^{n-1} \binom{n-1}{2} - 4 \cdot \binom{n-1}{n/2} \delta_n.$$

The ideal  $I_{p^*}$  is a zero dimensional ideal and the number of points in  $V_{\bar{\mathbb{Q}}}(I_{p^*})$  is half that of  $V_{\bar{\mathbb{Q}}}(I^s)$ :

$$\deg(I_{p^*}) = 2^{n-2} \binom{n-1}{2} - 2 \cdot \binom{n-1}{n/2} \delta_n.$$

This ideal corresponds to the Fermat-Weber point  $p^* = (x^*, y^*)$ , i.e. the polynomial system consisting of the two generators of  $I_{p^*}$  is the ‘smallest’ polynomial system in two variables with rational coefficients vanishing on  $p^* \in \mathbb{Q}$ . More precisely, among all the algebraic varieties defined by such polynomial systems, the variety defined by the generators of  $I_{p^*}$  over  $\mathbb{Q}$  has the least number of points.

Eliminating  $y$  from the two polynomial system, leaves a single polynomial in  $x$ . This is the minimal polynomial of  $x^*$  denoted by  $h_x$  in step 6. Similarly the minimal polynomial  $h_y$  of  $y^*$  is defined by eliminating  $x$ , and the following equality holds:

$$\deg(h_x) = \deg(h_y) = \deg(I_{p^*}).$$

## 5.2. The ideal of the derivatives is determinantal

In this section we compute the degree of the ideal  $D^s$  that is introduced in step 2 of the Algorithm 5.1.1. Let the polynomial rings  $R_1$  and  $R_2$  be:

$$\begin{aligned} R_1 &= \mathbb{Q}[u_1, v_1, \dots, u_n, v_n, x, y, d_1, \dots, d_n], \\ R_2 &= \mathbb{Q}(u_1, v_1, \dots, u_n, v_n)[x, y, d_1, \dots, d_n], \end{aligned}$$

and set the polynomials

$$\bar{D}_x = \sum_{i=1}^n (x - u_i) \prod_{\substack{j=1 \\ j \neq i}}^n d_j, \quad \text{and} \quad \bar{D}_y = \sum_{i=1}^n (y - v_i) \prod_{\substack{j=1 \\ j \neq i}}^n d_j.$$

Calculating the degree of the ideal  $D^s \subset \mathbb{Q}[x, y, d_1, \dots, d_n]$  for  $n$  given points  $\{(u_n, v_n)\}_{i=1}^n$  in general position in the real plane with nonzero integer coordinates is the same as finding the degree of the saturated ideal  $(\bar{D}_x, \bar{D}_y) : (d)^\infty$  in  $R_2$ . In other words we are looking for the algebraic degree of the Fermat-Weber point over the rational field  $\mathbb{Q}(u_1, \dots, u_n, v_1, \dots, v_n)$ . However, first we study  $D_1^s := (\bar{D}_x, \bar{D}_y) : (d)^\infty$  in the ring  $R_1$  since it has a nicer structure (Proposition 5.2.1) and from there we can pass to the ring  $R_2$  (Proposition 5.2.8).

**Proposition 5.2.1** *The ideal  $D_1^s = (\bar{D}_x, \bar{D}_y) : (d)^\infty$  in the ring  $R_1$  is generated by the maximal minors of the matrix*

$$M = \begin{bmatrix} x - u_1 & x - u_2 & \dots & \dots & x - u_n \\ y - v_1 & y - v_2 & \dots & \dots & y - v_n \\ d_1 & 0 & \dots & 0 & -d_n \\ 0 & d_2 & \ddots & \vdots & \vdots \\ \vdots & \ddots & \ddots & 0 & \vdots \\ 0 & \dots & 0 & d_{n-1} & -d_n \end{bmatrix}_{(n+1) \times n}$$

and has degree  $\binom{n+1}{2}$ .

The following definitions are needed in order to prove the above proposition. Let  $R$  be a Noetherian ring and  $M$  a  $R$ -module. The unique length of a maximal  $M$ -sequence in an ideal  $I \subset R$  is called the *depth* of  $I$ . The *codimension* of  $I$  is defined as

$$\text{codim}(I) = \min\{\sup\{n : p_0 \subsetneq p_1 \subsetneq \dots \subsetneq p_n = p\} : I \subseteq p\}.$$

The ring  $R$  is a *Cohen-Macaulay ring* if  $\text{depth}(m) = \text{codim}(m)$  for any maximal ideal  $m$  of  $R$ . Examples of Cohen-Macaulay rings are fields and therefore polynomial rings over a field. The ring  $R$  is *determinantal* if it can be written in the form  $R = S/I$  where  $S$  is a Cohen-Macaulay ring and  $I$  is the ideal generated by the  $r \times r$  minors of a  $p \times q$  matrix  $M$ , for some  $p, q, r$ , such that the codimension of  $I$  in  $S$  is  $(p-r+1)(q-r+1)$ . We say  $I$  is a *Cohen-Macaulay ideal* if the quotient ring  $R/I$  is a Cohen-Macaulay ring.

To prove Proposition 5.2.1, we decompose the ideal  $\bar{D} = (\bar{D}_x, \bar{D}_y) \subseteq R_1$  and study the codimension, Cohen-Macaulayness and the degree of the primary components. The following important theorems and lemmas help us to verify these properties.

**Theorem 5.2.2** *Determinantal rings are Cohen-Macaulay.*

See Bruns and Vetter [1988] for a treatment and proof.

**Lemma 5.2.3** *Let  $\bar{D}$  be the ideal generated by  $\bar{D}_x$  and  $\bar{D}_y$  in  $R_1$ . Then  $\bar{D}$  is a complete intersection of codimension 2 and degree  $n^2$ .*

PROOF. It suffices to show that  $\bar{D}_x$  and  $\bar{D}_y$  are irreducible. Let  $\bar{D}_x$  be written as

$$\bar{D}_x = h(u_1, v_1, d_1, \dots, u_n, v_n, d_n, x, y) \cdot g(u_1, v_1, d_1, \dots, u_n, v_n, d_n, x, y)$$

where  $h, g \in R_1$ . The polynomial  $\bar{D}_x$  is linear in

$$S = \mathbb{Q}(d_1, \dots, d_n)[u_1, v_1, \dots, u_n, v_n, x, y].$$

Therefore, one of  $h$  or  $g$  has to be an element of  $\mathbb{Q}(d_1, \dots, d_n)$ . Without loss of generality, let it be  $h$ . Thus,  $h$  is a polynomial in  $\mathbb{Q}[d_1, \dots, d_n]$  and it divides  $\bar{D}_x$ . For any  $1 \leq k \leq n$ , setting  $x = u_k$  implies that  $h$  divides  $\sum_{i=1, i \neq k}^n (x - u_i) \prod_{j=1, j \neq i}^n d_j$  and therefore for any  $1 \leq i \leq n$ ,  $h$  divides  $\prod_{j=1, j \neq i}^n d_j$ . This implies that  $h$  is a unit in  $R_1$ . Thus  $h \in \mathbb{Q}$ .

Similarly we can show that  $\bar{D}_y$  is irreducible. This implies that  $\bar{D}$  is a complete intersection of codimension 2. Since each of  $\bar{D}_x$  and  $\bar{D}_y$  are of degree  $n$ , the degree of  $\bar{D}$  is  $n \cdot n = n^2$ . This proves the statement.  $\square$

**Lemma 5.2.4** *Let  $I \in R_1$  be the ideal generated by polynomials  $\prod_{j=1, j \neq i}^n d_j$  where  $1 \leq i \leq n$ . Then  $I$*

- (1) *has codimension 2,*
- (2) *is Cohen-Macaulay,*
- (3) *has degree  $\binom{n}{2}$ .*

PROOF. The ideal  $\bar{D} = (\bar{D}_x, \bar{D}_y) \subset R_1$  is a subset of  $I$  and therefore,  $\text{codim}(I) \geq 2$  by Lemma 5.2.3. Also, it is easy to see that  $I$  is generated by the maximal minors of the matrix

$$\begin{bmatrix} d_1 & 0 & \dots & 0 \\ 0 & d_2 & \ddots & \vdots \\ \vdots & \ddots & \ddots & 0 \\ 0 & \dots & 0 & d_{n-1} \\ d_n & d_n & \dots & d_n \end{bmatrix}_{n \times (n-1)},$$

since in all rows except the last one, there is only one non-zero element to choose. Now the *Hilbert-Burch theorem* [25, Theorem 3.2] implies (1). The correctness of (2) follows from (1) and Theorem 5.2.2. Finally, the ideal  $I$  is a monomial ideal and has the following primary decomposition

$$I = \bigcap_{1 \leq i < j \leq n} (d_i, d_j)$$

which implies (3).  $\square$

**Lemma 5.2.5** *Let  $I_n(M)$  be the ideal generated by all  $n$ -minors of the matrix  $M$  in Proposition 5.2.1. Then  $I_n(M)$*

- (1) *has codimension 2,*
- (2) *is Cohen-Macaulay,*
- (3) *is prime.*

PROOF. The proof of (1), (2) are similar to the proof of Lemma 5.2.4. Let  $S$  be the polynomial ring  $S = \mathbb{Q}[x_1, y_1, d_1, \dots, x_n, y_n, d_n]$ . The ideal  $I_n(M)$  is prime in  $R_1$  if and only if  $I_n(M')$  is prime in  $S$ , where  $M'$  is the matrix

$$M' = \begin{bmatrix} x_1 & x_2 & \dots & \dots & x_n \\ y_1 & y_2 & \dots & \dots & y_n \\ d_1 & 0 & \dots & 0 & -d_n \\ 0 & d_2 & \ddots & \vdots & \vdots \\ \vdots & \ddots & \ddots & 0 & \vdots \\ 0 & \dots & 0 & d_{n-1} & -d_n \end{bmatrix}.$$

We prove (3) by induction on  $n$ . If  $n = 2$  then the entries of  $M'$  are distinct variables in the polynomial ring  $S$ , therefore by [9, Theorem 2.10],  $I_2(M')$  is prime. Let  $N$  be the matrix obtained from some row and column transformations of  $M'$  in the ring  $S[d_1^{-1}]$ :

$$N = \begin{bmatrix} 0 & x_2 & \dots & x_{n-1} & x_n - \frac{d_n}{d_1}x_1 \\ 0 & y_2 & \dots & y_{n-1} & y_n - \frac{d_n}{d_1}y_1 \\ 1 & 0 & \dots & 0 & 0 \\ 0 & \frac{d_2}{d_1} & \ddots & \vdots & -\frac{d_n}{d_1} \\ \vdots & \ddots & \ddots & 0 & \vdots \\ 0 & \dots & 0 & \frac{d_{n-1}}{d_1} & -\frac{d_n}{d_1} \end{bmatrix}.$$

Now let  $S' = \mathbb{Q}[x_1, y_1, \dots, x_{n-1}, y_{n-1}, x'_n, y'_n, d_1, d'_2, \dots, d'_n]$ . The substitution

$$x'_n \rightarrow x_n - \frac{d_n}{d_1}x_1, \quad y'_n \rightarrow y_n - \frac{d_n}{d_1}y_1, \quad d'_i \rightarrow \frac{d_i}{d_1}, \quad \text{for } 2 \leq i \leq n,$$

induces the isomorphism

$$\frac{S'[d_1^{-1}]}{I_{n-1}(N')} \cong \frac{S}{I_n(M')}[\tilde{d}_1^{-1}]$$

where  $\tilde{d}_1$  denotes the residue class of  $d_1$  in  $\frac{S}{I_n(M')}$ , and

$$N' = \begin{bmatrix} x_2 & x_3 & \cdots & x_{n-1} & x'_n \\ y_2 & y_2 & \cdots & y_{n-1} & y'_n \\ d'_2 & 0 & \cdots & 0 & -d'_n \\ 0 & d'_3 & \ddots & \vdots & \vdots \\ \vdots & \ddots & \ddots & 0 & \vdots \\ 0 & \cdots & 0 & d'_{n-1} & -d'_n \end{bmatrix}.$$

Let  $\phi$  be the natural localization map

$$\phi : \frac{S}{I_n(M')} \rightarrow \frac{S}{I_n(M')}[\tilde{d}_1^{-1}].$$

By [20, Lemma 3.1]  $\tilde{d}_1$  is a non-zero divisor of  $\frac{S}{I_n(M')}$  which implies that  $\phi$  is an injection. The isomorphism above together with the injectivity of  $\phi$  completes the proof.  $\square$

**Lemma 5.2.6** *Let  $I$  be the ideal generated by  $\prod_{\substack{j=1 \\ j \neq i}}^n d_j$ , for  $1 \leq i \leq n$ ,  $I_n(M)$  be the ideal generated by all  $n$ -minors of the matrix  $M$  in Proposition 5.2.1 and  $\bar{D}$  be the ideal  $(\bar{D}_x, \bar{D}_y)$ . Then*

$$\bar{D} = I \cap I_n(M).$$

**PROOF.** By Lemmas 5.2.4 and 5.2.5, we have  $\bar{D} \subseteq I_n(M)$  and  $\bar{D} \subseteq J$ ,

$$\text{codim}(\bar{D}) = \text{codim}(I_n(M)) = \text{codim}(I) = 2.$$

Since the columns of the matrix  $M$  are homogeneous of degree one, a special case of Thom-Porteous-Giambelli formula [30, §14.4] evaluates the degree of  $I_n(M)$  into  $\binom{n}{2} + n \times 1 = \binom{n+1}{2}$ . Therefore,

$$\deg(\bar{D}) = \deg(I_n(M)) + \deg(I).$$

The ideals  $I$  and  $I_n(M)$  do not have embedded components since they are both Cohen-Macaulay. Thus, Bézout's theorem implies the result.  $\square$

**Proof of Proposition 5.2.1:** By using the notations of Lemma 5.2.6, this is enough to show that

$$\bar{D} : (d)^\infty = I_n(M) : (d)^\infty = I_n(M).$$

The first equality holds because of 5.2.6. Note that

$$(I \cap I_n(M)) : (d)^\infty = (I : (d)^\infty) \cap (I_n(M) : (d)^\infty),$$

and  $I : (d)^\infty = R_1$ . The second equality holds because  $I_n(M)$  is a prime ideal by Lemma 5.2.5.  $\square$

We can now use this result in the following way. Let  $m_y$  and  $m_x$  be minors which are the determinant of the matrix  $M$  without the first and the second row, respectively. Let  $m_i$  be the minor which is the determinant of the matrix  $M$  without  $(i+2)$ -th row for  $1 \leq i \leq n-1$ . By Proposition 5.2.1,  $D_1^s = (\bar{D}_x, \bar{D}_y)$  is minimally generated by the  $(n+1)$  minors  $m_x, m_y, m_1, \dots, m_{n-1}$  where  $m_x$  and  $m_y$  are both of degree  $n$  and  $m_1, \dots, m_{n-1}$  are all of degree  $(n-1)$ . Explicitly, the generators are

$$\begin{aligned} m_x &= (-1)^{n+1} \bar{D}_x, \\ m_y &= (-1)^{n+1} \bar{D}_y, \\ m_i &= (-1)^{n-i+1} \sum_{\substack{j=1 \\ j \neq i}}^n [(x(v_i - v_j) - y(u_i - u_j) + (u_i v_j - u_j v_i)) \cdot \prod_{\substack{k=1 \\ k \neq i, j}}^n d_k], \end{aligned}$$

where  $1 \leq i \leq n-1$ .

This completes the calculations in  $R_1$ . Now by using the next two proposition, we pass to the ring  $R_2$  and we find the degree of the ideal  $D_2^s := (\bar{D}_x, \bar{D}_y) \subset R_2$ . That is  $\deg D^s$  for the ideal  $D^s \subset R$  defined in step 2 of Algorithm 5.1.1.

**Proposition 5.2.7** *The ideal  $D_2^s \subset R_2$  is generated by polynomials  $m_1, \dots, m_{n-1}$ .*

PROOF. First we show that in the ring  $R_2$ ,  $m_x$  and  $m_y$  both can be generated by  $m_1, m_2, m_3$ . For this purpose, let

$$a_1 = \frac{(u_2 - u_3)}{l}, \quad a_2 = \frac{(u_1 - u_3)}{l}, \quad a_3 = \frac{(u_1 - u_2)}{l},$$

and

$$b_1 = \frac{(v_2 - v_3)}{l}, \quad b_2 = \frac{(v_1 - v_3)}{l}, \quad b_3 = \frac{(v_1 - v_2)}{l},$$

where  $l$  is the determinant of the matrix

$$\begin{bmatrix} u_1 & u_2 & u_3 \\ v_1 & v_2 & v_3 \\ 1 & 1 & 1 \end{bmatrix}.$$

Then

$$\begin{aligned} m_x &= a_1 d_1 m_1 + a_2 d_2 m_2 + a_3 d_3 m_3, \\ m_y &= b_1 d_1 m_1 + b_2 d_2 m_2 + b_3 d_3 m_3. \end{aligned}$$

□

**Proposition 5.2.8** *Let  $m_{(i,j,k)}$  be the 3-minor of the matrix*

$$\begin{bmatrix} u_1 & u_2 & \dots & u_n \\ v_1 & v_2 & \dots & v_n \\ 1 & 1 & \dots & 1 \end{bmatrix}$$

*with columns  $i, j, k \in \{1, \dots, n\}$ . The ideal  $D_2^s \subseteq R_2$  is the ideal generated by the maximal minors of the  $(n-1) \times (n-2)$  matrix  $M_{R_2}$ :*

$$M_{R_2} = \begin{bmatrix} M_{11} & M_{12} & M_{13} \\ M_{21} & M_{22} & M_{23} \end{bmatrix},$$

where

$$M_{11} = \begin{bmatrix} m_{(2,3,4)}d_1 & m_{(2,3,5)}d_1 & \dots & m_{(2,3,n-1)}d_1 \\ m_{(1,3,4)}d_2 & m_{(1,3,5)}d_2 & \dots & m_{(1,3,n-1)}d_2 \\ m_{(1,2,4)}d_3 & m_{(1,2,5)}d_3 & \dots & m_{(1,2,n-1)}d_3 \end{bmatrix},$$

$$M_{12} = \begin{bmatrix} m_{(2,3,n)}d_1 + m_{(1,2,3)}d_n \\ m_{(1,3,n)}d_2 - m_{(1,2,3)}d_n \\ m_{(1,2,n)}d_3 + m_{(1,2,3)}d_n \end{bmatrix},$$

$$M_{13} = \begin{bmatrix} ((v_2 - v_3)x - (u_2 - u_3)y + (u_2v_3 - u_3v_2))d_1 \\ ((v_3 - v_1)x - (u_3 - u_1)y + (u_3v_1 - u_1v_3))d_2 \\ ((v_1 - v_2)x - (u_1 - u_2)y + (u_1v_2 - u_2v_1))d_3 \end{bmatrix},$$

and

$$M_{21} = \begin{bmatrix} d_4 & 0 & \dots & 0 \\ 0 & d_5 & \dots & 0 \\ \vdots & \vdots & \ddots & \vdots \\ 0 & 0 & \dots & d_{n-1} \end{bmatrix}, \quad M_{22} = \begin{bmatrix} -d_n \\ -d_n \\ \vdots \\ -d_n \end{bmatrix}, \quad M_{23} = \begin{bmatrix} 0 \\ 0 \\ \vdots \\ 0 \end{bmatrix}.$$

Moreover,  $D_2^s$  has degree  $\binom{n}{2} + 1$ .

PROOF. Let  $m'_i$  be the minor which is the determinant of the matrix  $M_{R_2}$  without the  $i$ -th row for  $1 \leq i \leq n-1$ . We have the following relations:

$$(5.2) \quad m'_i = \frac{(-1)^n}{m_{(1,2,3)}} m_i,$$

for  $i = 1, 2, 3$ , and

$$(5.3) \quad m'_i = \frac{(-1)^{(n+1)}}{m_{(1,2,3)}^2} m_i,$$

for  $i = 4, \dots, n-1$ . Therefore, the maximal minors of  $M_{R_2}$  are generators of  $D_2^s$ . After homogenizing the last column, the first  $n-3$  columns of  $M_{R_2}$  are linear in  $d_i$  and the last column is bilinear in  $x, y, z$  and  $d_i$ .

Using a special case of Thom-Porteous-Giambelli formula [30, §14.4] the degree of  $D_2^s$  evaluates

$$\binom{n-3}{2} \times (1 \times 1) + (n-3) \times 1^2 + (n-3) \times (1 \times 2) + 1 \times 2^2 = \binom{n}{2} + 1.$$

□

### 5.3. Computational results

This section reports on the computational results on the degree of the ideals  $I_i$  in step 3 and  $I^s$  in step 4 of the Algorithm 5.1.1 for  $n = 5, \dots, 10$ . This leads us to obtain the desired formula for the algebraic degree of the Fermat-Weber point over  $\mathbb{Q}$ . Notice that in this section we use the notations defined in Algorithm 5.1.1.

Implementation of Algorithm 5.1.1 in SINGULAR is available on <https://software.mis.mpg.de>. It results in the following formulas: let  $n$  be an integer such that  $5 \leq n \leq 10$ , and  $\delta_n$  be zero for odd  $n$  and one for even  $n$ . The degree of the ideals  $I_1$

$$\deg(I_1) = 2 \cdot \deg(D^s),$$

and for  $2 \leq i \leq n-1$ ,

$$\deg(I_i) = 2 \cdot \deg(I_{i-1}) - 2^{i-2} \cdot (i-2)$$

and

$$\deg(I_n) = 2 \cdot \deg(I_{n-1}) - 2^{n-2} \cdot (n-2) - 4 \cdot \binom{n-1}{n/2} \delta_n.$$

Therefore, always there is only a drop of  $2^{i-2} \cdot (i-2)$  from  $\deg(g_i) \cdot \deg(I_{i-1})$  in the degree of  $I_i = I_{i-1} + (g_i)$ , except for the last step where there is an extra drop of  $4 \cdot \binom{n-1}{n/2}$  for odd  $n$ . Thus, for  $1 \leq i \leq n-1$ ,

$$\begin{aligned} \deg(I_i) &= 2^{i-1} (2 \cdot \deg(D^s) - \binom{i-1}{2}) \\ &= 2^{i-1} (2(\binom{n}{2} + 1) - \binom{i-1}{2}), \end{aligned}$$

and for  $i = n$ ,

$$\begin{aligned} \deg(I_n) &= 2^{n-1} (2(\binom{n}{2} + 1) - \binom{n-1}{2}) - 4 \cdot \binom{n-1}{n/2} \delta_n \\ &= 2^{n-1} \cdot (\binom{n+1}{2} + 1) - 4 \cdot \binom{n-1}{n/2} \delta_n. \end{aligned}$$

Saturating the ideal  $I_n$  by the ideal generated by  $d$  is the same as saturation by the ideals  $(d_i)$  for all  $1 \leq i \leq n$ . In each



step of saturation the degree drops by  $2^n$ . Thus, the final ideal  $I^s := (\cdots (I_n : (d_1)) : \cdots : (d_n) \cdots) \subseteq R$  has degree

$$\begin{aligned} \deg(I^s) &= \deg(I_n) - n \cdot 2^n \\ &= 2^{n-1} \cdot \left( \binom{n+1}{2} + 1 \right) - 4 \cdot \binom{n-1}{n/2} \delta_n - n \cdot 2^n \\ &= 2^{n-1} \binom{n-1}{2} - 4 \cdot \binom{n-1}{n/2} \delta_n. \end{aligned}$$

Elimination of  $\{d_1, d_2, \dots, d_n\}$  from the ideal  $I^s$  drops the degree by a factor of 2. Note that  $(x, y) \in V_{\mathbb{Q}}(I_{p^*})$  implies  $(x, y, \pm d_1, \dots, \pm d_n) \in V_{\mathbb{Q}}(I^s)$ . Therefore, the ideal  $I_{p^*}$  has degree

$$\begin{aligned} \deg(I_{p^*}) &= \deg(I^s)/2 \\ &= 1/2 \cdot (2^{n-1} \binom{n-1}{2} - 4 \cdot \binom{n-1}{n/2} \delta_n) \\ &= 2^{n-2} \binom{n-1}{2} - 2 \cdot \binom{n-1}{n/2} \delta_n. \end{aligned}$$

The ideal  $I_{p^*}$  is a zero-dimensional ideal in  $\mathbb{Q}[x, y]$  that has the conjectured degree. Therefore, the following proposition holds:

**Proposition 5.3.1** *Let  $n$  be an integer such  $5 \leq n \leq 10$ . For  $n$  general points in  $\mathbb{R}^2$  with integer coordinates, the algebraic degree of the Fermat-Weber point over  $\mathbb{Q}$  is*

$$2^{n-2} \binom{n-1}{2} - 2 \cdot \binom{n-1}{n/2} \delta_n.$$

For giving an algebraic explanation of the conjecture on the algebraic degree of the Fermat-Weber point over  $\mathbb{Q}$ , we have broken it into smaller steps. We proved some of the steps for  $n$  number of points, where  $n \geq 5$ . However, in some steps we are restricted to computational results where  $n \leq 10$ . The formulas that are calculated in the last section suggest the steps of a general proof.

## Bibliography

- [1] H. Abo, A. Seigal, and B. Sturmfels. “Eigenconfigurations of tensors”. In: *Algebraic and geometric methods in discrete mathematics*. Vol. 685. Contemp. Math. American Mathematical Society, 2017, pp. 1–25.
- [2] V. I. Arnold. “On the arrangement of ovals of real plane algebraic curves, involutions of four-dimensional smooth manifolds, and the arithmetic of integral quadratic forms”. In: *Vladimir I. Arnold - Collected Works*. 1971, pp. 239–249.
- [3] S. Aronhold. “Über den gegenseitigen Zusammenhang der 28 Doppeltangenten einer allgemeinen Curve 4ten Grades”. In: *Monatberichte der Akademie der Wissenschaften zu Berlin*. 1864, pp. 499–523.
- [4] C. Bajaj. “Geometric optimization and computational complexity”. PhD thesis. Cornell University, Department of Computer Science, 1984.
- [5] J. Bochnak, M. Coste, and M. Roy. *Real Algebraic Geometry*. Vol. 36. Ergebnisse der Mathematik und ihrer Grenzgebiete/ A Series of Modern Surveys in Mathematics. Springer, Berlin, Heidelberg, 2013.
- [6] W. Bosma, J. Cannon, and C. Playoust. “The Magma algebra system. I. The user language”. In: *Journal of Symbolic Computation* 24.3-4 (1997), pp. 235–265.
- [7] C. W. Brown. “Constructing cylindrical algebraic decomposition of the plane quickly”. Manuscript. 2002.
- [8] E. Brugallé and L. López de Medrano. “Inflection points of real and tropical plane curves”. In: *Journal of Singularities* 4 (2012), pp. 74–103.
- [9] W. Bruns and U. Vetter. *Determinantal rings*. Vol. 1327. Springer, 2006.
- [10] L. Brusotti. “Sulla “piccola variazione” di una curva piana algebrica reale”. In: *Accademia dei Lincei, Rendiconti*. 5th ser. 30 (1921), pp. 375–379.
- [11] P. Bürgisser and F. Cucker. *Condition. The Geometry of Numerical Algorithms*. 1st ed. Vol. 349. Grundlehren der mathematischen Wissenschaften. Springer-Verlag Berlin Heidelberg, 2013.
- [12] L. Busé and I. Nonkané. “Discriminants of complete intersection space curves”. In: *Proceedings of the 2017 ACM on International*

- Symposium on Symbolic and Algebraic Computation*. ISSAC '17. Association for Computing Machinery, 2017, pp. 69–76.
- [13] L. Caporaso and E. Sernesi. “Characterizing curves by their odd theta characteristics”. In: *Journal für die Reine und Angewandte Mathematik. [Crelle’s Journal]* 562 (2003), pp. 101–135.
  - [14] T. Ö. Çelik. “Propriétés géométriques et arithmétiques explicites des courbes”. PhD thesis. Université de Rennes 1, IRMAR, 2018.
  - [15] T. Ö. Çelik, A. Kulkarni, Y. Ren, and M. Sayyary Namin. “Tritangents and their space sextics”. In: *Journal of Algebra* 538 (2019), pp. 290–311.
  - [16] J. Cheng, S. Lazard, L. Peñaranda, M. Pouget, F. Rouillier, and E. Tsigaridas. “On the Topology of Planar Algebraic Curves”. In: *Mathematics in Computer Science* 4 (2010), pp. 113–137.
  - [17] L. Chua, M. Kummer, and B. Sturmfels. “Schottky algorithms: classical meets tropical”. In: *Mathematics of Computation* 88.319 (2019), pp. 2541–2558.
  - [18] A. Coble. *Algebraic Geometry and Theta Functions*. Algebraic Geometry and Theta Functions v. 1. American mathematical society, 1929.
  - [19] S. J. Colley and G. Kennedy. “A higher-order contact formula for plane curves”. In: *Communications in Algebra* 19.2 (1991), pp. 479–508.
  - [20] A. Conca. “Gröbner bases of powers of ideals of maximal minors”. In: *Journal of Pure and Applied Algebra* 121.3 (1997), pp. 223–231.
  - [21] F. Dalla Piazza, A. Fiorentino, and R. Salvati Manni. “Plane quartics: the universal matrix of bitangents”. In: *Israel Journal of Mathematics* 217.1 (2017), pp. 111–138.
  - [22] A. Degtyarev and V. Zvonilov. “Rigid isotopy classification of real algebraic curves of bidegree (3,3) on quadrics”. In: *Mathematical Notes* 66 (1999), pp. 670–674.
  - [23] I. V. Dolgachev. *Classical Algebraic Geometry: A Modern View*. Cambridge University Press, 2012.
  - [24] A. Eigenwillig, M. Kerber, and N. Wolpert. “Fast and exact geometric analysis of real algebraic plane curves”. In: *Proceedings of the 2007 International Symposium on Symbolic and Algebraic Computation*. ISSAC '07. Association for Computing Machinery, 2007, pp. 151–158.
  - [25] D. Eisenbud. “Lectures on the geometry of syzygies”. In: *Trends in commutative algebra*. Vol. 51. Math. Sci. Res. Inst. Publ. With a chapter by Jessica Sidman. Cambridge Univ. Press, 2004, pp. 115–152.
  - [26] A. Emch. “Mathematical models”. In: *University of Illinois Bulletin* XXV.43 (1928), pp. 5–38.

- [27] G. Farkas and A. Verra. “The geometry of the moduli space of odd spin curves”. In: *Annals of Mathematics*. 2nd ser. 180.3 (2014), pp. 927–970.
- [28] J. C. Faugère, P. Gianni, D. Lazard, and T. Mora. “Efficient computation of zero-dimensional Gröbner bases by change of ordering”. In: *Journal of Symbolic Computation* 16.4 (1993), pp. 329–344.
- [29] T. Fiedler. “Eine Beschränkung für die Lage von reellen ebenen algebraischen Kurven”. In: *Beiträge zur Algebra und Geometrie* 11 (1981), pp. 7–19.
- [30] W. Fulton. *Intersection theory*. Vol. 2. Springer Science & Business Media, 2013.
- [31] A. Gabard. *Ahlfors circle maps and total reality: from Riemann to Rohlin*. 2012. arXiv: 1211.3680 [math.HO].
- [32] I. M. Gelfand, M. M. Kapranov, and A. V. Zelevinsky. *Discriminants, resultants and multidimensional determinants*. Modern Birkhäuser Classics. Reprint of the 1994 edition. Birkhäuser Boston, MA, 2008, pp. x+523.
- [33] L. Gonzalez-Vega and I. Necula. “Efficient topology determination of implicitly defined algebraic plane curves”. In: *Computer Aided Geometric Design* 19.9 (2002), pp. 719–743.
- [34] D. Gudkov. “Complete topological classification of the disposition of ovals of a sixth order curve in the projective plane”. In: *Nine Papers on Hilbert’s 16th Problem*. Vol. 112. 2. American Mathematical Society Translations, 1978, pp. 97–122.
- [35] D. Gudkov. “Ovals of sixth order curves”. In: *Nine Papers on Hilbert’s 16th Problem*. Vol. 112. 2. American Mathematical Society Translations, 1978, pp. 9–14.
- [36] D. Gudkov and A. Krahnov. “Periodicity of the Euler characteristic of real algebraic  $(m-1)$ -manifolds Funkcional”. In: *Anal. i Priložen* 7 (1973).
- [37] A. Harnack. “Über die Vieltheiligkeit der ebenen algebraischen Curven”. In: *Mathematische Annalen* 10.2 (1876), pp. 189–198.
- [38] C. Harris and Y. Len. “Tritangent planes to space sextics: the algebraic and tropical stories”. In: *Combinatorial Algebraic Geometry*. Ed. by G. G. Smith and B. Sturmfels. Vol. 80. Fields Inst. Commun. Fields Inst. Res. Math. Sci., 2018, pp. 47–63.
- [39] R. Hartshorne. *Algebraic geometry*. Graduate Texts in Mathematics, No. 52. Springer-Verlag, New York-Heidelberg, 1977, pp. xvi+496.
- [40] J. D. Hauenstein, A. Kulkarni, E. C. Sertöz, and S. N. Sherman. “Certifying Reality of Projections”. In: *Mathematical Software – ICMS 2018*. Ed. by J. H. Davenport, M. Kauers, G. Labahn, and J. Urban. Cham: Springer International Publishing, 2018, pp. 200–208.

- [41] D. Hilbert. “Über die reellen Züge algebraischer Kurven”. In: *Algebra · Invariantentheorie · Geometrie*. Springer Berlin Heidelberg, 1933, pp. 415–436.
- [42] R. Hudson, R. Hudson, W. Barth, and H. Baker. *Kummer’s Quartic Surface*. Cambridge Mathematical Library. Cambridge University Press, 1990.
- [43] I. V. Itenberg. “Rigid isotopy classification of curves of degree 6 with one nondegenerate double point”. In: *Topology of manifolds and varieties*. Ed. by O. Viro. Vol. 18. Advances in Soviet Mathematics. American Mathematical Society, 1994, pp. 193–208.
- [44] G. Kahn. “Eine allgemeine Methode zur Untersuchungen der Gestalten algebraischer Kurven”. PhD thesis. Göttingen, 1909.
- [45] N. Kaihnsa, M. Kummer, D. Plaumann, M. Sayyary Namin, and B. Sturmfels. “Sixty-Four Curves of Degree Six”. In: *Experimental Mathematics* 28.2 (2019), pp. 132–150.
- [46] C. Kalla and C. Klein. “Computation of the topological type of a real Riemann surface”. In: *Mathematics of Computation* 83.288 (2014), pp. 1823–1846.
- [47] V. M. Kharlamov. “Isotopic types of nonsingular surfaces of fourth degree in  $\mathbb{RP}^3$ ”. In: *Functional Analysis and Its Applications* 12 (1978), pp. 68–69.
- [48] V. M. Kharlamov. “Rigid isotopic classification of real planar curves of degree 5”. In: *Functional Analysis and Its Applications* 15 (1981), pp. 73–74.
- [49] V. M. Kharlamov. “Classification of nonsingular surfaces of degree 4 in  $\mathbb{RP}^3$  with respect to rigid isotopies”. In: *Functional Analysis and Its Applications* 18 (1984), pp. 39–45.
- [50] V. Kharlamov. “New congruences for the Euler characteristic of real algebraic varieties, Funktsional. Anal. Prilozhen. 7 (1973), 74–78”. In: *English translation in Functional Anal. Appl* 7 (1973), pp. 147–150.
- [51] H. Kuhn. “On a pair of dual nonlinear programs. I. Nonlinear Programming”. In: *Nonlinear programming*. Amsterdam : North-Holland, 1967, pp. 37–54.
- [52] A. Kulkarni. *An arithmetic invariant theory of curves from  $E_8$* . 2017. eprint: 1711.08843.
- [53] A. Kulkarni. “An explicit family of cubic number fields with large 2-rank of the class group”. In: *Acta Arithmetica* 182.2 (2018), 117–132.
- [54] A. Kulkarni, Y. Ren, M. Sayyary Namin, and B. Sturmfels. “Real space sextics and their tritangents”. In: *Proceedings of the 2018 ACM International Symposium on Symbolic and Algebraic Computation*. ISSAC ’18. Association for Computing Machinery, 2018, pp. 247–254.

- [55] A. Kulkarni, M. Sayyary, Y. Ren, and B. Sturmfels. *Data and scripts for this article*. Available at: `software.mis.mpg.de`. 2017.
- [56] M. Kummer. “Totally real theta characteristics”. In: *Annali di Matematica Pura ed Applicata*. 4th ser. 198.6 (2019), pp. 2141–2150.
- [57] A. Kunert and C. Scheiderer. “Extreme positive ternary sextics”. In: *Transactions of the American Mathematical Society* 370.6 (2017), 3997–4013.
- [58] H. Lee and B. Sturmfels. “Duality of multiple root loci”. In: *Journal of Algebra* 446 (2016), pp. 499–526.
- [59] D. Lehavi. “Any smooth plane quartic can be reconstructed from its bitangents”. In: *Israel Journal of Mathematics* 146.1 (2005), 371–379.
- [60] D. Lehavi. “Effective reconstruction of generic genus 4 curves from their theta hyperplanes”. In: *International Mathematics Research Notices. IMRN* 19 (2015), pp. 9472–9485.
- [61] A. Lerario and E. Lundberg. “Statistics on Hilbert’s 16th problem”. In: *Int. Math. Res. Not. IMRN* 12 (2015), pp. 4293–4321.
- [62] K. Löbenstein. “Ueber den Satz, dass eine ebene, algebraische Kurve 6. Ordnung mit 11 sich einander ausschliessenden Ovalen nicht existiert”. PhD thesis. Göttingen, 1910.
- [63] M. Maccioni. “The number of real eigenvectors of a real polynomial”. In: *Bollettino dell’Unione Matematica Italiana* 11.2 (2018), pp. 125–145.
- [64] Y. Manin. *Cubic Forms: Algebra, Geometry, Arithmetic*. North-Holland Mathematical Library. Elsevier Science, 1986.
- [65] J. H. McDonald. “The Ovals of the Plane Sextic Curve”. In: *American Journal of Mathematics* 49.4 (1927), pp. 523–526.
- [66] M. Michalek, H. Moon, B. Sturmfels, and E. Ventura. “Real rank geometry of ternary forms”. In: *Annali di Matematica Pura ed Applicata*. 4th ser. 196.3 (2017), pp. 1025–1054.
- [67] J. Nie, P. A. Parrilo, and B. Sturmfels. “Semidefinite representation of the k-ellipse”. In: *Algorithms in algebraic geometry*. Springer, 2008, pp. 117–132.
- [68] V. V. Nikulin. “Integral symmetric bilinear forms and some of their applications”. In: *Mathematics of the USSR-Izvestiya* 14.1 (1980), pp. 103–167.
- [69] I. Petrowsky. “On the Topology of Real Plane Algebraic Curves”. In: *Annals of Mathematics* 39.1 (1938), pp. 189–209.
- [70] D. Plaumann, B. Sturmfels, and C. Vinzant. “Quartic curves and their bitangents”. In: *Journal of Symbolic Computation* 46.6 (2011), pp. 712–733.
- [71] B. Poonen. *Rational points on varieties*. Vol. 186. Graduate Studies in Mathematics. American Mathematical Society, 2017, pp. xv+337.

- [72] K. Ranestad and B. Sturmfels. “On the convex hull of a space curve”. In: *Advances in Geometry* 12.1 (2012), pp. 157–178.
- [73] H. E. Rauch and H. M. Farkas. *Theta functions with applications to Riemann surfaces*. The Williams & Wilkins Co., Baltimore, Md., 1974, pp. xii+232.
- [74] B. Reznick. “Some concrete aspects of Hilbert’s 17th Problem”. In: *Real algebraic geometry and ordered structures (Baton Rouge, LA, 1996)*. Vol. 253. Contemp. Math. Amer. Math. Soc., Providence, R.I., 2000, pp. 251–272.
- [75] K. Rohn. “Die Maximalzahl und Anordnung der Ovale bei der ebenen Kurve 6. Ordnung und bei der Fläche 4. Ordnung”. In: *Mathematische Annalen* 73 (1913), pp. 177–229.
- [76] A. V. Rokhlin. “Complex topological characteristics of real algebraic curves”. In: *Russian Mathematical Surveys*. Vol. 33. 5. 1978, pp. 85–98.
- [77] V. A. Rokhlin. “Congruence modulo 16 in Hilbert’s sixteenth problem. II”. In: *Functional Analysis and Its Applications* 7.2 (1973), pp. 163–164.
- [78] R. Seidel and N. Wolpert. “On the exact computation of the topology of real algebraic curves”. In: *Proceedings of the Twenty-First Annual Symposium on Computational Geometry*. SCG ’05. Association for Computing Machinery, 2005, pp. 107–115.
- [79] E. Sertöz. *Enumerative Geometry of Double Spin Curves*. Doctoral Dissertation, HU Berlin, <https://edoc.hu-berlin.de/handle/18452/19134>. 2017.
- [80] R. Silhol. *Real Algebraic Surfaces*. Springer, Berlin, Heidelberg, 1989.
- [81] D. Testa, A. Várilly-Alvarado, and M. Velasco. “Cox rings of degree one del Pezzo surfaces”. In: *Algebra Number Theory* 3.7 (2009), pp. 729–761.
- [82] G. A. Utkin. “Construction of certain types of nonsingular fourth order surfaces”. In: *Nine Papers on Hilbert’s 16th Problem*. Vol. 112. 2. American Mathematical Society Translations, 1978, pp. 158–170.
- [83] N. Vervliet, O. Debals, L. Sorber, M. Van Barel, and L. De Lathauwer. *Tensorlab 3.0*. 2016. URL: <http://www.tensorlab.net>.
- [84] O. Y. Viro. “Gluing of plane real algebraic curves and constructions of curves of degrees 6 and 7”. In: *Topology (Leningrad, 1982)*. Vol. 1060. Lecture Notes in Math. Springer, Berlin, 1984, pp. 187–200.
- [85] O. Y. Viro. “From the sixteenth Hilbert problem to tropical geometry”. In: *Japanese Journal of Mathematics* 3.2 (2008), pp. 185–214.
- [86] A. Weber. *Alfred Weber’s Theory of the Location of Industries*. CreateSpace Independent Publishing Platform, 2017.

- [87] J. E. Wright. “The Ovals of the Plane Sextic Curve”. In: *American Journal of Mathematics* 29.3 (1907), pp. 305–308.
- [88] O. Y. Viro. “Progress in the topology of real algebraic varieties over the last six years”. In: *Russian Mathematical Surveys* 41.3 (1986), pp. 55–82.



## Bibliographische Daten

---

Real Algebraic Geometry of the Sextic Curves  
(Reelle algebraische Geometrie von sextischen Kurven)  
Sayyary Namin, Mahsa  
Universität Leipzig, Dissertation, 2020  
122 Seiten,  
25 Abbildungen,  
88 Referenzen

## Selbstständigkeitserklärung

Hiermit erkläre ich, die vorliegende Dissertation selbständig und ohne unzulässige fremde Hilfe angefertigt zu haben. Ich habe keine anderen als die angeführten Quellen und Hilfsmittel benutzt und sämtliche Textstellen, die wörtlich oder sinngemäß aus veröffentlichten oder unveröffentlichten Schriften entnommen wurden, und alle Angaben, die auf mündlichen Auskünften beruhen, als solche kenntlich gemacht. Ebenfalls sind alle von anderen Personen bereitgestellten Materialien oder erbrachten Dienstleistungen als solche gekennzeichnet.

Leipzig, den 2. September 2020



.....

(Mahsa Sayyary Namin)

## Daten zum Autor

---

<b>Name:</b>	Mahsa Sayyary Namin
<b>Geburtsdatum:</b>	24.04.1990 in Teheran, Iran
<b>09/2008 - 09/2013</b>	Studium der Mathematik (B. Sc.) Sharif University of Technology, Tehran, Iran
<b>09/2013 - 07/2016</b>	Studium der Mathematik (M. Sc.) University of Tehran, Tehran, Iran
<b>04/2015 - 06/2015</b>	Studium der Mathematik (Austausch-Studentin) Sorbonne University Pierre and Marie Curie Campus, Paris, France
<b>09/2015 - 09/2016</b>	Studium der Mathematik (Prädoktorandin) International Center for Theoretical Physics, Trieste, Italy
<b>seit 09/2016</b>	Doktorandin Max-Planck-Institut für Mathematik in den Natur- wissenschaften, Leipzig
<b>07/2019 - 11/2020</b>	Wissenschaftlicher Mitarbeiterin Mathematisches Institut, Universität Leipzig